Simulation of Condensation on Vertical Fluted Tubes

A Thesis
Presented to
The Faculty of the
Chemical Engineering Department
University of Houston
Houston, Texas

In Partial Fulfillment
of the Requirements for the Degree
Master of Science in Chemical Engineering

By
Gregory Y. Weeter
December, 1973

Acknowledgments

I would like to thank Dr. A. E. Dukler for his advice and direction throughout this project. I also appreciate the help and consideration of the Engineering System Simulation Laboratory. Thanks also to my mother, Earlene Y. Weeter, for typing the manuscript.

Simulation of Condensation on Vertical Fluted Tubes

An Abstract of a Thesis
Presented to
The Faculty of the
Chemical Engineering Department
University of Houston
Houston, Texas

In Partial Fulfillment
of the Requirements for the Degree
Master of Science in Chemical Engineering

By
Gregory Y. Weeter
December, 1973

ABSTRACT

Heat transfer coefficients on the condensing side of a heat exchanger can be markedly increased by designing the condensing surface to take advantage of surface tension. This is accomplished by using a waved or "fluted" surface. A mathematical model for the prediction of heat transfer coefficients on these surfaces was developed earlier, but the method of solution is poorly understood. In addition, the original model made some approximations which are either not necessary or else not accurate over the entire surface. These problems are alleviated in the modified model.

For the most part, the original and modified models predict heat transfer coefficients which are quite similar, but for distances far down the condenser, where the flutes are fairly full, the difference begins to become evident. The shape of the condensate profile is predicted by the two methods varies to some extent between the two methods as the flute fills.

The variation of heat transfer coefficient with the temperature driving force across the film was determined; and it was found that increasing the driving force caused a decrease in heat transfer coefficient, since the steam condensed faster than it could run off. Despite

the fact that increasing the temperature lowers the surface tension, it also increases the heat transfer coefficient. This occurs because the increase in temperature also decreases the viscosity, and thus there is less resistance to flow.

Comparison of the predictions of the new model with experimental data shows that, considering the spread of the data, the predictions are fairly good.

The effect of varying the dimensions of a sinusoidal flute on the heat transfer coefficient was determined. It was found that flutes with high, closely spaced peaks would greatly enhance the heat transfer; but the validity of the assumption of uniform temperature in the metal surface was questioned.

A comparison of the sinusoidal condenser profile with the GE Profile-9 surface indicated that the GE Profile-9 surface is less effective than a sinusoidal surface.

A new surface profile was developed which would allow a much larger amount of liquid to flow downward in the trough than the sinusoidal profile. This surface showed somewhat better heat transfer than the sinusoidal surface.

TABLE OF CONTENTS

LIST OF FIGURES

Chapter I

INTRODUCTION

When heat is exchanged between two streams, the transferred heat is $q = UA(-\Delta T)$. In order to increase the rate of heat transfer, it is thus necessary to increase the heat transfer coefficient, the area for heat transfer, or the temperature driving force. Of these three, the latter two are most generally used, although new ways of changing the heat transfer coefficient have been developed.

When one of the streams has a much higher resistance to heat transfer than the other, as in an air-cooled heat exchanger, it is often helpful to increase the surface area by adding fins along the side of the exchanger in contact with the high resistance stream.

The heat transfer coefficient may be increased in several ways. Since the total resistance to heat transfer is made up of several resistances, the reduction of any of these is bound to improve the performance of the equipment; but it is most helpful to adjust the largest contributors to the resistance. Since the wall is usually made of material with high thermal conductivity, its resistance is generally quite small compared to the other resistances. Naturally, fouling should be avoided; but in practice it is uneconomical to try to completely eliminate it, since this involves frequent shut-downs to clean the exchanger. Thus the main areas where improvement can be made and have a significant effect are in the regions surrounding the wall where the bulk of the temperature gradient lies. One means of improving the heat transfer is to decrease the thickness of these regions. When the fluid inside the tube has a high resistance to heat transfer, it has been found advantageous to use a helically twisted ribbon inside the tube to establish vortex shear-flow (1), (2). This obstruction in the tube increases the turbulence and thus produces more effective mixing and therefore decreases the effective thickness of the region where the temperature gradient exists. In addition, in two-phase flow such as evaporating sea water inside a tube, it has been found that the ribbon causes, by means of centrifugal force, the denser liquid to move to the outside, along the wall, while keeping the vapor in the center of the tube. Thus, besides causing additional turbulence, the system keeps the liquid near the surface. Since the liquid will transfer heat more readily than the vapor, this results in further enhancement of heat transfer.

For condensing-evaporating systems, one of the large resistances to heat transfer may be that of the liquid condensate film. There are, at present, three means of decreasing this resistance: spinning a horizontal condensing surface, promoting dropwise condensation, and fluting the tubes. The first of these produces a centrifugal force greater than the force of gravity, thereby speeding up the rate at which the condensate is removed, and thus decreasing the film thickness. The disadvantage of this scheme is that it is relatively expensive, both in capital and operating costs. Dropwise condensation, which is often many times more efficient than filmwise condensation, can be promoted by coating the condensing surface with a hydrophobic film. However, it is difficult to maintain dropwise condensation over long periods of time.

The most promising means of changing the thickness of the condensate film is by the use of vertically fluted surfaces, as seen in Figures 1 and 2. For a fluid system whose surface is curved, there is a pressure resulting from the surface tension which is inversely proportional to the radius of curvature of the surface. As predicted by Gregorig (3), surface tension causes a pressure gradient in the condensate film because the radius of curvature of the free surface is changing, so that there is flow away from the peak, where the high pressure exists, into the valley. This results in a thin film near the peak at the expense of increased thickness in the valley. Thus, although the surface appears somewhat similar to longitudinally finned tubes, the effect is quite different. In fact, the gain in heat transfer rate is greater than the gain in surface area. Even though the resistance to heat transfer is large in the valley (because of the thick film), the increased heat transfer in the peak

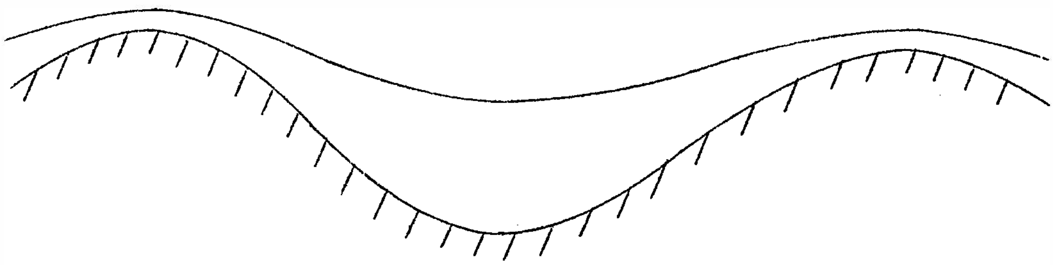

Figure 1
Drawing of Fluted Surface

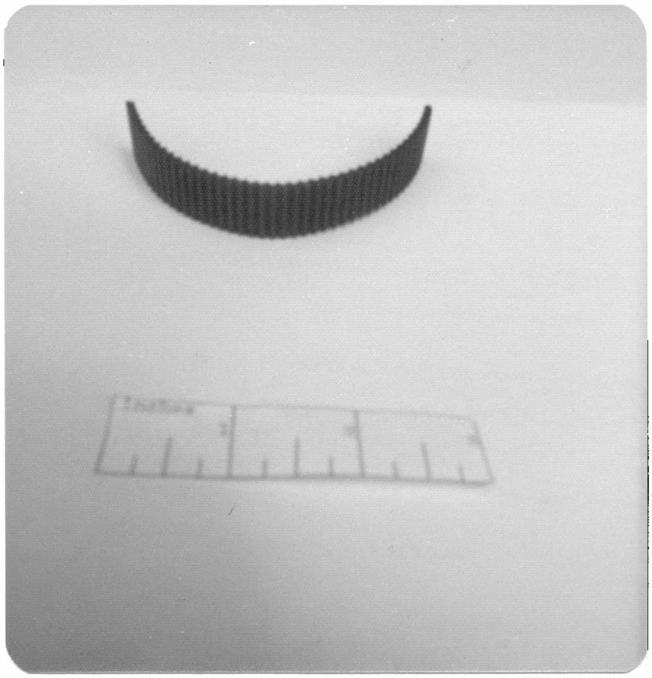

Figure 2
Photograph of Fluted Surface

section is great enough to result in a considerable net improvement over smooth tubes.

Chapter II

REVIEW OF EARLIER WORK

The first experimental work utilizing the surface tension to increase heat transfer were performed by Gregorig (3). He established that the condensing heat transfer coefficient was, indeed, improved by using fluted surfaces. He further demonstrated that the numerical method he worked out gave verifiable predictions of the heat transfer coefficient. Lustenader, Richter, and Neugebauer (4) performed experiments which showed that the heat transfer coefficient was a weak function of the tube length, as predicted by Gregorig, but that at a sufficient length the heat transfer dropped off sharply. This was attributed to the fact that the valley became so full that there was no longer a significant curvature of the free surface, and hence no pressure gradient to act as the horizontal driving force for flow. Thus, material condensed at the peak tended to stay at the peak, which increased the film thickness in the important condensing region. This, too, was predicted by Gregorig's model. An "optimized" surface configuration was used for these experiments, but no method was suggested for this optimization. In the discussion of this paper, Trefethen (5) noted that the pressure gradient would act on the vapor near the free surface, as well as on the liquid film, thus forcing any non-condensible vapor toward the valley, where its effect would be minimized. In a later paper, Lustenader and Staub (2) presented data over a considerable ΔT temperature driving force range. Experimental data was presented by Carnivos (6) and Christ (7), which further demonstrated the great improvement in heat transfer coefficient that could be obtained by fluting the condensing surface. Christ's experiments were of special interest because they were essentially extensions of Gregorig's work, using the same surface configuration as Gregorig used. Carnivos (8) conducted experiments using doubly fluted tubes (that is, both the condensing and evaporating sides were fluted), and, while he did not measure the individual contributors (condensing and evaporating coefficients), determined that whether the flutes were in phase or out of phase with each other had little effect on the overall heat transfer coefficient.

Other work, by Thomas (9), (10), employed loosely attached wires and rectangular fins on the surface of smooth tubes to increase the heat transfer. The basis for this work was, like Gregorig's, the fact that surface tension would cause an increase in thickness of the condensate film in one place while decreasing it at another location. In this case, the thick region was at the base of the fins or wires, while the film between the extensions was relatively thin. This surface was not an extended surface in the sense that regular finned tubes are, since the wires and fins were loosely attached, thus allowing only negligible heat transfer from the fin to the tube. Most of the condensate was drawn into rivulets next to the fins, while the bulk of the condensation took place between the fins. Thomas found experimentally that the rectangular fins caused a greater increase in heat transfer coefficient than the wires, but concluded that this was due, not to the surface tension effects, but to hydrodynamic considerations for the downward flow.

A recent work (11) used "dimpled" tubes, somewhat similar to the dimples on a golf ball, to enhance heat transfer (see Figure 3). This appeared to utilize surface tension to promote a semblance of dropwise condensation, in which the condensate was collected in the indentations. Apparently, however, the main influence on the heat transfer coefficient for this type of surface was on the evaporating side of the tube. (The tube was of uniform thickness, so that indentations on the condensing side corresponded to mounds on the evaporating side.) The dimples increased turbulence in the falling evaporating film; and, moreover, the film thickness along the mounds on the evaporating side was kept small by surface tension but was continually renewed by the falling film.

Theoretical Work

The original mathematical description of the effect of fluted surfaces on condensing heat transfer coefficients in vertical tubes was done by

Major Axis

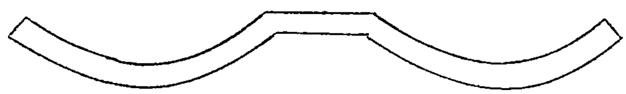

Minor Axis

Figure 3
Dimpled Surface

Gregorig (3). He broke the problem down into two parts. First was the problem of horizontal flow, which included condensation of vapor and movement of the condensate, through the influence of surface tension, into the valley of the flute. This determined the shape and thickness of the condensate profile along the flute. The horizontal flow problem was simulated by a one-dimensional flow equation, making use of steady-state and creeping flow assumptions. The boundary conditions, besides no slip at the wall and no shear at the free surface, were that symmetry in the condensate profile must be preserved at both the peak and the valley. The method for determining the profile was to begin at the peak and integrate the equation to the valley. Because one of the boundary conditions (symmetry) was at the center of the valley, the solution was, of necessity, trial and error and very laborious. Once the profile was found, the downward flow rate through the profile could be easily found by solving a two-dimensional Poisson equation numerically. Knowing the rate of condensation and downward flow rate for a pair of profiles, the vertical separation distance between them could be found by means of a mass balance. The experiments by Christ (7) showed that the Gregorig model resulted in good predictions, particularly when the trough was not filled. However, the method became less accurate as the trough filled.

As a suggested improvement, in order to eliminate the trial and error process involved in determining the profile, Markowitz, Mikic, and

Bergles (12) proposed a simpler method for determining the film thickness at the peak of the flute. The method broke the problem down into two areas: one where the film thickness was small compared to the radius of curvature of the metal surface (near the peak), and one where it was significant in comparison to the radius of curvature (in the valley). The assumption was made that the film thickness was practically constant in the trough. This assumption is not bad near the top of the tube, but as the trough fills it becomes progressively worse. An expression similar to the Nusselt (13) equation for determining the condensate thickness was developed to determine the thickness at the crest of the flute, using the surface tension-induced pressure gradient rather than gravity as the driving force. This method showed moderately good agreement with the single published point determined by Gregorig; but the predicted heat transfer was, in general, substantially different from experimental results determined by Markowitz, et al (12). It was suggested in the paper that the experimental results might be in error to some extent because of the presence of non-condensible gas in the feed steam; but, as has been mentioned earlier (5), this problem should be minimized by the fluted surface. This method, while clearly faster and easier than the original Gregorig method, seems to hold little promise, since the original method yielded much better agreement with experimental data. The fact that the predicted film was even fairly close to the Gregorig prediction appears to be coincidental, since the peak film thickness predicted by Gregorig did not vary monotonically with pipe length, while this method predicted that it would.

Chapter III

DETAIL OF GREGORIG METHOD

Gregorig worked with a vertical condensing tube with a fluted surface similar to that shown in Figure 1. In deriving the original numerical method for determining the condensate film profile on fluted tubes, Gregorig first assumed that, as far as the horizontal (peak to valley of the flute) flow was concerned, the metal surface from the crest to the trough of the rill was flat (see Figure 4). This assumption enabled him to use a single equation of motion to represent the horizontal flow, rather than having to use a pair of coupled equations.

The starting point of the analysis is the x-component of the Navier-Stokes equation of motion:

$$\frac{\rho}{g_c}\left(\frac{\partial u_x}{\partial t} + u_x\frac{\partial u_x}{\partial x} + u_y\frac{\partial u_x}{\partial y} + u_z\frac{\partial u_x}{\partial z}\right) = -\frac{\partial P}{\partial x} + \frac{\mu}{g_c}\left(\frac{\partial^2 u_x}{\partial x^2} + \frac{\partial^2 u_x}{\partial y^2} + \frac{\partial^2 u_x}{\partial z^2}\right) + \frac{\rho g_x}{g_c} \quad (1)$$

Assuming that the flow is steady and slow, the acceleration terms (the left-hand side of equation 1) are negligible. Since gravity is in the z-direction, g_x is zero. The film thickness varies slowly with the tube length, so the viscous term involving $\frac{\partial^2 u_x}{\partial z^2}$ is small. In addition, since the film thickness is small, it is likely that U_x will vary much faster with y than with x. Thus equation 1 can be reduced to

$$\frac{\partial P}{\partial x} = \frac{\mu}{g_c}\frac{\partial^2 u_x}{\partial y^2} \quad (2)$$

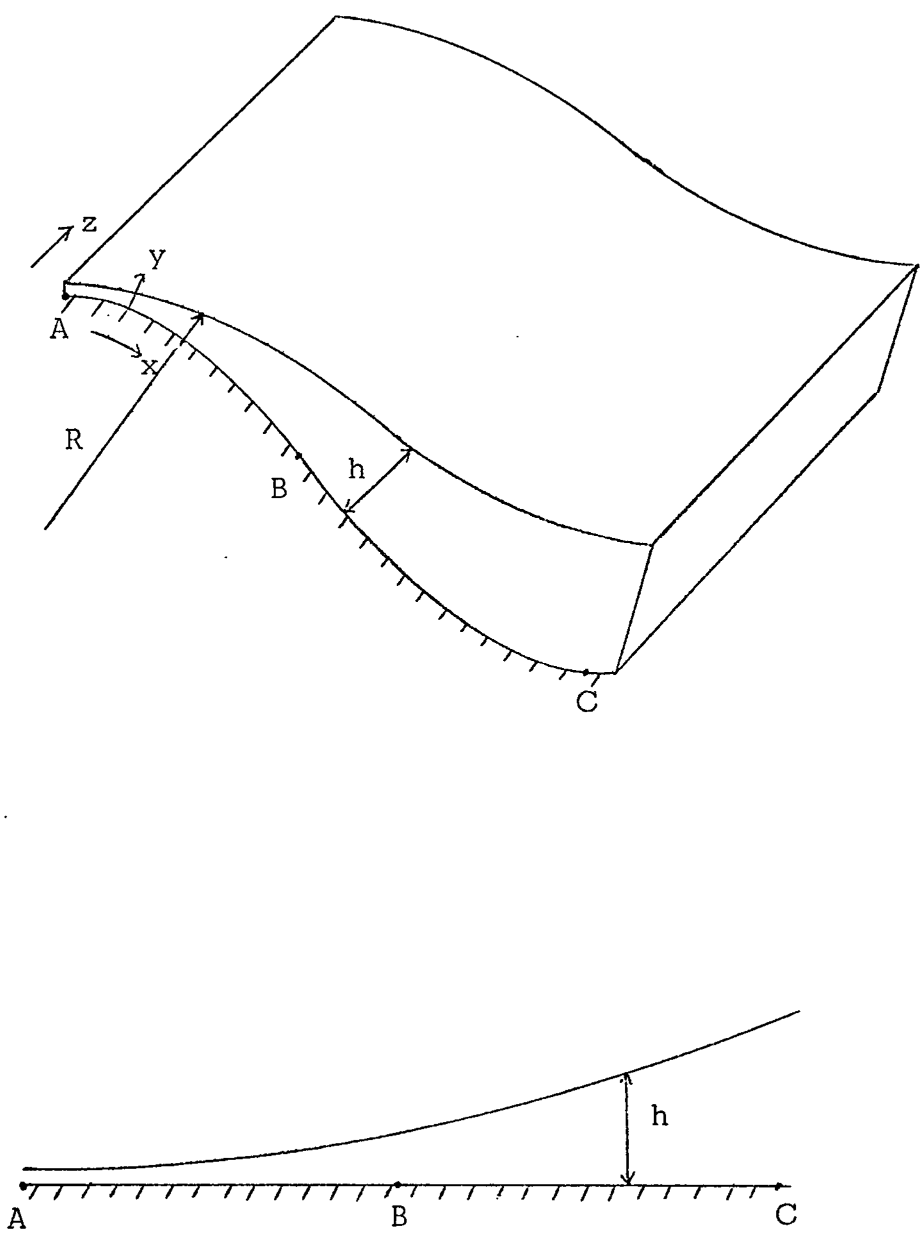

Figure 4

Transformation of Curved Metal Surface
to a Flat Surface

The boundary conditions for the solution of this problem are: (1) no slip at the wall (implies that the velocity is zero at the wall) and (2) no shear at the free surface (implying that the velocity reaches a maximum here). Integrating equation (2) and applying the boundary conditions,

$$U_x = \frac{g_c}{\mu}\frac{\partial P}{\partial x}\left(\frac{y^2}{2} - hy\right). \tag{3}$$

Averaging U_x over the film thickness from $y=0$ to $y = h$ and rearranging,

$$-\frac{\partial P}{\partial x} = \frac{3\,\bar{U}_x\,\mu}{g_c\,h^3} . \tag{4}$$

The pressure resulting from surface tension is determined by the radius of curvature of the free surface:

$$P = \frac{\sigma}{R\,g_c} . \tag{5}$$

The convective diffusion in two dimensions is

$$U_x\frac{\partial T}{\partial x} + U_y\frac{\partial T}{\partial y} = \frac{k}{C_p\rho}\left[\frac{\partial^2 T}{\partial x^2} + \frac{\partial^2 T}{\partial y^2}\right]. \tag{6}$$

Assuming that $\frac{\partial T}{\partial x}$ is negligible and U_y is small, equation (6) is reduced to

$$\frac{\partial^2 T}{\partial x^2} + \frac{\partial^2 T}{\partial y^2} = 0 . \tag{7}$$

However, the temperature varies much more rapidly in the y-direction than in the x-direction, so equation (7) may be simplified to

$$\frac{\partial^2 T}{\partial y^2} = 0 . \tag{8}$$

Integrating this once, the result is

$$\frac{\partial T}{\partial y} = \text{constant} . \tag{9}$$

However, the heat flux is defined in terms of the temperature gradient at the boundary ($y = 0$):

$$-\left(\frac{\partial T}{\partial y}\right)_0 \equiv \frac{q}{kA} . \tag{10}$$

Since, according to equation (9), $\frac{\partial T}{\partial y}$ is constant, the right-hand side of equation (10) must also be constant, thus equation (10) may be integrated to yield

$$q = \frac{kA}{h}(-\Delta T) \ . \tag{11}$$

Or, defining $Q = \frac{q}{A}$

$$Q = \frac{k}{h}(-\Delta T) \ . \tag{12}$$

It should be noted that in obtaining equation (8), it was assumed that, for the purpose of heat transfer, the condensing surface was flat, rather than fluted, as was assumed for the flow equation in equation (2). However, it is not strictly true that the area for heat transfer is independent of the y-position, but it is instead wedge-shaped. The heat flow is essentially one-dimensional, but the direction of heat flow is not parallel at various x-positions. Equation (10) should allow A to be a function of y, rather than being constant.

Utilizing a heat balance and allowing m_n to represent the rate of mass condensed per unit length per unit time between the peak of the flute and the position x_n distance along the flute (see Figure 5),

$$Q = \lambda \frac{dm_n}{dx} \ . \tag{13}$$

Setting equations (12) and (13) equal and integrating, assuming that h is constant,

$$\Delta m_n = m_{n+1} - m_n = \frac{k(-\Delta T)\Delta x}{h_n \lambda} \ . \tag{14}$$

The relation between m_n and U_{x_n} is found by assuming that all

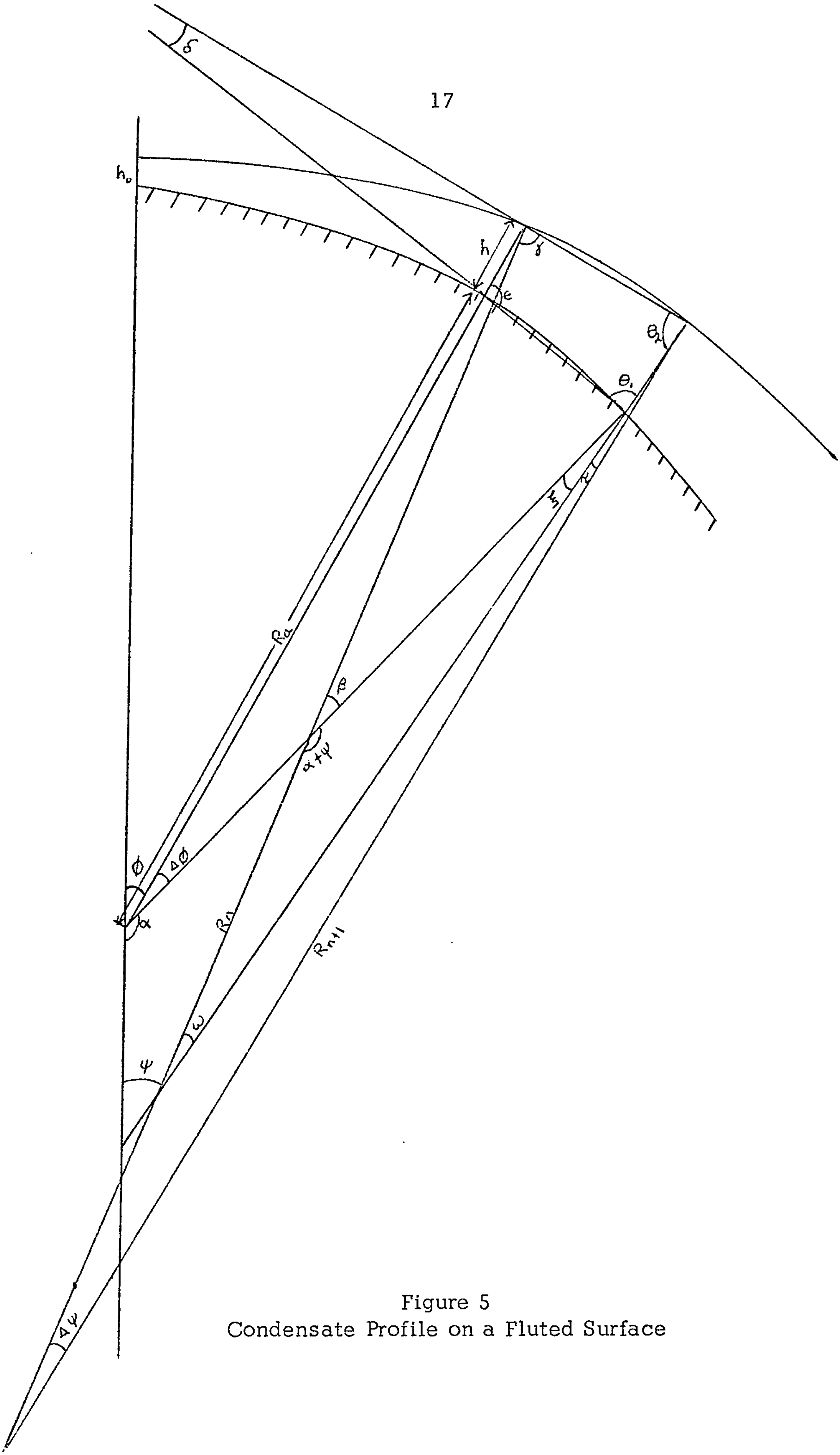

Figure 5
Condensate Profile on a Fluted Surface

flow is horizontal. Then one obtains

$$m_n = \rho h_n \bar{U}_{x_n} \quad . \tag{15}$$

Substituting equation (15) into (4), it may be seen that

$$\frac{\partial P}{\partial x} = -\frac{3\mu}{\rho h_n^3 g_c} m_{n+1} \quad . \tag{16}$$

At this point it is important to introduce the fact that the surface is not flat, but is instead curved in order to have a pressure gradient in the x-direction. To aid in notation, the symbol s is used to represent distance along the curved surface, where x was the distance along the flat surface. Thus equations (14) and (16) become

$$\Delta m_n = \frac{k(-\Delta T)}{h_n \lambda} \Delta s \tag{17}$$

and

$$\frac{\partial P}{\partial s} = \frac{-3\mu}{\rho h_n^3 g_c} m_{n+1} \quad . \tag{18}$$

Assuming that h is constant over the interval, an assumption that is valid for small steps, equation (18) is integrated and equation (5) is substituted in:

$$R_{n+1} = \frac{1}{1/R_n - \frac{3\mu m_{n+1}}{h_n^3 \rho \sigma} \Delta s} \quad . \tag{19}$$

From Figure 5 it is clear that

$$\Delta \phi = \Delta s / R_A \tag{20}$$

and

$$\Delta \Psi = \Delta s / R_n \tag{21}$$

Equation (20) is used to find $\Delta\phi$, the change in angle of the metal surface. However, this is not really necessary, since the shape of the metal surface is known. Thus the angle $\Delta\phi$ can be found directly from the equation of the surface.

In order to use equation (21), it is necessary to assume that the radius of curvature is constant over the interval Δs at the value R_n. However, as seen in Figure 5, it is clear that, since the two radii of curvature R_n and R_{n+1} do not intersect at the pivot point of R_n, but intersect close to the pivot point of R_{n+1}, it would be better to use R_{n+1}, rather than R_n in equation (21). The use of R_n does not introduce a large error as long as the radius of curvature is fairly constant, but at some point along the surface the radius of curvature must go to infinity, reverse sign, and decrease rapidly, as the free surface goes from convex to concave. In this region, the use of R_n in equation (21) is not a good approximation.

As shown in Appendix 1,

$$\delta = \phi - \psi + \frac{\Delta\phi}{2} - \frac{\Delta\psi}{2} \ . \tag{22}$$

Then the change in h is given by

$$\Delta h = [(\phi - \psi) + \tfrac{1}{2}(\Delta\phi - \Delta\psi)]\Delta s \tag{23}$$

Equation (23) (together with the relation $h_{n+1} = h_n + \Delta h$) gives a film thickness which is likely to be greater than the actual thickness. The process used in finding a position on the free surface is to take equal-sized steps along both the free and solid surfaces, so that a position on the solid surface which is a distance s from the peak corresponds to a position on the free surface which is likewise a distance s from the peak, when measured along the free surface. The actual film thickness should be the shortest distance from a point on the free surface to the solid surface. Thus the thickness calculated by equation (23) will always be at least as large as the true thickness, and in the case where the trough is nearly full may be significantly larger than the true thickness.

The actual numerical procedure used in the original Gregorig method is:

1) Choose h_o (film thickness at peak), R_o (radius of curvature of free surface at peak), and Δs.

2) Determine $\Delta\phi$ from equation (20).

3) Determine Δm from equation (17) and set

$$m_{n+1} = m_n + \Delta m_n$$

4) Determine $\Delta\Psi$ from equation (21).

5) Find h_{n+1} $(= h_n + \Delta h)$ from equation (23).

6) Find R_{n+1} from equation (19).

7) Make another Δs step and go to step 2. Continue to step off along the metal surface, calculating the film thickness at each point, until h goes negative (which is physically unrealizable) or Ψ goes negative (implying that the line of symmetry of the metal surface does not correspond to the line of symmetry of the free surface), or the line of symmetry in the valley is reached. If convergence has not been reached (ie, $\Psi \neq 0$ at the line of symmetry), choose

another value of h_o and try again. The last two possibilities represent the satisfaction of the boundary condition that symmetry must be preserved (that is, the slope of the free surface must be zero) at the center of the valley (the line of symmetry of the metal surface).

At this point Gregorig has determined the profile of the condensate film, but not the vertical position of that profile. At this point he states that relaxation is used to determine the downward flow rate, but does not go into any further detail as to method. The method used here is to begin with the equation of motion in the z-direction to determine the downward flow rate (see Figure 6):

$$\frac{\rho}{g_c}\left(\frac{\partial u_z}{\partial t} + u_x\frac{\partial u_z}{\partial x} + u_y\frac{\partial u_z}{\partial y} + u_z\frac{\partial u_z}{\partial z}\right) = -\frac{\partial p}{\partial z} + \frac{\mu}{g_c}\left(\frac{\partial^2 u_z}{\partial x^2} + \frac{\partial^2 u_z}{\partial y^2} + \frac{\partial^2 u_z}{\partial z^2}\right) + \rho\frac{g_z}{g_c} \,. \qquad (24)$$

Neglecting the acceleration terms and assuming negligible pressure drop, equation (24) reduces to the three-dimensional Poisson equation

$$\frac{\partial^2 u_z}{\partial x^2} + \frac{\partial^2 u_z}{\partial y^2} + \frac{\partial^2 u_z}{\partial z^2} = -\frac{\rho}{\mu} g_z \,. \qquad (25)$$

However, U_z varies much more slowly in the z-direction than in the x- and y-directions, so equation (25) becomes

$$\frac{\partial^2 u_z}{\partial x^2} + \frac{\partial^2 u_z}{\partial y^2} = -\frac{\rho}{\mu} g_z \,. \qquad (26)$$

By using a Taylor series to represent U_z the finite difference approximations of the derivatives $\frac{\partial^2 u_z}{\partial x^2}$ and $\frac{\partial^2 u_z}{\partial y^2}$ may be found (14) as (see

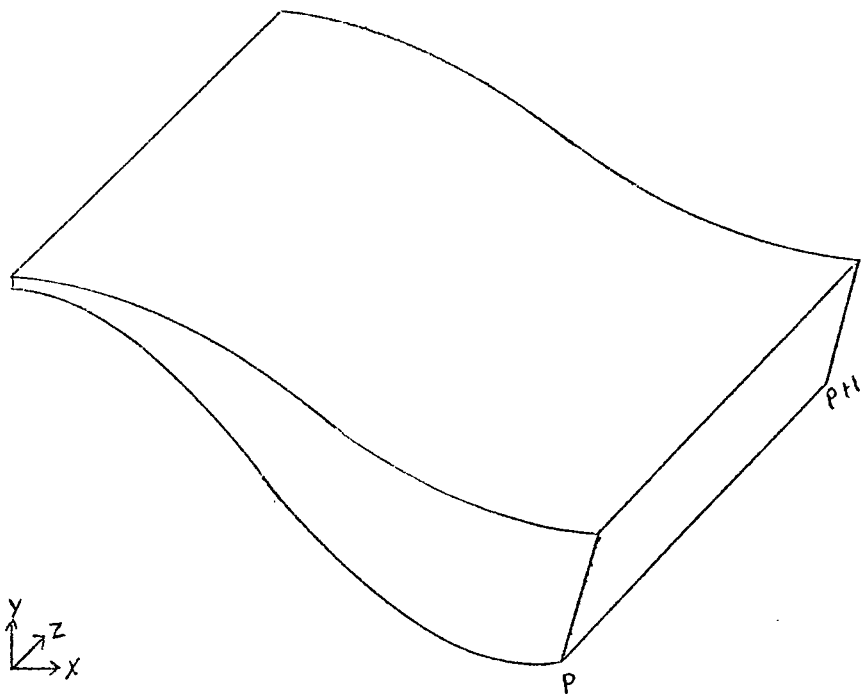

Figure 6
Fluted Surface Showing Coordinates for Downward Flow

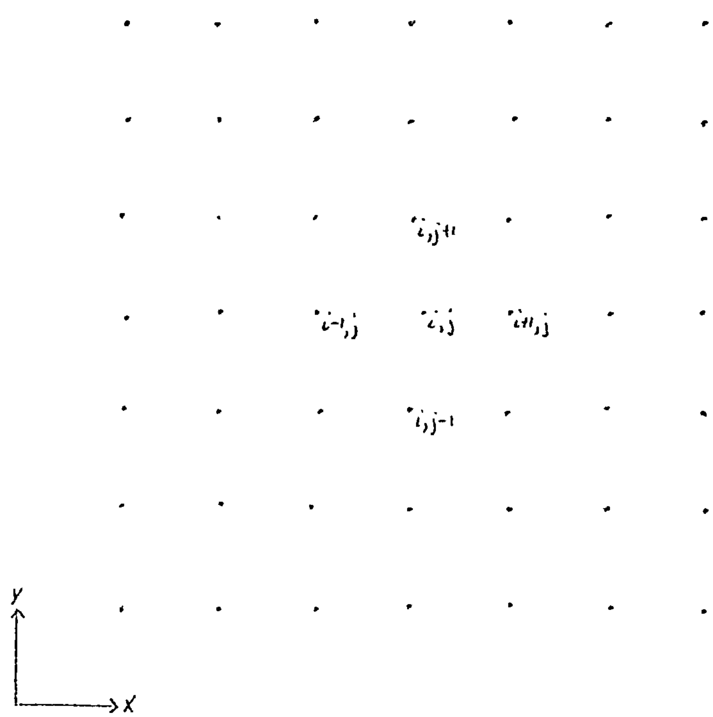

Figure 7
Grid System for Finite Differences

Figure 7):

$$\frac{\partial^2 U_z}{\partial x^2} \cong \frac{U_{i+1,j} - 2U_{i,j} + U_{i-1,j}}{(\Delta x)^2} \tag{27}$$

$$\frac{\partial^2 U_z}{\partial y^2} \cong \frac{U_{i,j+1} - 2U_{i,j} + U_{i,j-1}}{(\Delta y)^2} \tag{28}$$

If the grid is uniform in both directions, Δx and Δy are equal. Substituting equations (27) and (28) into equation (26) and solving for U_{ij}, the result is:

$$U_{i,j} = \frac{1}{4}\left(U_{i+1,j} + U_{i-1,j} + U_{i,j+1} + U_{i,j-1} + \frac{\rho}{\mu} g_z (\Delta x)^2\right) \tag{29}$$

Using the successive over-relaxation technique for solution, in order to obtain rapid conversion,

$$U_{i,j}^{(n+1)} = U_{i,j}^{(n)} + \omega\left[\frac{1}{4}\left(\frac{g_z (\Delta x)^2}{\mu}\rho + U_{i-1,j} + U_{i+1,j} + U_{i,j-1} + U_{i,j+1}\right) - U_{i,j}^{(n)}\right] \tag{30}$$

The factor ω is an acceleration parameter which varies from 1.0 to 2.0. A value of 1.0 for ω reduces equation (30) to equation (29) and results in slow convergence, while higher values bring about faster convergence, up to a limiting value of ω, which varies with the system of equations and the boundaries. If a value of ω is chosen that is too high, the system of equations will not converge. It was found that a relaxation parameter (ω) of 1.9 enabled convergence to be obtained in about 1/4 the number of iterations required for $\omega = 1.0$. However, the system did not always converge for $\omega = 1.9$, particularly when the film was very thin in the valley. This is probably due to the coarseness of the grid ($\Delta x = 0.0004$). In these cases, $\omega = 1.0$ was used to obtain convergence.

Once the velocity at each of the grid points was determined, the flow rate was found by integrating the velocity over the flow area.

In this way the downward flow rate for a known profile was determined. Let the subscripts p and p + 1 represent the downward flow rate and rate of condensation (as determined above) for a given pair of profiles. Further, let m represent the total rate of condensation over the entire flute. This is the same as the m used in equation (13), which deals with intermediate values of the rate of condensation at points along the flute. Then the vertical separation distance between the two profiles can be determined by the use of a mass balance:

$$\Delta z = \frac{W_{p+1} - W_p}{(m_p + m_{p+1})/2} \,. \tag{31}$$

In the case where the profile in question is the closest one to the top of the condenser tube, p = 0; and the value of m_o is not known, while $W_p = 0$. However, the highest profile can be found thin enough that it should cause a negligible error if the position of this point is found by

$$z = W_1 / m_1 \tag{32}$$

Actually, the true value of z will be somewhat smaller than that found by equation (32), since the rate of condensation at the very top of the tube [m_p in equation (31)] is larger than m_1, but the distance found using equation is so small that the error is quite negligible.

Chapter IV

DEVELOPMENT OF MODIFIED MODEL

It is very simple to improve equation (20) in the original Gregorig method, since the metal surface's shape is known. Thus $\Delta\phi$ can be calculated directly, rather than calculating R_a and using the geometric approximation of equation (20) to determine it. The value of $\Delta\phi$ can be found by using Figure 8. Let D_1 represent the slope of the surface at point 1 and D_2 represent the slope at point 2.

Then
$$\phi_1 = -\tan^{-1}(1/D_1) \tag{33}$$

$$\phi_2 = -\tan^{-1}(1/D_2) \tag{34}$$

thus
$$\Delta\phi = \phi_2 - \phi_1 = -\tan^{-1}(1/D_2) + \tan^{-1}(1/D_1). \tag{35}$$

Equation (10), when integrated over x, yields

$$q(x \rightarrow x+\Delta x) = \frac{1}{\Delta x}\int_{x}^{x+\Delta x} -kA\left(\frac{dT}{dy}\right)_0 dx. \tag{36}$$

Since the film thickness and thus the derivative $\left(\frac{dT}{dy}\right)_0$ is a function of x, it becomes necessary to determine an average value of $\left(\frac{dT}{dy}\right)_0$ in order to invoke the mean value theorem to integrate equation (36). Thus the integral may be changed to

$$q(x \rightarrow x+\Delta x) = \frac{kA(-\Delta T)}{h_{avg}}. \tag{37}$$

Now, provided that h is not changing very rapidly, it should be possible to use the value of h at x in equation (37) instead of an average

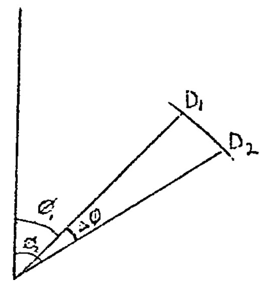

Figure 8
Profile of Metal Surface Showing
Determination of $\Delta\phi$

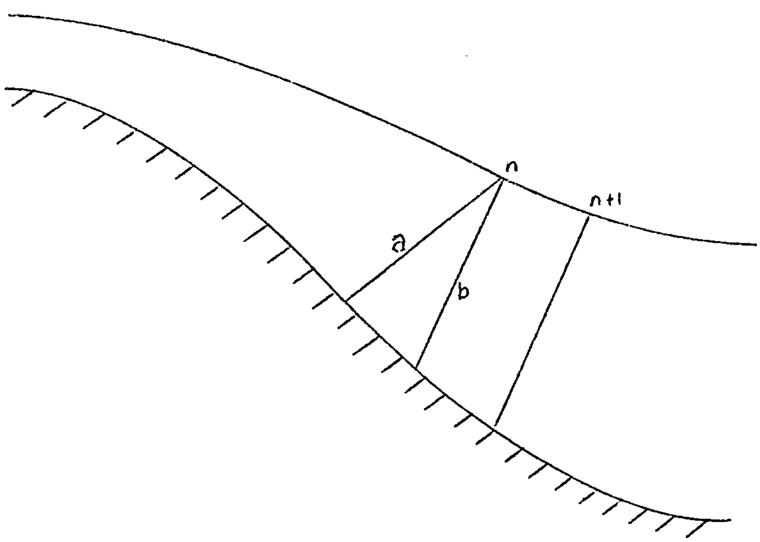

Figure 9
Deviation of Film Thickness as Determined
by Gregorig from True Thickness

a actual length for heat transfer
b length used by Gregorig for
heat transfer

h. However, the value of h used in equations (4) and (12) in Gregorig's method is not determined rigorously. Clearly, if one represents $\frac{dT}{dy}$ by $\frac{\Delta T}{h}$, h must be normal to the condensing surface. However, in Gregorig's method, while the h calculated in equation (23) is approximately perpendicular to the surface for thin films (while the two liquid surfaces are nearly parallel), as the trough fills this value becomes less and less accurate. In addition, when the trough fills appreciably, the distance from the peak to the valley along the free surface is much shorter than the distance along the metal surface; so the integration step along the free surface is not associated with the proper portion of the metal surface, as shown in Figure 9. Since the film thickness for the horizontal flow should also be measured perpendicular to the surface, any improvement in the height for heat transfer should, likewise, result in an improvement in calculating the horizontal flow rate.

Since the area for heat transfer between the two lines representing the boundaries of the integration increment is not constant, but decreases as one proceeds from the free surface through the film, it is necessary to change equation (12). The volume under consideration is wedge-shaped, as shown in Figure 10.

The rate of heat transfer is

$$q = -k\, dA \frac{dT}{dh}, \tag{38}$$

where $dA = (ah + b)\, dz$.

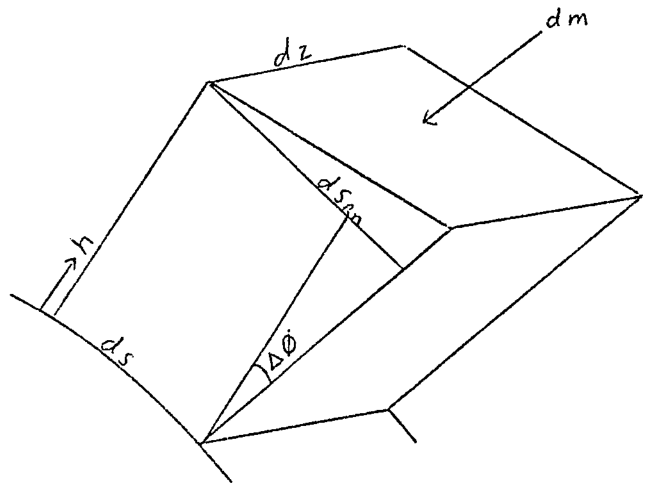

Figure 10
Actual Area for Heat Transfer

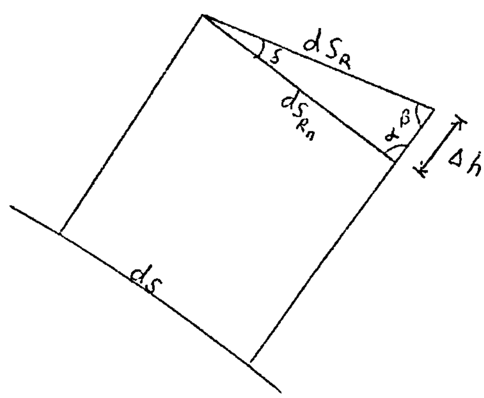

Figure 11
Distance along Free Surface Associated with Δs on Metal Surface

Then, making the substitution,

$$dq = -k\,dz\,(ah+b)\frac{dT}{dh}\,. \tag{39}$$

Assuming that the temperature driving force is uniform and integrating,

$$dq = \frac{a k\,dz\,(-\Delta T)}{\ln(ah+b)-\ln(b)}. \tag{40}$$

Since there is no subcooling,

$$dq = \lambda\,\Delta m_n\,dz \tag{41}$$

or

$$\Delta m_n = \frac{ak(-\Delta T)/\lambda}{\ln(\frac{ah}{b}+1)}, \tag{42}$$

where $a = \Delta\phi$

$b = \Delta s$.

As shown in Appendix 2, the change in film thickness Δh may be calculated, as a first approximation, as

$$\Delta h = \Delta s_{Rn}\,\frac{\sin[\phi-\psi+\frac{1}{2}(\Delta\phi-\Delta\psi)]}{\sin[\psi-\phi-\Delta\phi+\frac{1}{2}(\pi+\Delta\psi)]}\,. \tag{43}$$

Equation (43) results in the calculation of the profile if the distance along the free surface increment is not affected by the change in film thickness. However, a change does occur, so it is necessary to make a further calculation (see Figure 11). From the cosine law,

$$\Delta s_R = \sqrt{(\Delta h)^2+(\Delta s_{Rn})^2-2\Delta h\,\Delta s_{Rn}\cos(\tfrac{\pi+\Delta\phi}{2})}\,. \tag{44}$$

A better approximation of Δh than equation (43) can now be found, using Δs_R as found in equation (44) and the law of sines:

$$\Delta h = \frac{\Delta s_R\,\sin[\phi-\psi+\frac{1}{2}(\Delta\phi-\Delta\psi)]}{\sin[\frac{\pi+\Delta\phi}{2}]} \tag{45}$$

It has been found that when the radius of curvature of the free surface is changing rapidly, equation (20) does not yield an accurate estimate of $\Delta\Psi$, which is very important, since Ψ is used to determine whether convergence has been obtained. Instead, it has been found that $\Delta\Psi$ can be better represented by

$$\Delta\Psi = \frac{\Delta s_R}{(|R_n| + |R_{n+1}|)/2} \text{ (sign of } R_{n+1}\text{)}. \tag{46}$$

Rather than using Δs in equation (19), it is now necessary to use the free surface increment Δs_R, since the integration is performed along the free surface:

$$R_{n+1} = \frac{1}{1/R_n - \frac{3\mu m_{n+1}}{h_n^3 \rho \sigma} \Delta s_R} . \tag{47}$$

The numerical procedure for the new model is:

1) Chose h_o, R_o, and Δs.

2) Determine $\Delta\phi$ from equation (35).

3) Find Δm_n from equation (42) and set

$$m_{n+1} = m_n + \Delta m_n$$

4) Solve equation (19) for R_{n+1}, using $\Delta s_{Rn} = \Delta s + h\Delta\phi$ in place of Δs.

5) Obtain $\Delta\Psi$ from equation (46).

6) Determine Δh from equation (43).

7) Get Δs_R from equation (44).

8) Solve equation (47) for R_{n+1}.

9) Determine $\Delta\Psi$ from equation (46).

10) Determine Δh from equation (45).

11) Continue to move along the surface until h goes negative, Ψ goes negative, or the center of the trough is reached. If convergence has not been reached, choose a different value of h and go back to step 2.

The method of determining the downward flow rate and vertical position of a given profile for the modified model is the same as that of the original Gregorig model.

Chapter V

NOTES ON THE TWO MODELS

The results of the predictions of the two models are, in general, of the same form. An important point of interest in the results is that the values of h_o associated with a given R_o are not necessarily unique. A plot of the relation between the two in a typical example is shown in Figure 12. This results in a variation in peak height as one proceeds down the tube that is not monatonically increasing, as one would expect, but oscillates, as in Figures 13-16. This unexpected behavior is probably fictional, a result of the computational scheme, although it is not clear what the source of the anomaly is. However, before discarding the method, it would be beneficial to determine the actual profile of condensate experimentally to make certain that the fluctuations do not actually occur in practice. As one closes in on the center of the spiral in Figure 12, which corresponds to the top of the condenser, the solution becomes very sensitive to the value of h_o that is chosen. However, after distances several feet down the tube, the solution may be largely insensitive to h_o.

It may be noted that the film thickness is generally not a minimum at the peak of the flute, but that the minimum occurs at a point along the side of the flute. This occurs because the radius of curvature of the

Peak Values of Radius of Curvature and Film Thickness

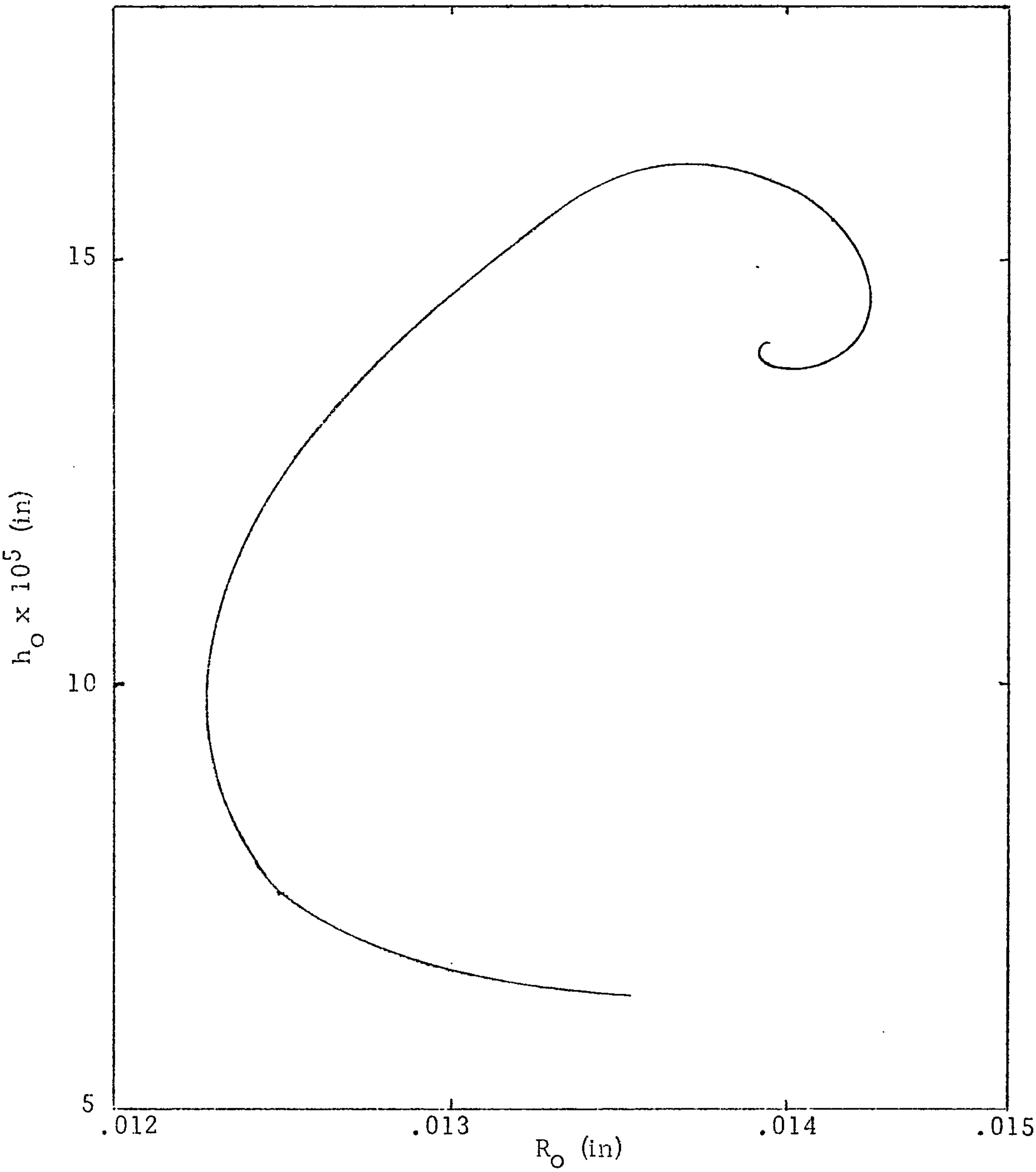

Figure 12

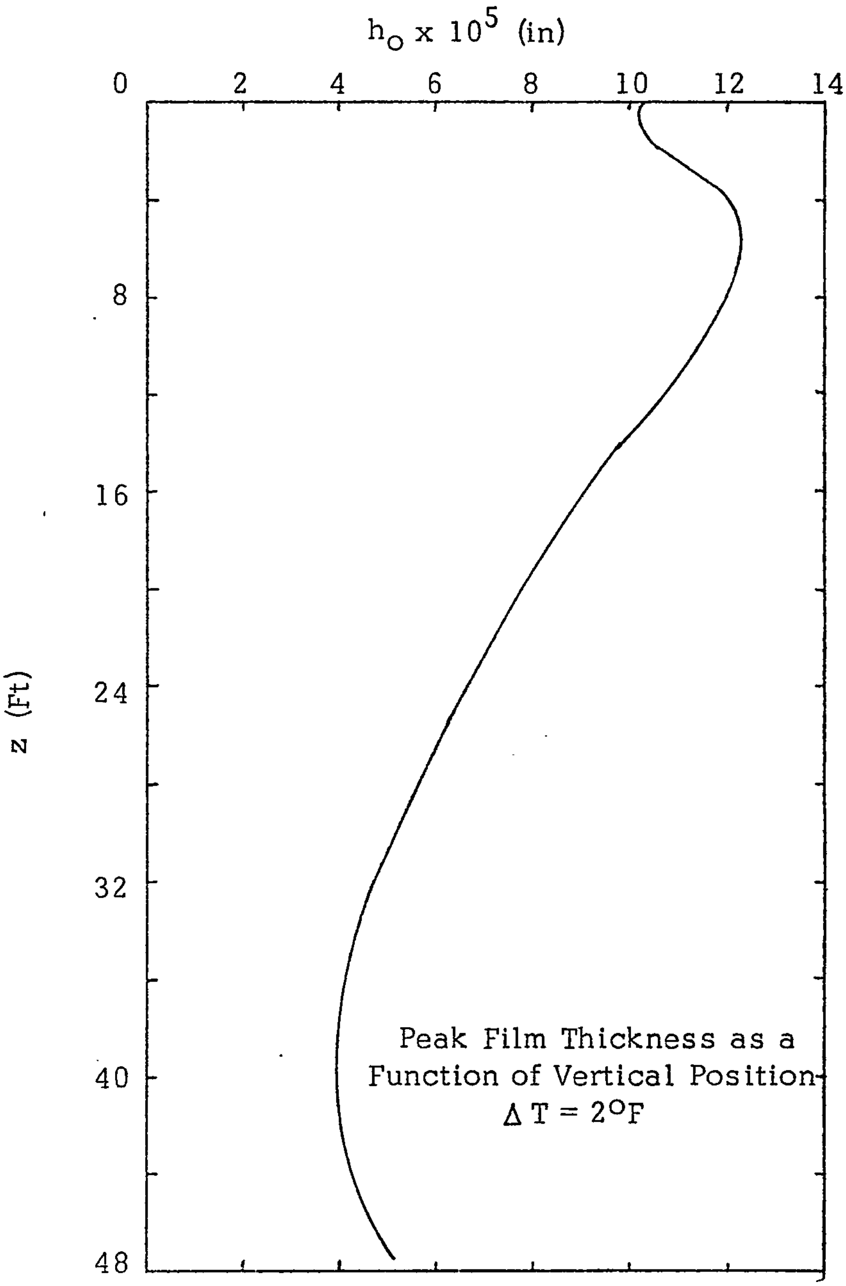

$h_o \times 10^5$ (in)
0
2
4
6
8
10
12
14
8
16
24
32
40
48
z (Ft)
Peak Film Thickness as a
Function of Vertical Position
$\Delta T = 2^oF$

Figure 13

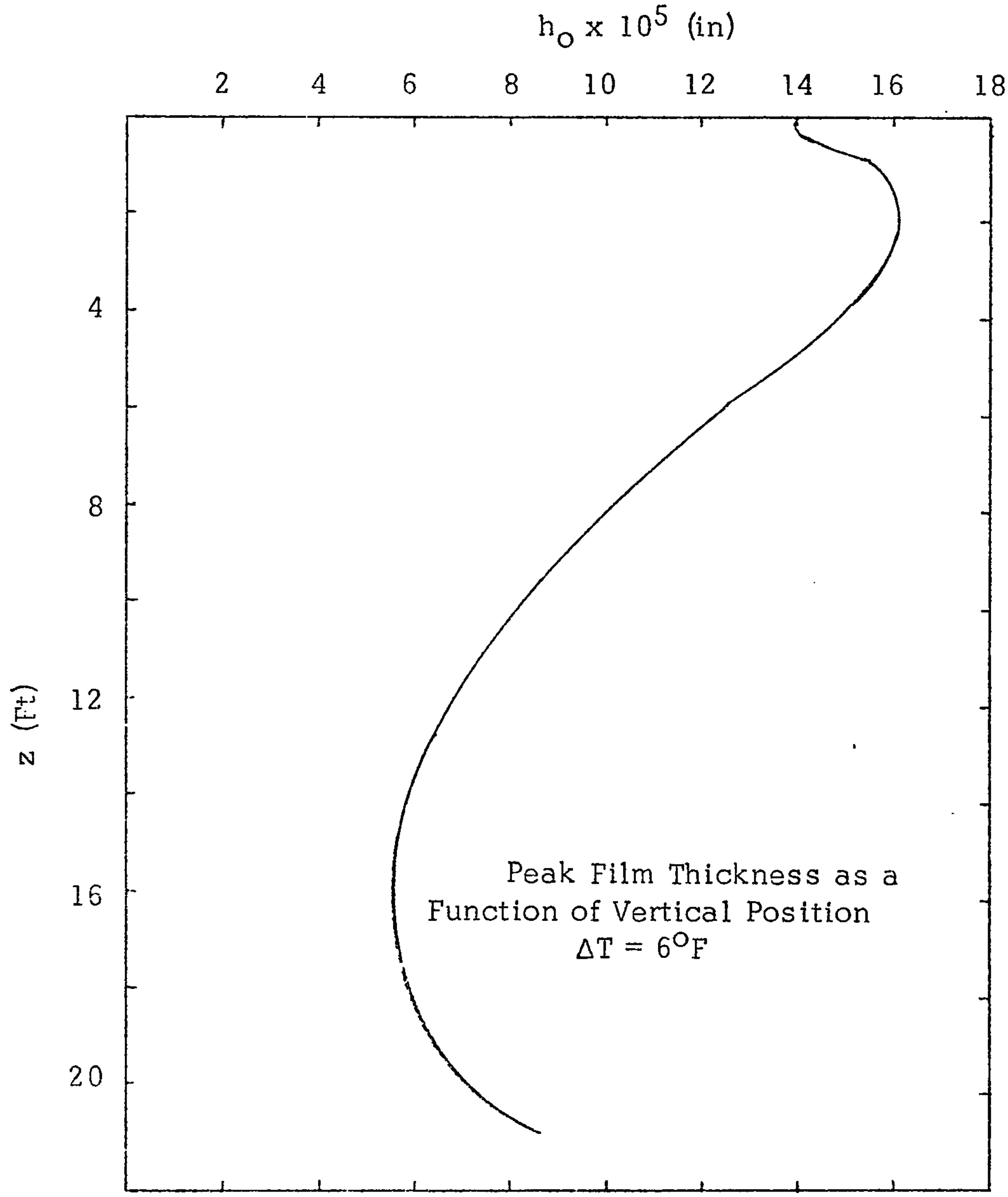

$h_o \times 10^5$ (in)
2
4
6
8
10
12
14
16
18
z (Ft)
4
8
12
16
20
Peak Film Thickness as a Function of Vertical Position
$\Delta T = 6^oF$

Figure 14

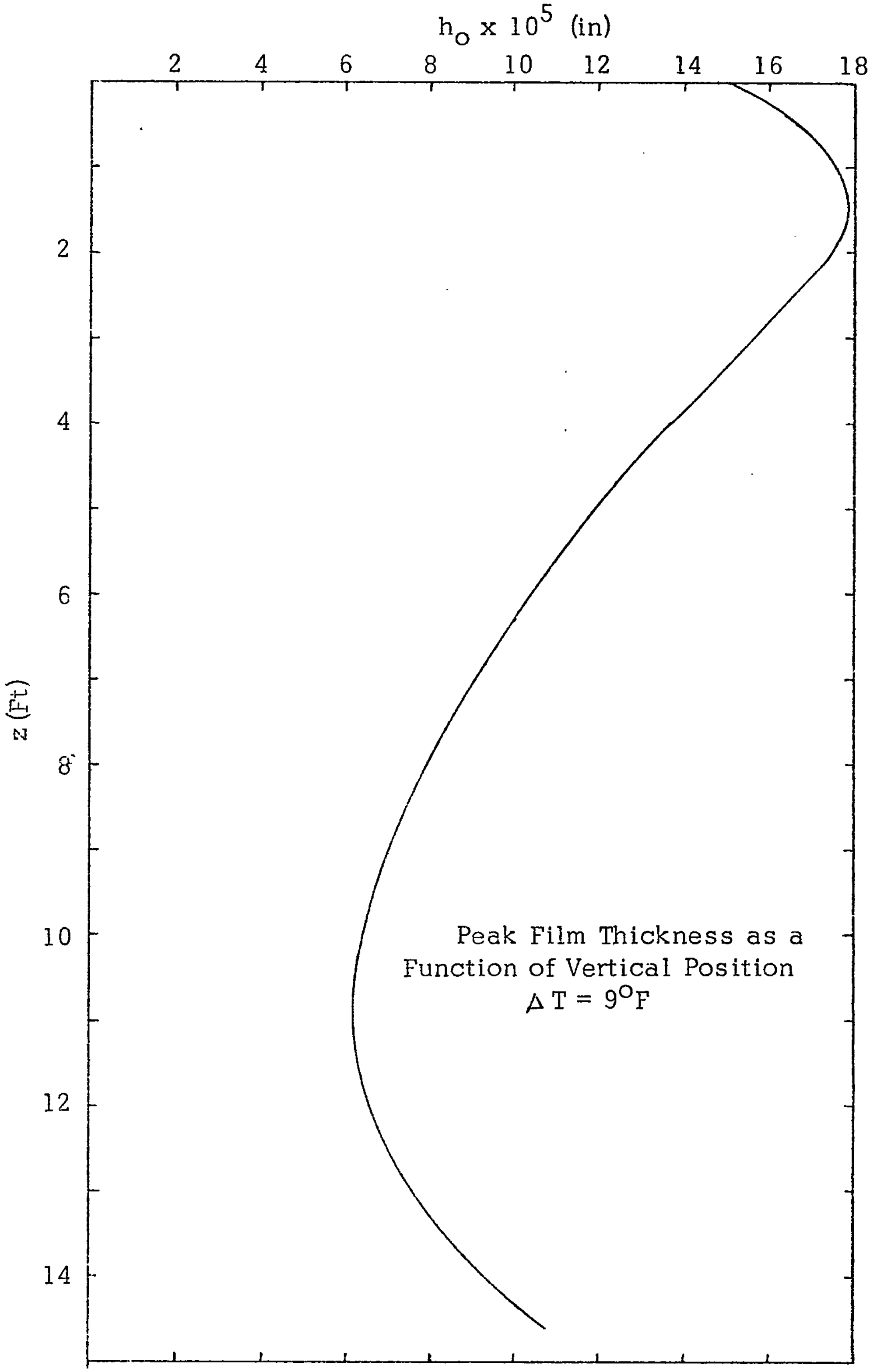
h_o x 10^5 (in)
2
4
6
8
10
12
14
16
18
z (Ft)
2
4
6
8
10
12
14
Peak Film Thickness as a
Function of Vertical Position
ΔT = 9°F

Figure 15

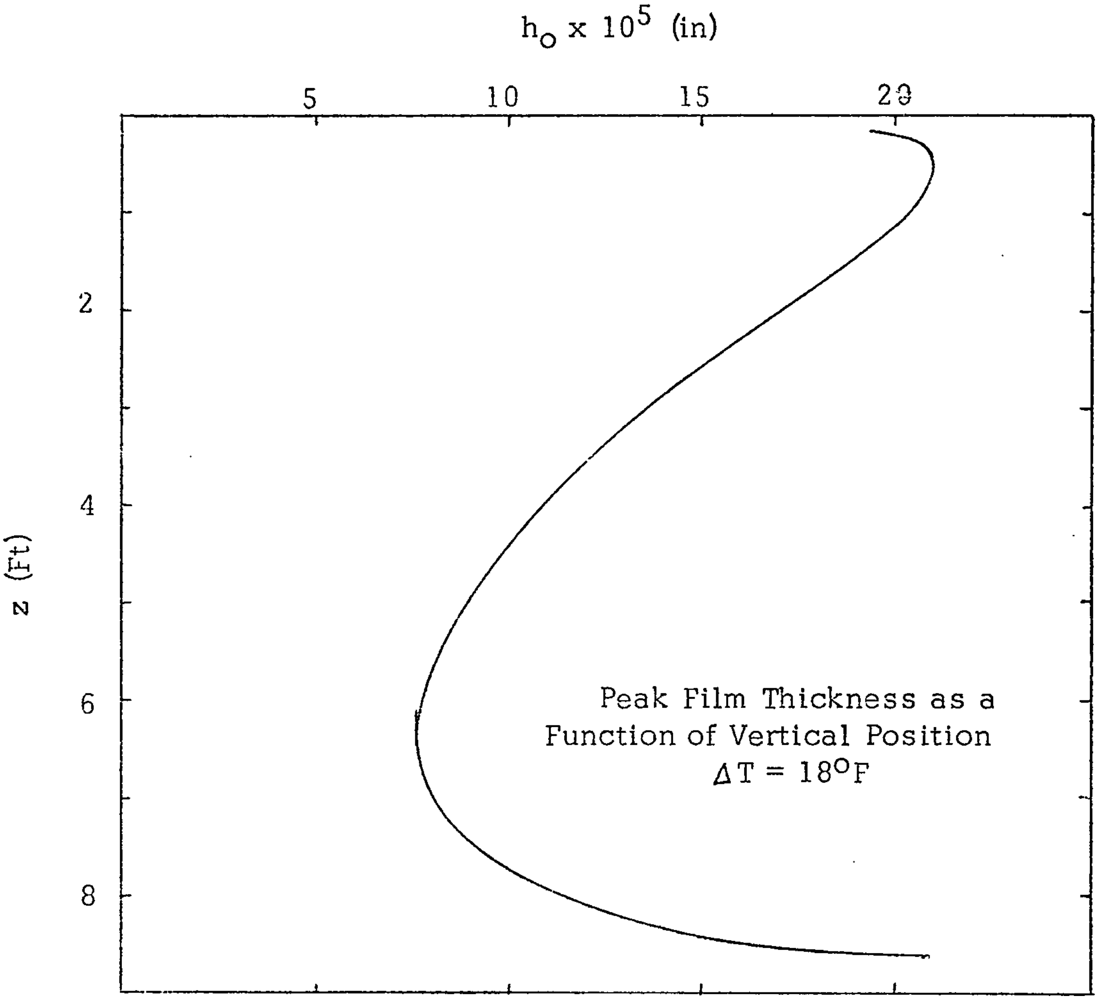

$h_o \times 10^5$ (in)
5
10
15
20
2
4
6
8
z (Ft)
Peak Film Thickness as a
Function of Vertical Position
$\Delta T = 18^oF$

Figure 16

metal surface increases faster than the radius of curvature of the free surface. Since, in some cases, the radius of curvature of the free surface is tighter than the radius of curvature of the metal surface, it is unavoidable that the film thickness will decrease.

As with any finite integration scheme, the method is somewhat sensitive to the size of the steps used in integration along the flute. However, this dependence is not very strong as long as the steps are about 1% or less of the period of the flute.

Chapter VI

COMPARISON OF THE MODELS

The two models were compared for predicting the heat transfer in the condensate film on a metal profile (see Figure 17) of:

$$y = 0.012 \cos\left(\frac{x\pi}{0.04}\right) + 0.012 , \tag{48}$$

Local heat transfer coefficients as functions of the vertical position in the tube for temperature driving forces of 2, 6, 9, and 18 degrees F are shown for the original and modified Gregorig methods in Figures 18-21, and compared to those predicted by the Nusselt (13) equation. It may be noted that both methods predict that the heat transfer coefficient decreases very slowly over most of the tube length, as opposed to the Nusselt prediction. This is a direct result of the effect of surface tension, which maintains a film thickness in the peak region which does not change substantially until flooding occurs. It is apparent that the original method predicts local heat transfer coefficients that are very close to those predicted by the new method near the top of the condenser; but, as the film thickness increases, the heat transfer coefficient determined by the original method falls off much more rapidly. In addition, the sharp decrease in heat transfer coefficient, indicative of flooding the grooves, occurs appreciably earlier in the original method. The primary difference between the two methods, the different means of measuring

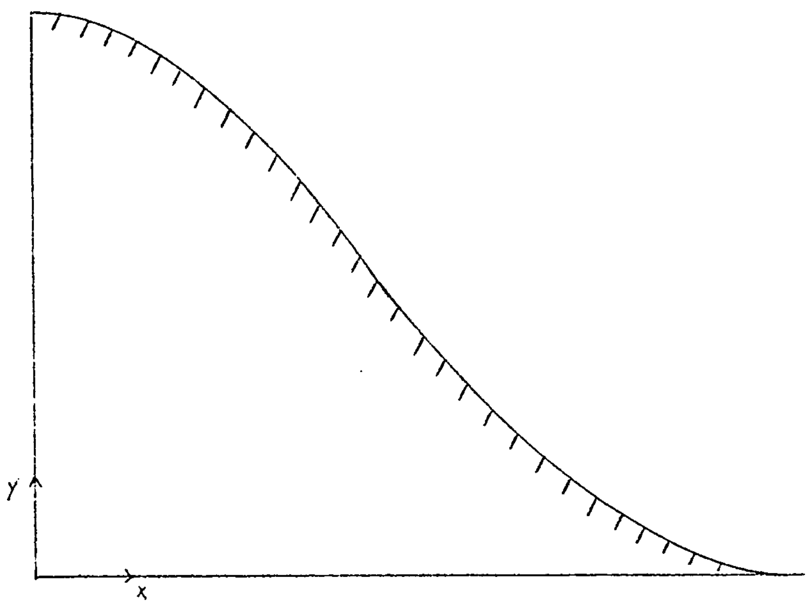

Figure 17
Profile of Sinusoidal Condensing Surface

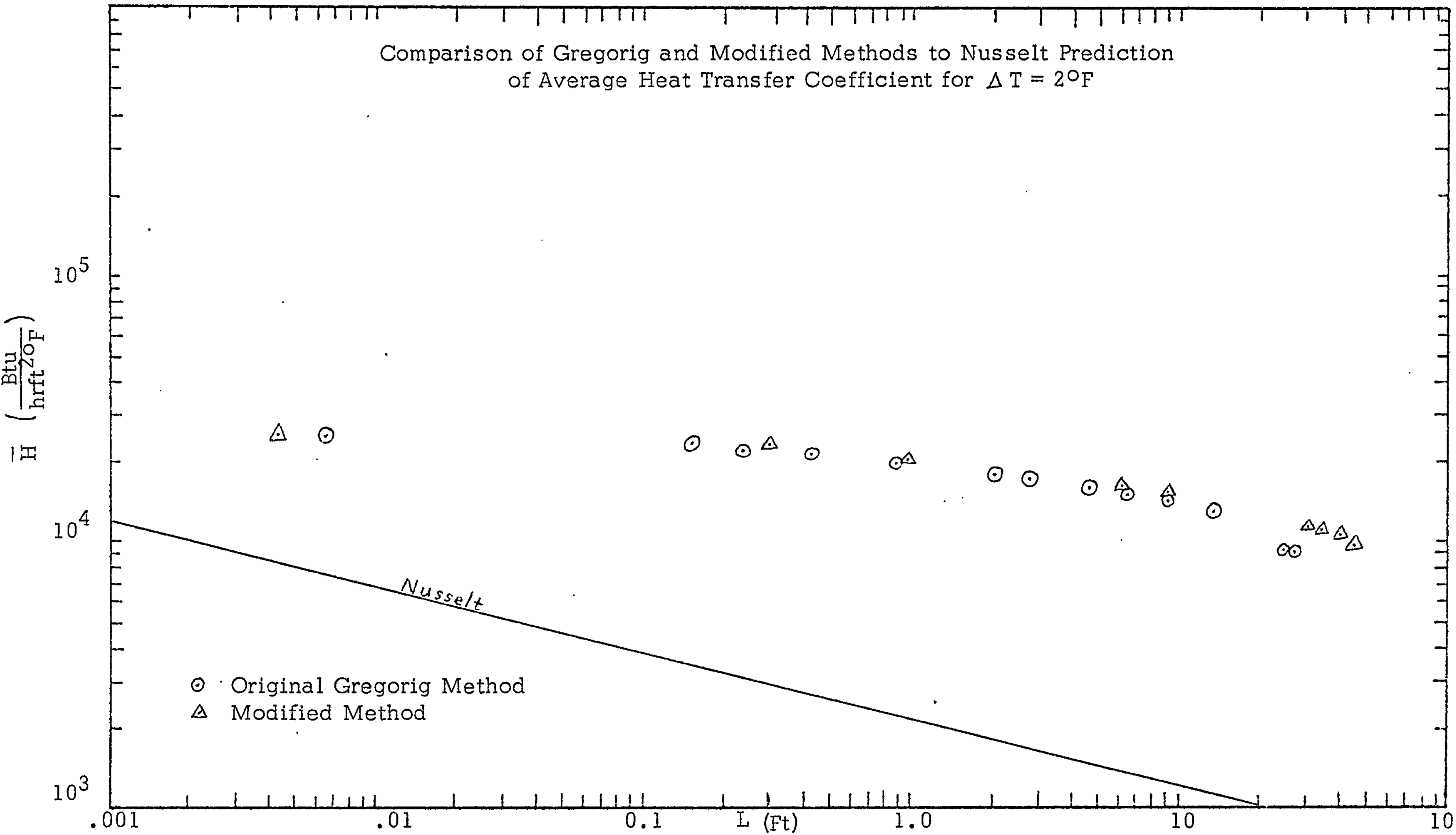
Comparison of Gregorig and Modified Methods to Nusselt Prediction
of Average Heat Transfer Coefficient for $\Delta T = 2^{\circ}F$
$\bar{H}\ \left(\frac{Btu}{hrft^2\,{}^{\circ}F}\right)$
10^5
10^4
10^3
Nusselt
Original Gregorig Method
Modified Method
.001
.01
0.1
1.0
10
100
L (Ft)

Figure 18

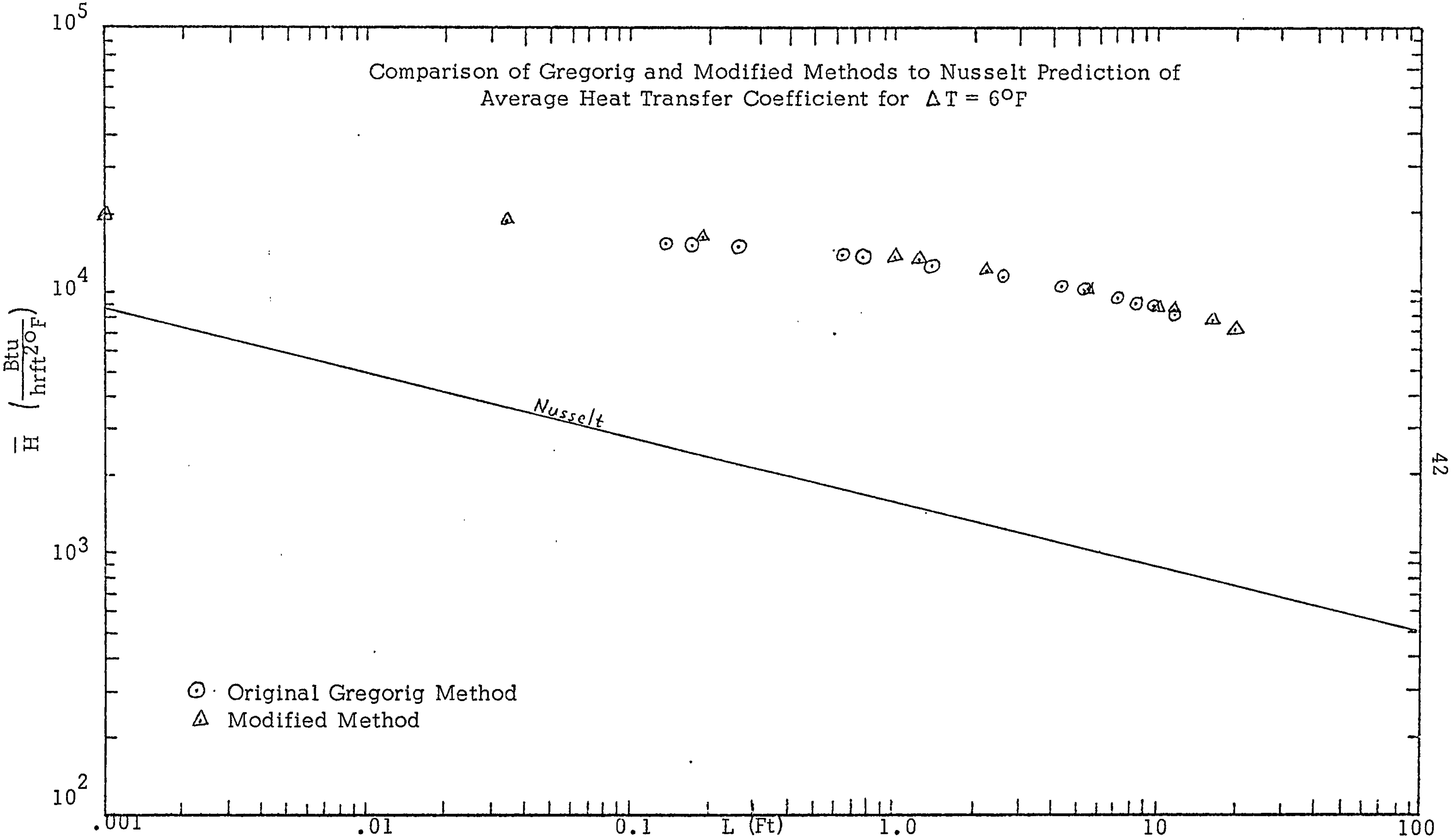

Comparison of Gregorig and Modified Methods to Nusselt Prediction of Average Heat Transfer Coefficient for $\Delta T = 6^{o}F$
10^5
10^4
10^3
10^2
$\bar{H}\ \left(\frac{Btu}{hrft^2\,{}^oF}\right)$
Nusselt
Original Gregorig Method
Modified Method
.001
.01
0.1
1.0
10
100
L (Ft)

Figure 19

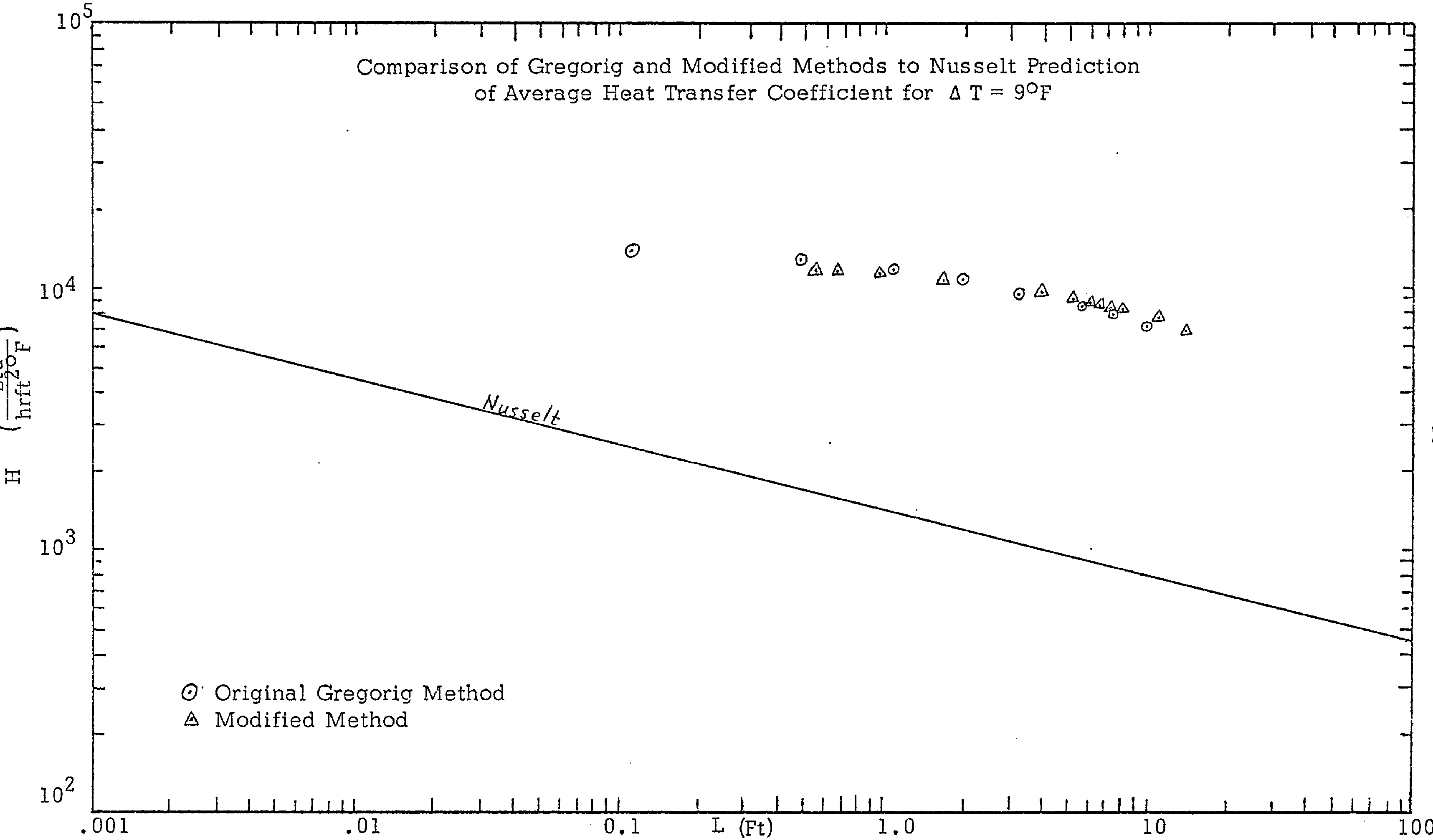
Comparison of Gregorig and Modified Methods to Nusselt Prediction
of Average Heat Transfer Coefficient for Δ T = 9°F
Nusselt
Original Gregorig Method
Modified Method
10^5
10^4
10^3
10^2
.001
.01
0.1
1.0
10
100
L (Ft)
H
Figure 20

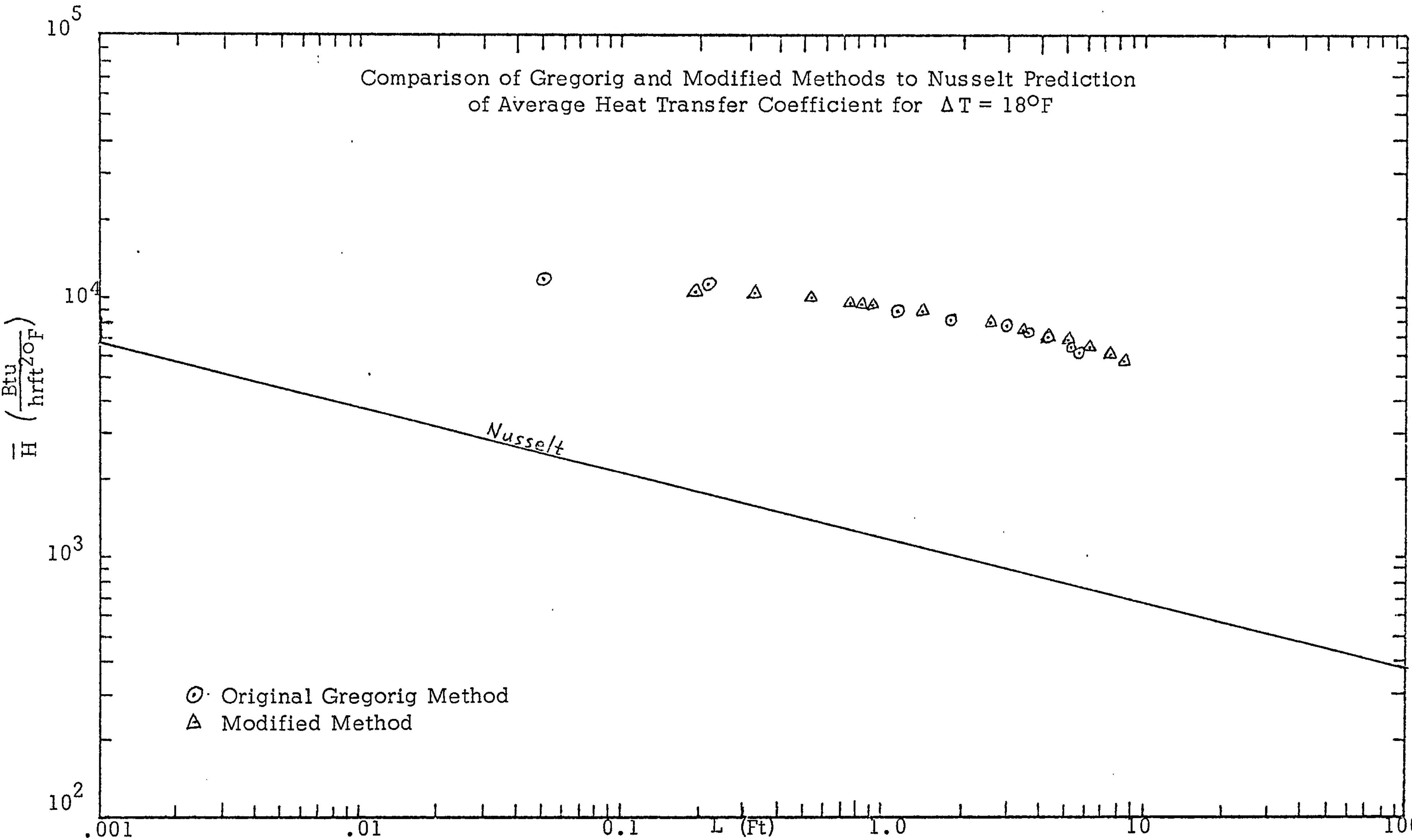

Comparison of Gregorig and Modified Methods to Nusselt Prediction
of Average Heat Transfer Coefficient for $\Delta T = 18^oF$
10^5
10^4
10^3
10^2
$\overline{H}\ \left(\frac{Btu}{hrft^2\,^oF}\right)$
Nusselt
Original Gregorig Method
Modified Method
.001
.01
0.1
1.0
10
100
L (Ft)

Figure 21

the film thickness for heat transfer, would account for the difference between the two methods in the lower regions of the condenser, since the original method tends to predict more resistance to heat transfer than the new method. This is because the new method uses the shortest path through the film from a point on the free surface as the length for resistance to heat flow, while the original method uses a somewhat longer value for heat transfer. This discrepancy shows up most markedly as the trough fills. The two methods predict fairly close heat transfer coefficients over most of the range of tube lengths because the effects of the different ways of measuring film thickness are muted by the fact that the difference shows up most markedly in the trough when it is fairly full. At this point, the local heat transfer contributes very little to the horizontally-averaged value, it being about two orders of magnitude smaller than the peak rate of heat transfer.

A comparison of the profiles predicted by the two models at a vertical position of about 0.2 feet from the top of the condenser may be found using Figure 22. It may be noted that there is very little difference between the two -- the fact that the profile obtained using the original Gregorig method is slightly thicker than the modified result is accounted for by the fact that it is slightly farther down the condenser (0.024 feet), and thus the flow downward through it is greater. The most pronounced difference between the two methods, as noted in the discussion of the

Comparison of Condensate Profiles Determined by Gregorig and Modified Methods
for $\Delta T = 18^{\circ}$ at a Vertical Position 0.2 Feet Down from Top on Condenser

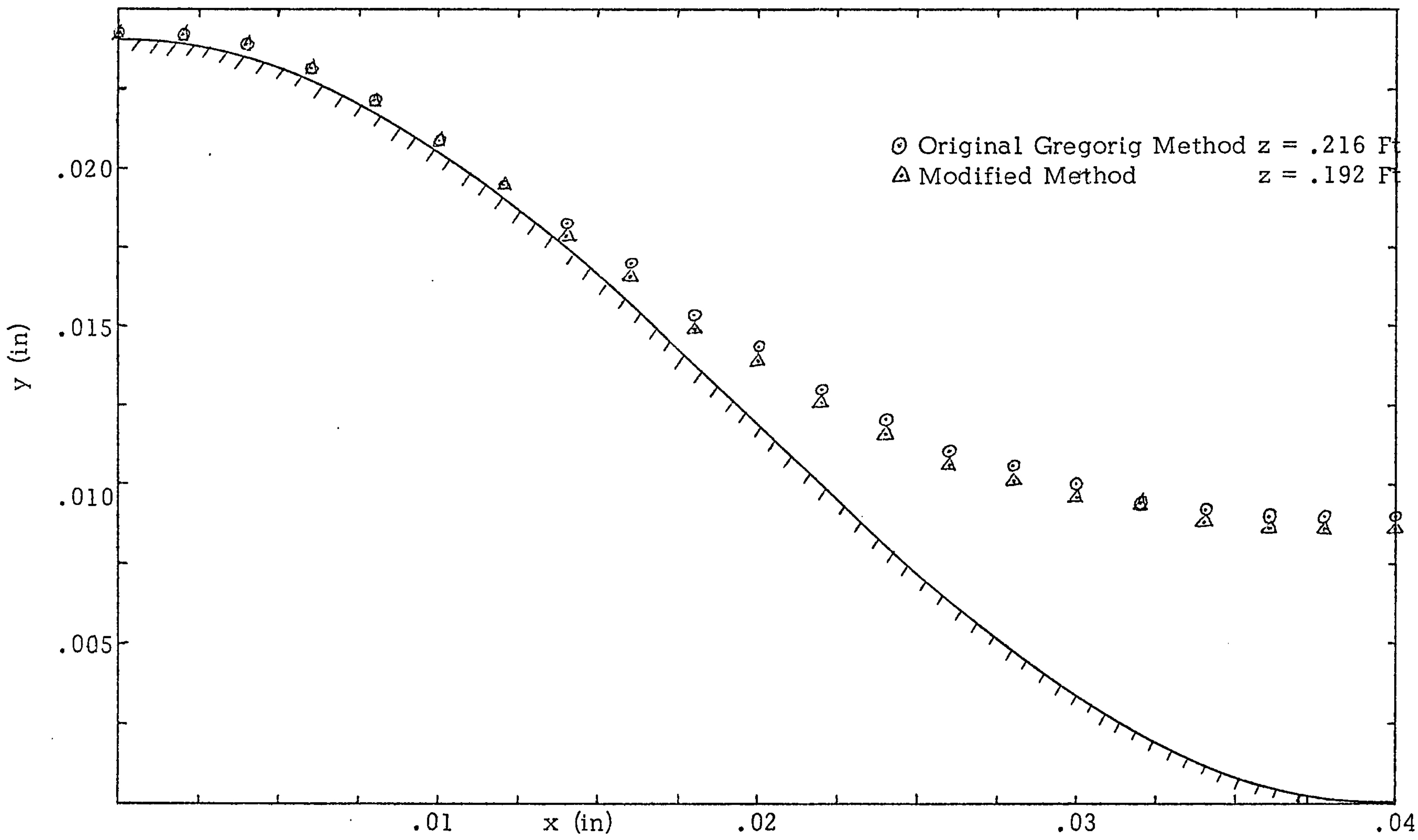

Figure 22

Comparison of Condensate Profiles Determined by Gregorig and Modified Methods
for $\Delta T = 18^{\circ}$ at a Vertical Position 4.5 Feet Down from Top of Condenser

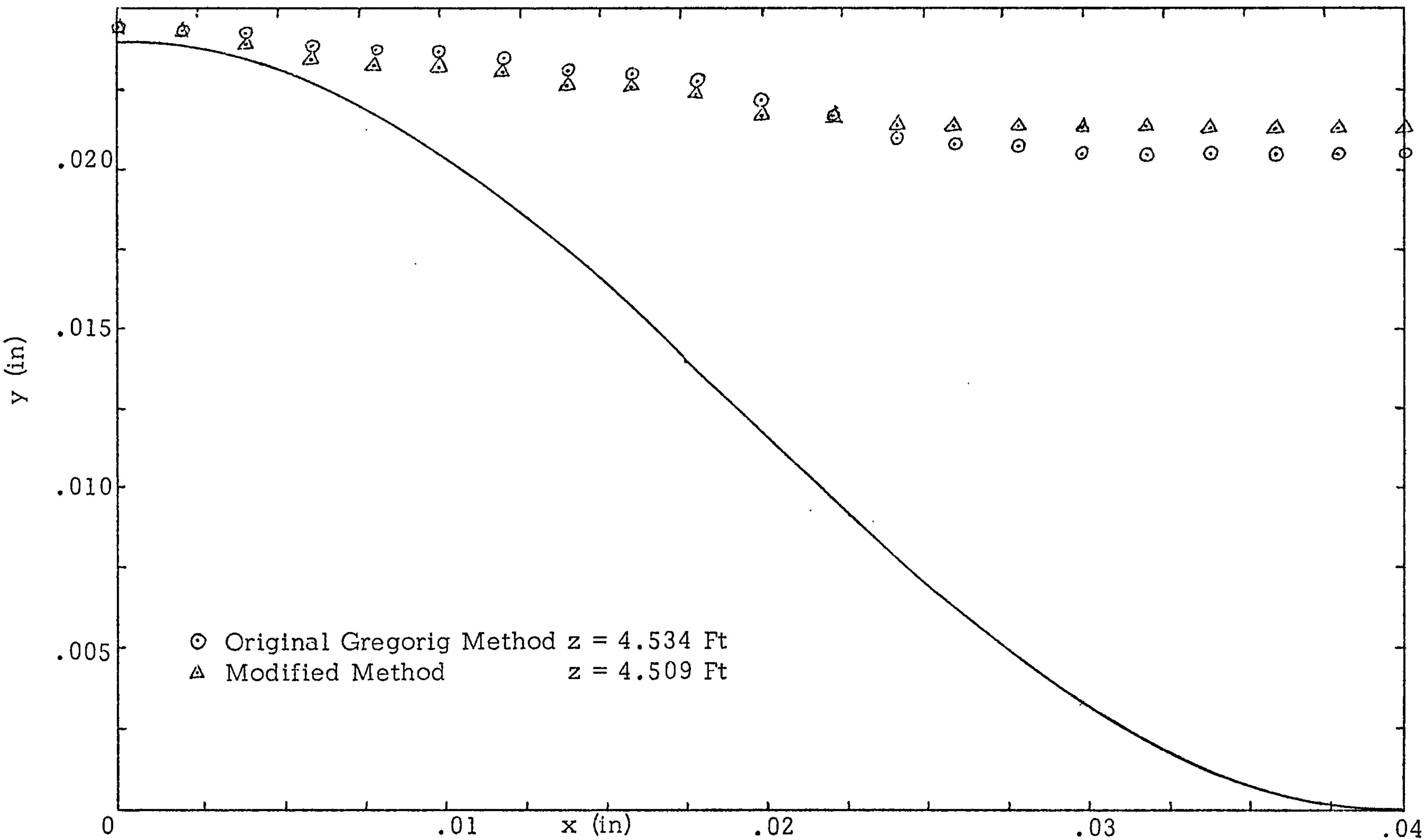

Figure 23

heat transfer coefficients, occurs in the region where flooding occurs. As seen in Figure 23, at a distance of 4.5 feet from the top of the condenser, there is a definite difference in the profiles. The modified method predicts a thinner film at the peak, with the free surface more nearly paralleling the condenser surface near the crest of the flute than does the original method. The film thickness near the center of the trough, then, must be thicker for the modified method in order to allow the condensate to run off. Since the whole concept of using surface tension to increase heat transfer is to reduce the film thickness at one point while increasing it at another, the result is that the modified model predicts that the heat transfer coefficient will be higher than does the original method. While this in itself does not appear significant, it would be possible to choose between the methods if the actual free surface were determined experimentally because of this difference in shapes.

Chapter VII

MODIFIED MODEL

The effect of changing the temperature driving force is shown in Figure 24 for the new model. Two facts are readily apparent; increasing the temperature driving force causes a decrease in the heat transfer coefficient, and increasing the driving force also causes flooding higher in the condenser. The first effect, that of lower heat transfer coefficient, is caused by the fact that the steam condenses at a higher rate than it can run off; and thus the film thickens as the driving force increases. Figure 25 shows the film thickness along the surface as a function of the driving force for a sample downward flow rate. It may be noted that the film at the peak is thinnest for the lowest ΔT and increases with ΔT, while the thickness in the valley is greatest for the low driving force and decreases for larger ΔT. The earlier onset of flooding with increased ΔT is also expected, since the higher the driving force, the more mass will be condensed, while the rate of vertical run-off is independant of ΔT except for the effect that changing the driving force has on the profile itself. Thus the liquid level should build up faster for a higher temperature driving force.

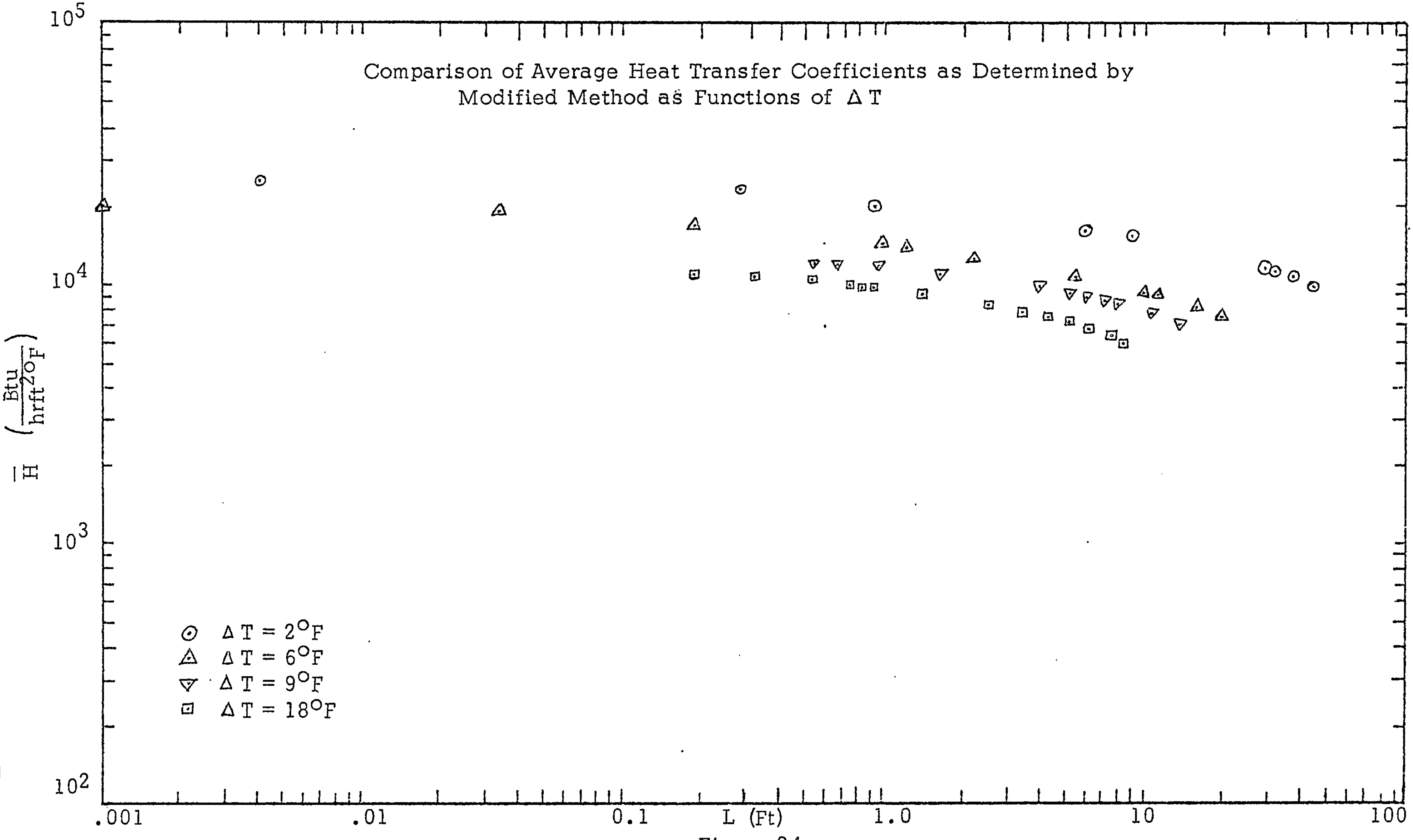

Comparison of Average Heat Transfer Coefficients as Determined by Modified Method as Functions of ΔT
10^5
10^4
10^3
10^2
$\bar{H}$ $\left(\frac{Btu}{hrft^2 {}^\circ F}\right)$
.001
.01
0.1
1.0
10
100
L (Ft)
$\Delta T = 2^\circ F$
$\Delta T = 6^\circ F$
$\Delta T = 9^\circ F$
$\Delta T = 18^\circ F$

Figure 24

Comparison of Film Thicknesses for Same Downward Flow (0.0000350 lb/sec) at $\Delta T = 2$ and $18^{o}F$

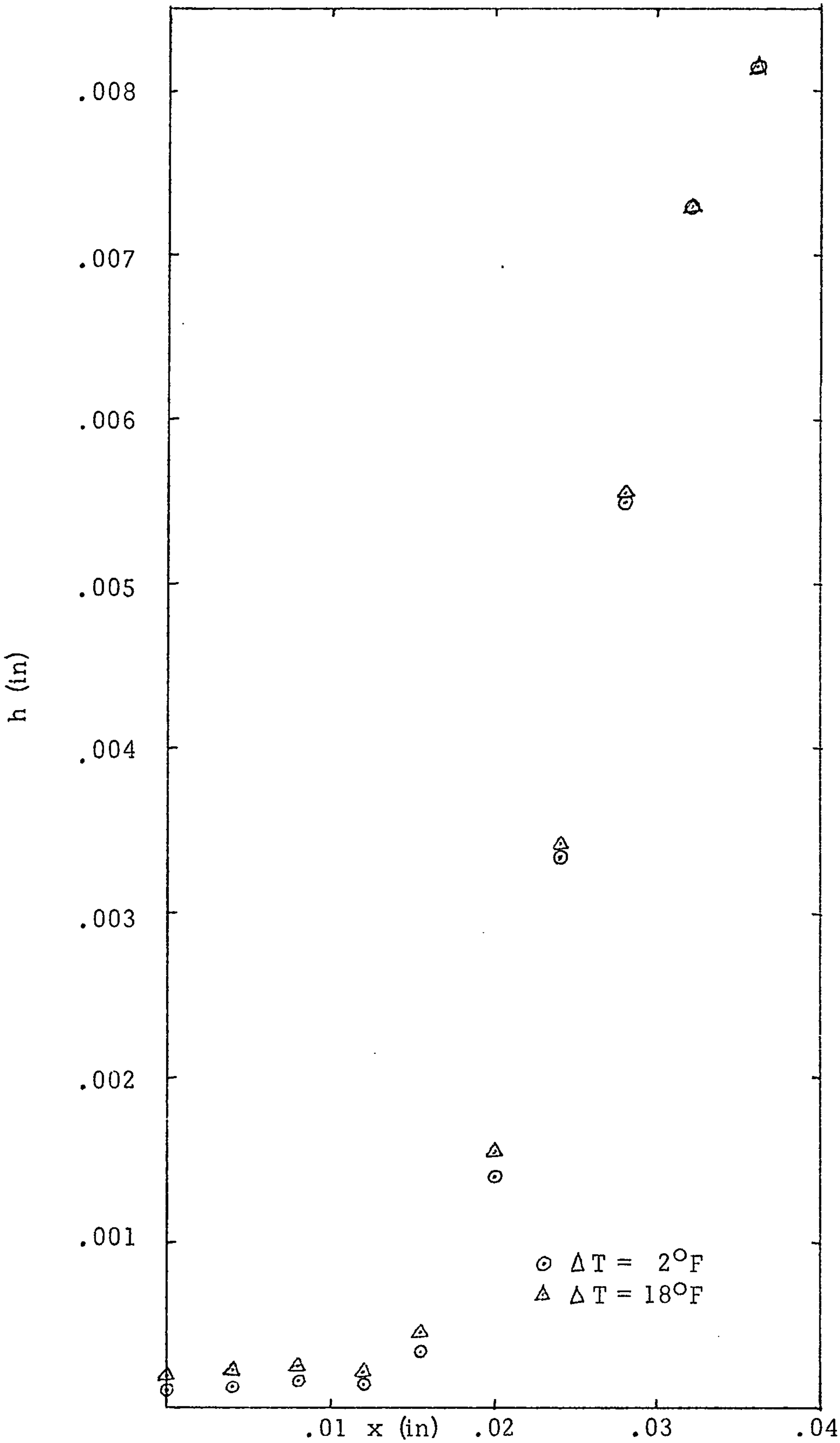

Figure 25

Varying the operating temperature has the effect shown in Figures 26 and 27. Increasing the temperature lowers the surface tension, but it also decreases the viscosity. It may be noted that the heat transfer coefficient increases with the operating temperature. This occurs because the viscosity, which influences both horizontal and vertical flows, allows for faster horizontal flow, since it offers less resistance, even though the pressure driving force (resulting from surface tension) is lower. In addition, the flute can drain faster because there is less viscous resistance. This enables depression of the flooding point to lower positions in the condenser by increasing the operating temperature. Thus increasing the operating temperature results in higher heat transfer coefficients and less danger of flooding the flutes. Increasing the operating temperature from $212^{\circ}F$ to $300^{\circ}F$ causes a depression of the flooding point to a position further down the condenser, and even in the region where the trough is only slightly filled, the heat transfer coefficient increases by about 15%. Decreasing the operating temperature to $100^{\circ}F$ brings about just the opposite: flooding occurs earlier and the heat transfer coefficient well above the flooding point is decreased by about 30%. It appears that the kinematic viscosity, which is used in determining the downward flow rate, is very sensitive to the operating temperature. The limiting factor in the heat transfer process for condensing steam appears to be the rate at which the condensate can run off, just as it is for

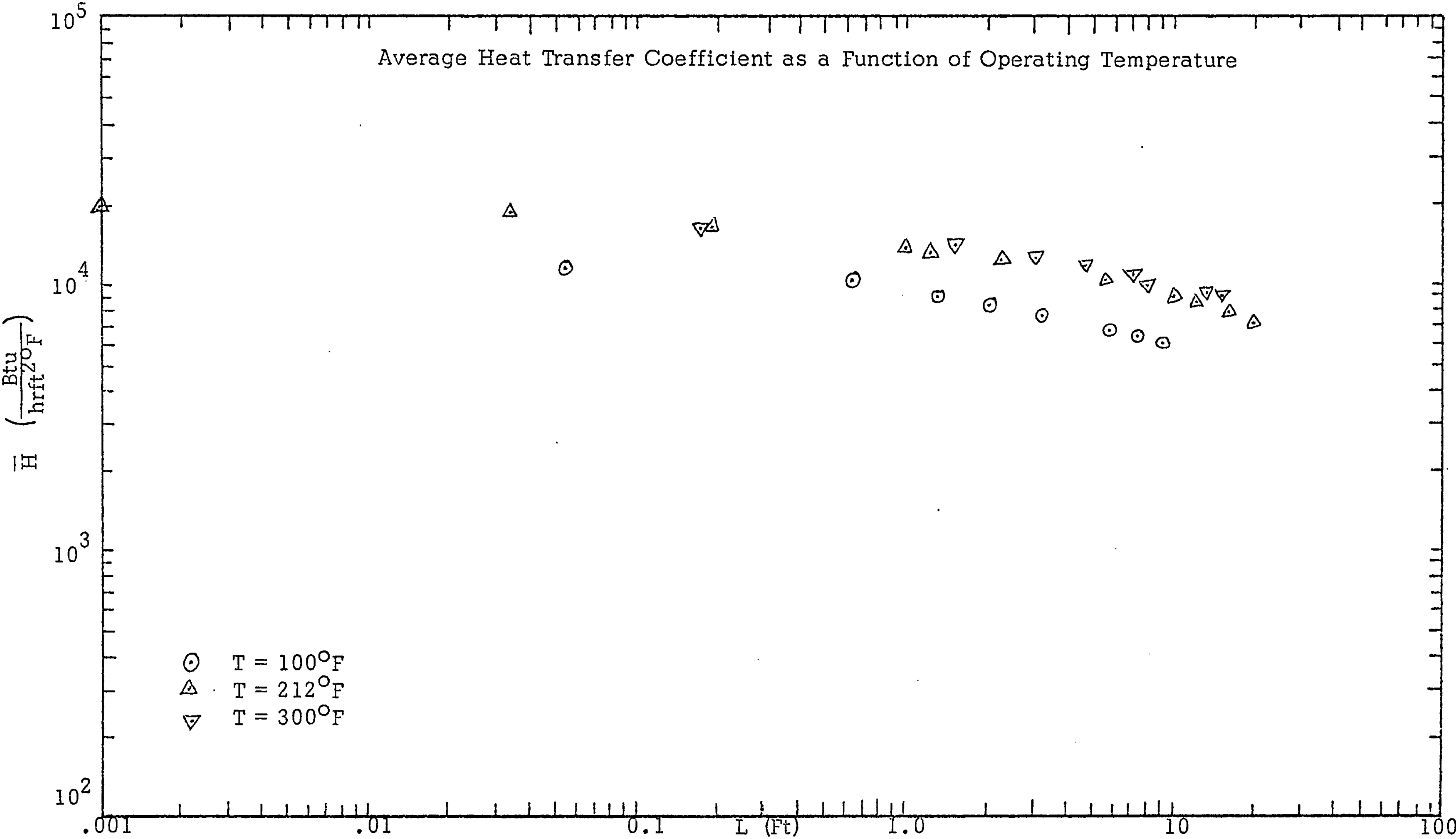

Average Heat Transfer Coefficient as a Function of Operating Temperature
10^5
10^4
10^3
10^2
$\overline{H}$ $\left(\frac{Btu}{hrft^2 {}^oF}\right)$
.001
.01
0.1
1.0
10
100
L (Ft)
T = 100°F
T = 212°F
T = 300°F

Figure 26

Local Heat Transfer Coefficient as a Function of Operating Temperature

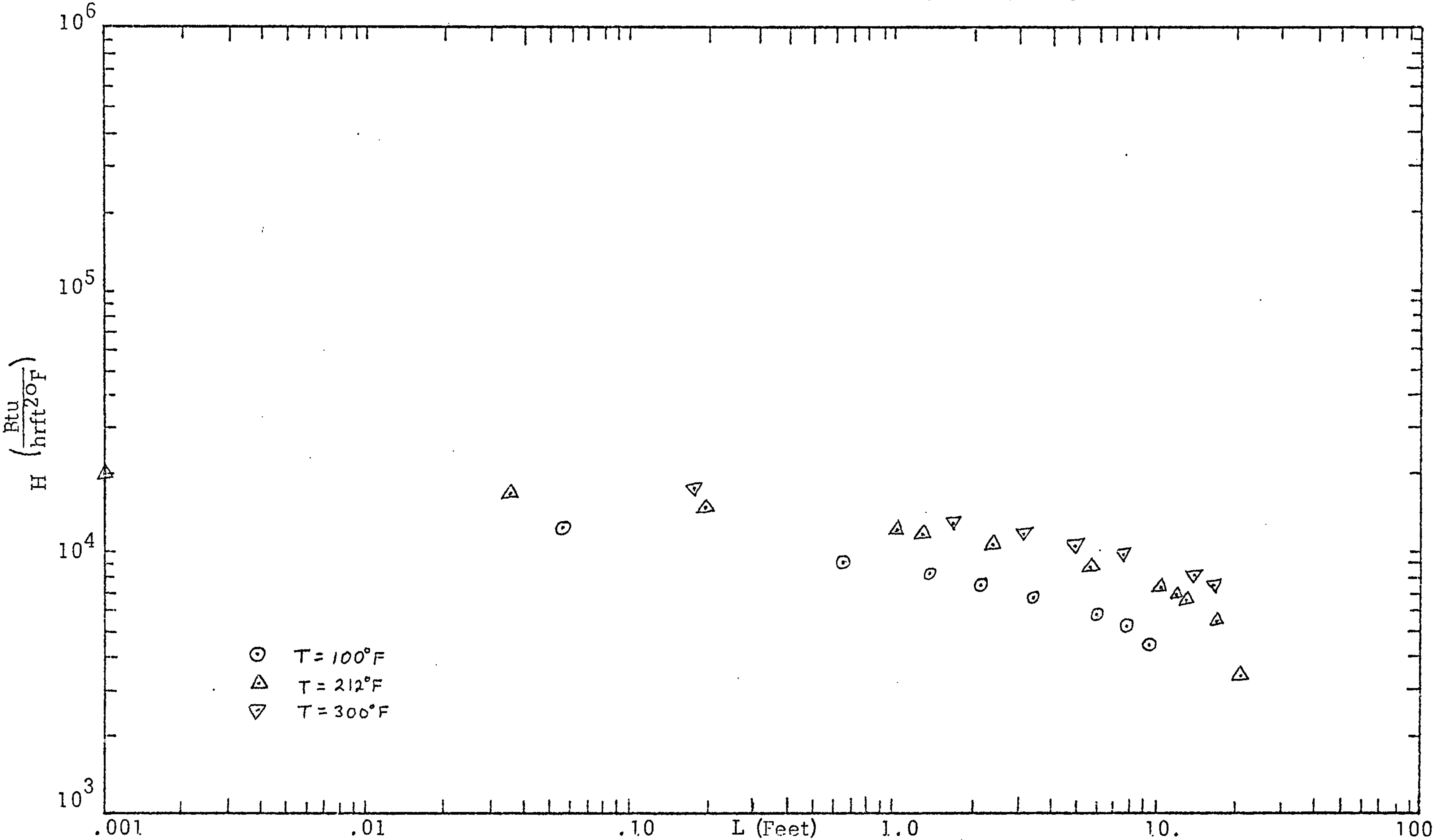

Figure 27

condensation on a smooth surface, but the difference is that the heat transfer coefficient has been increased dramatically by fluting the surface. The fact that the downward flow rate is the limiting factor for heat transfer is borne out by a comparison of the sizes of the horizontal and vertical velocities averaged over the film thickness, as shown in Figure 28. It may be noted that, except near the peak, the horizontal velocity is several orders of magnitude smaller than the downward flow rate. Plots of the variation of horizontal flow rate with position along the flute are shown in Figures 28-32 for various vertical positions. Aside from the expected maximum in the middle of the flute and zero velocity at the peak and valley, the most notable phenomenon on the curves is the fact that there is a "plateau" on the curve for $z = 0.034$ feet (Figure 28). This is a result of the fact that the radius of curvature of the free surface varies at a fairly constant rate in this region. In the other curves, the radius of curvature varies much faster, thus there is no flat region in those curves.

Plots of the local heat transfer coefficient as a function of the horizontal position are shown in Figures 33-37. Clearly, the heat transfer coefficient starts high at the crest, decreases slowly, then increases sharply before dropping off quickly. This increase in coefficient is a result of the film's being thinner along the side of the flute than at the

Horizontal Flow Rate Averaged Over Film Thickness as a Function of Position Along Flute Compared to Vertical Flow Rate

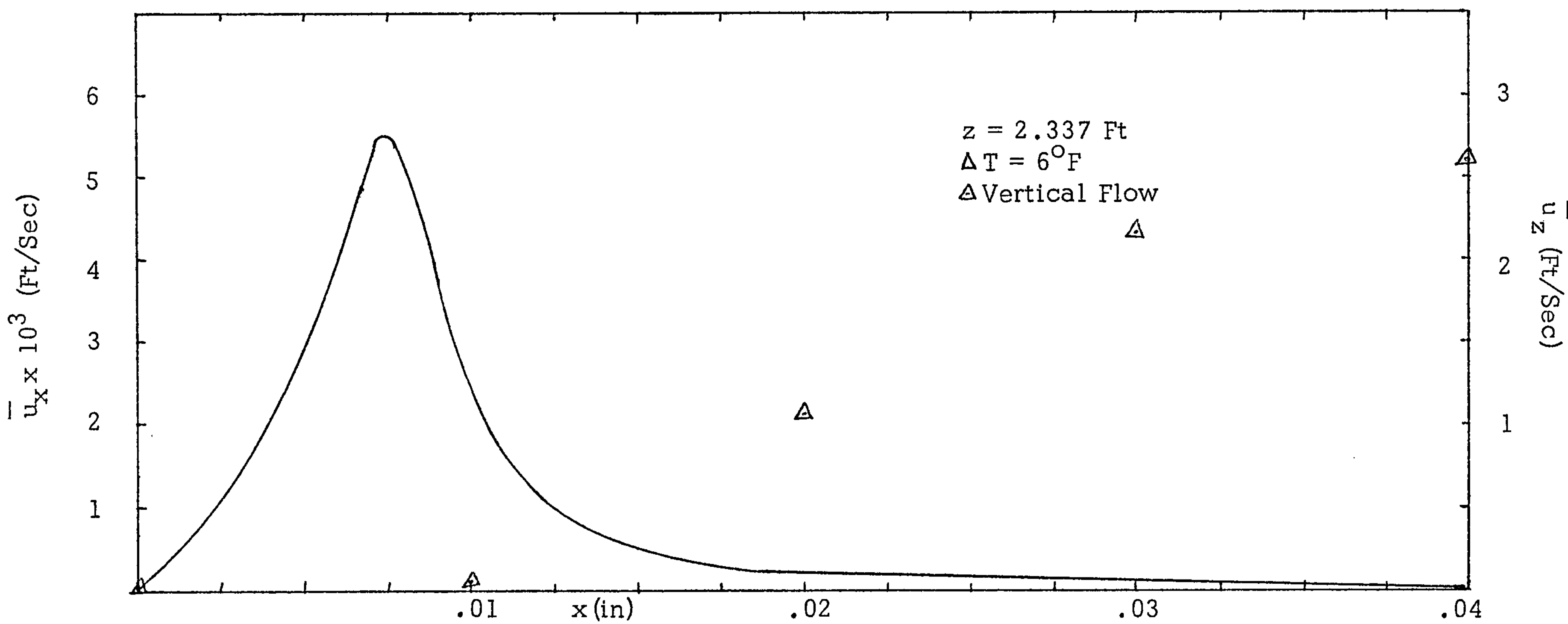

Figure 28

Horizontal Flow Rate Averaged Over Film Thickness as a Function of Position Along the Flute at z = .034 Feet

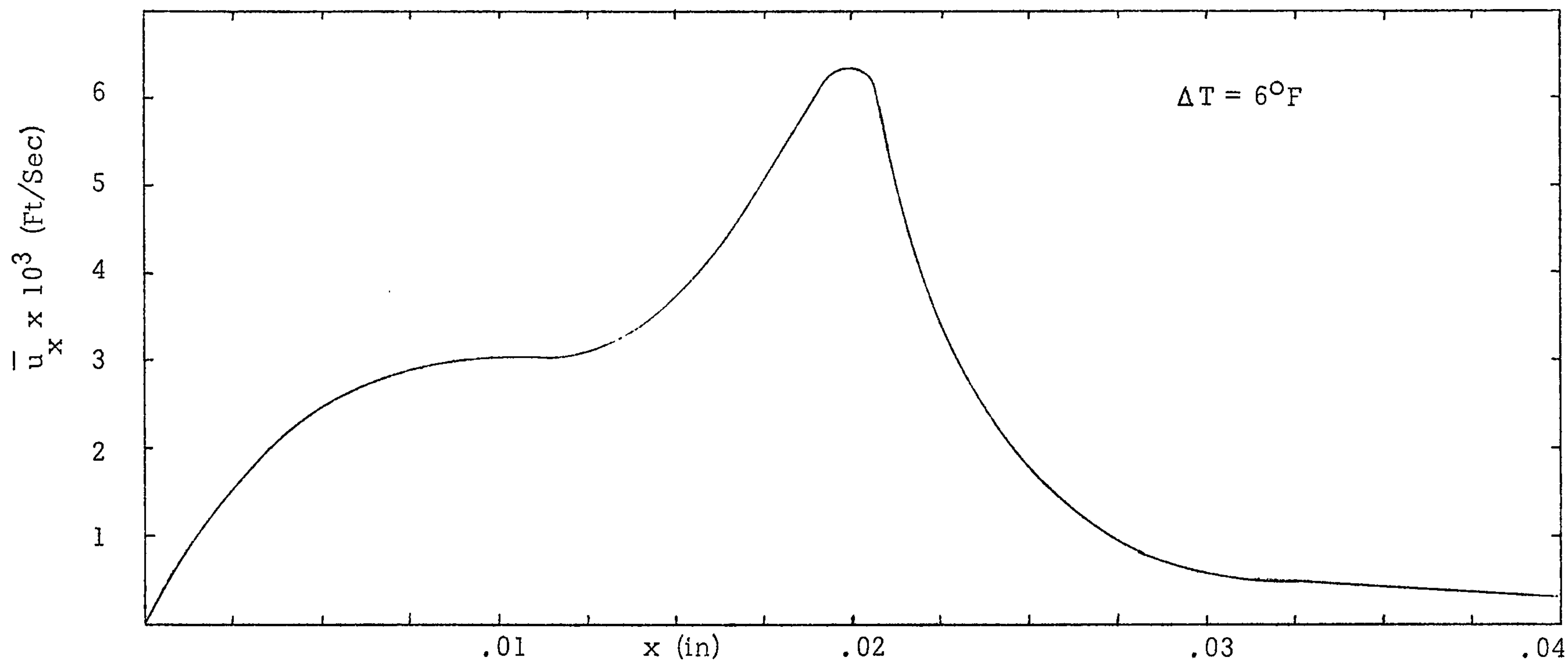

Figure 29

Horizontal Flow Rate Averaged Over Film Thickness as a Function of Position Along the Flute at z = .192 Feet

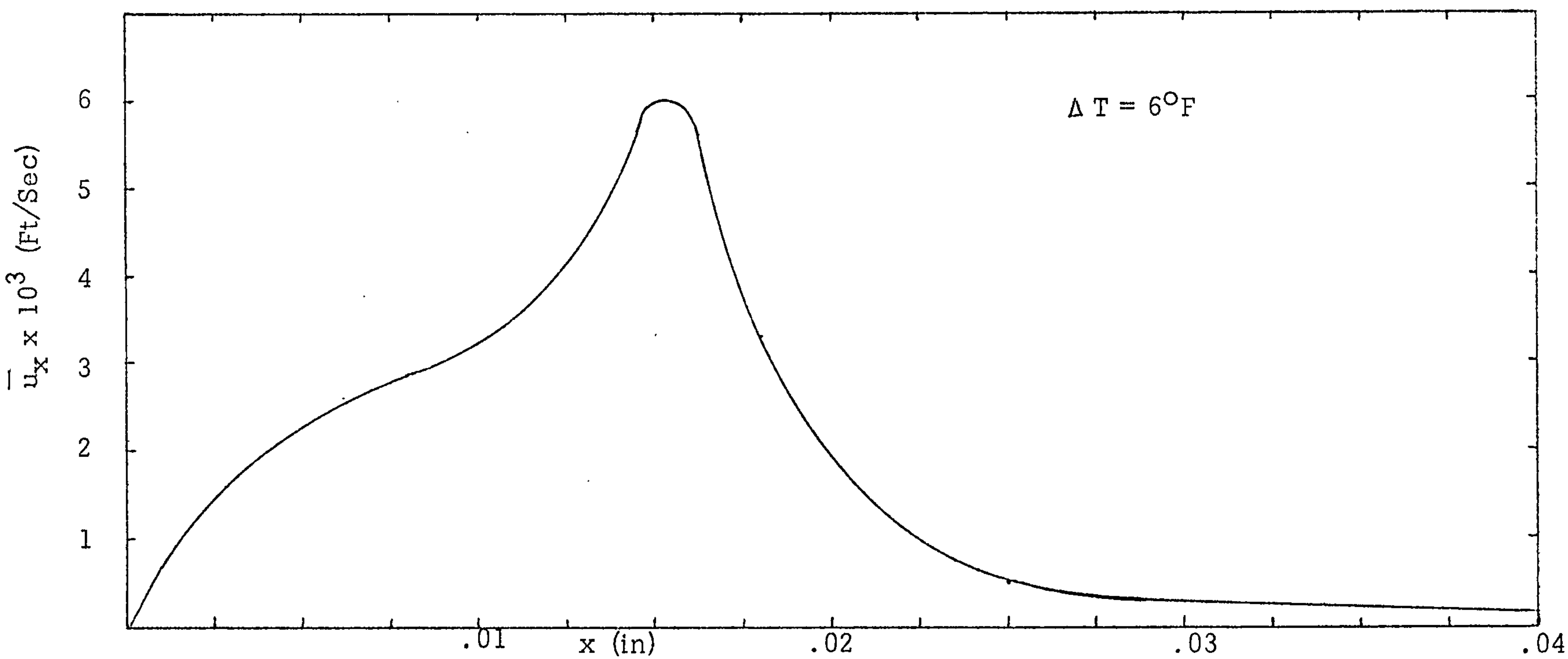

Figure 30

Horizontal Flow Rate Averaged Over Film Thickness as a Function of Position Along Flute at z = 1.036

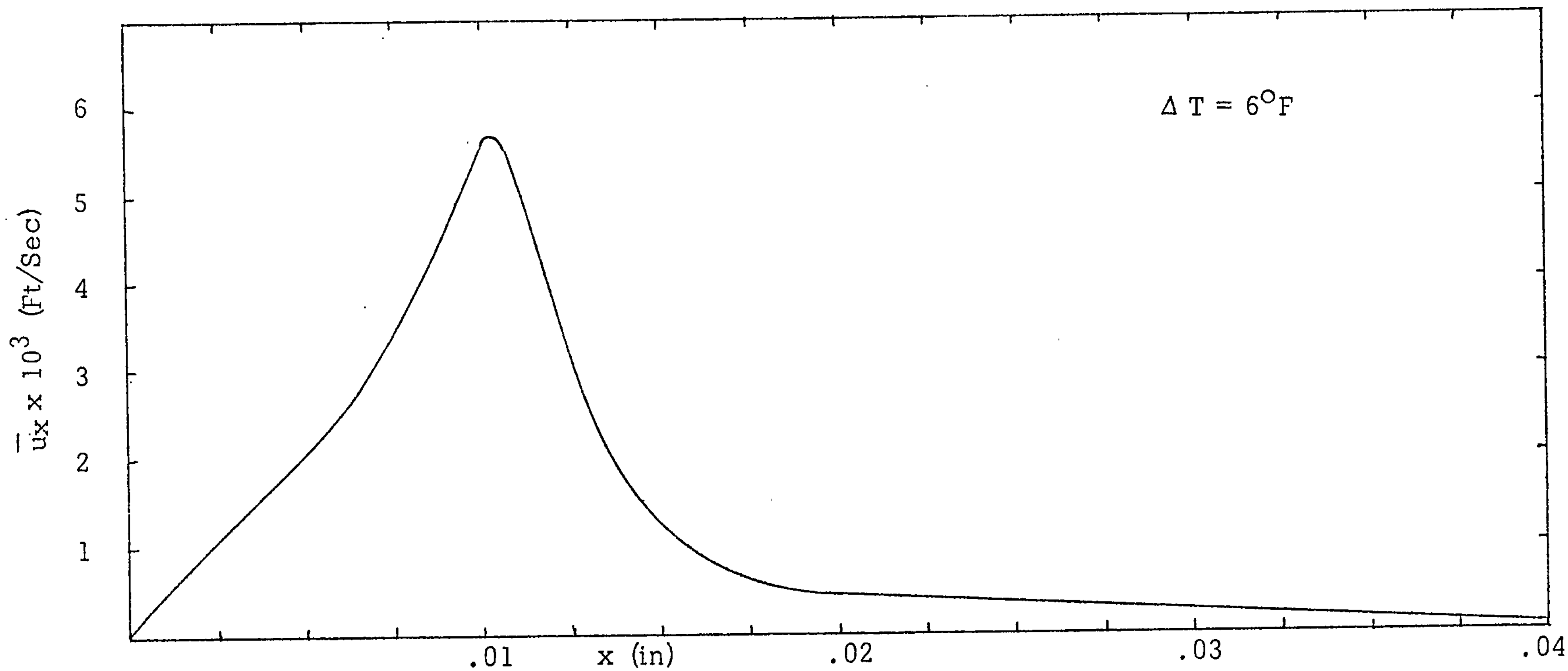

Figure 31

Horizontal Flow Rate Averaged Over Film Thickness as a Function of Position Along Flute at z = 5.777 Feet

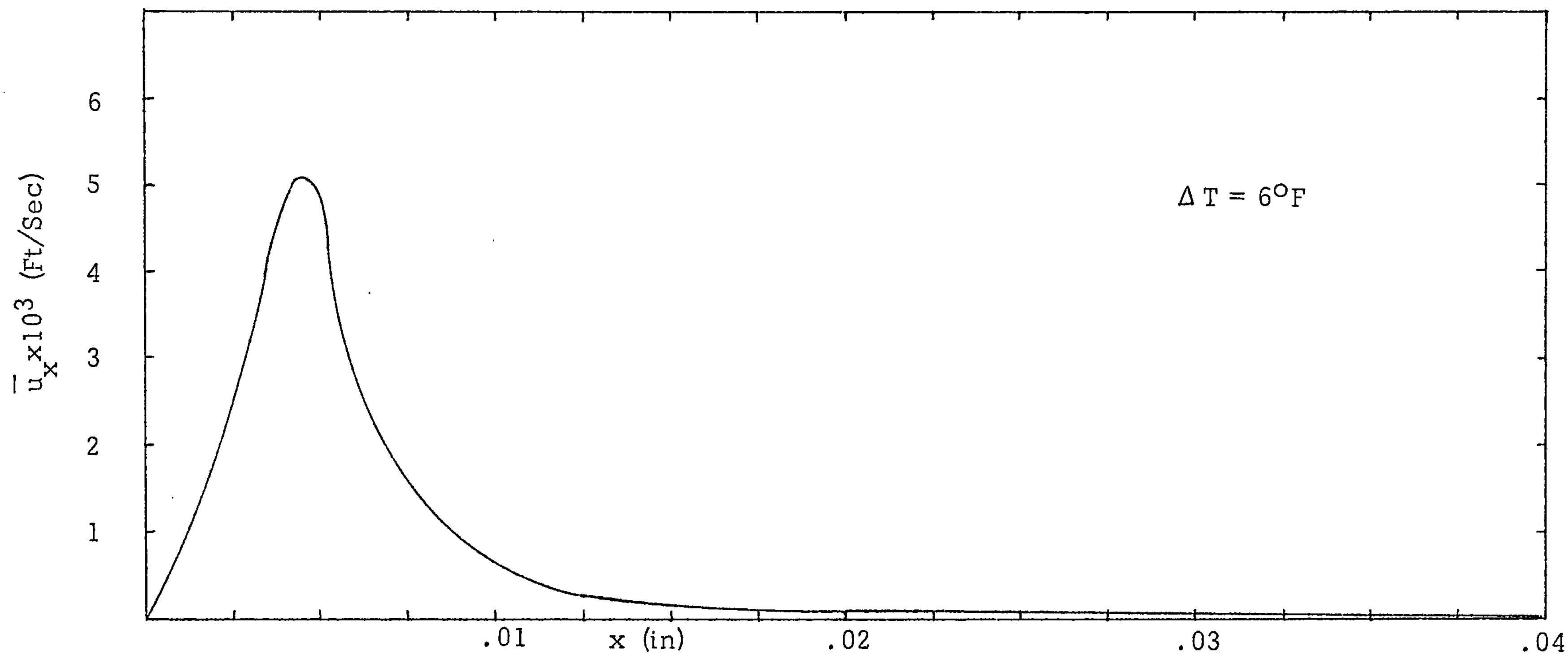

Figure 32

Local Heat Transfer Coefficient as a Function of Position Along the Flute at z = 0.034 Feet

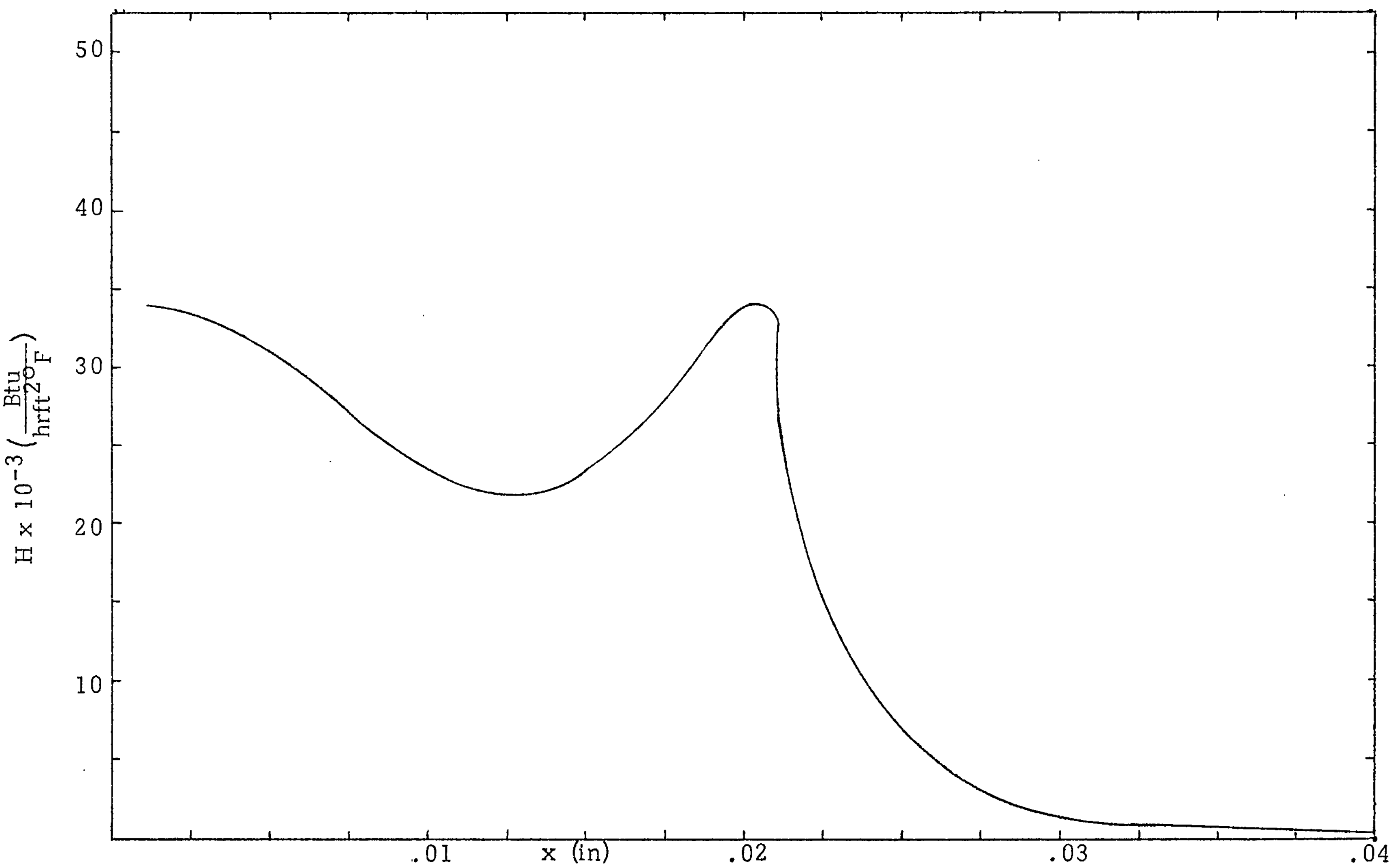

Figure 33

Local Heat Transfer Coefficient as a Function of Position Along the Flute at $z = 0.192$ Feet

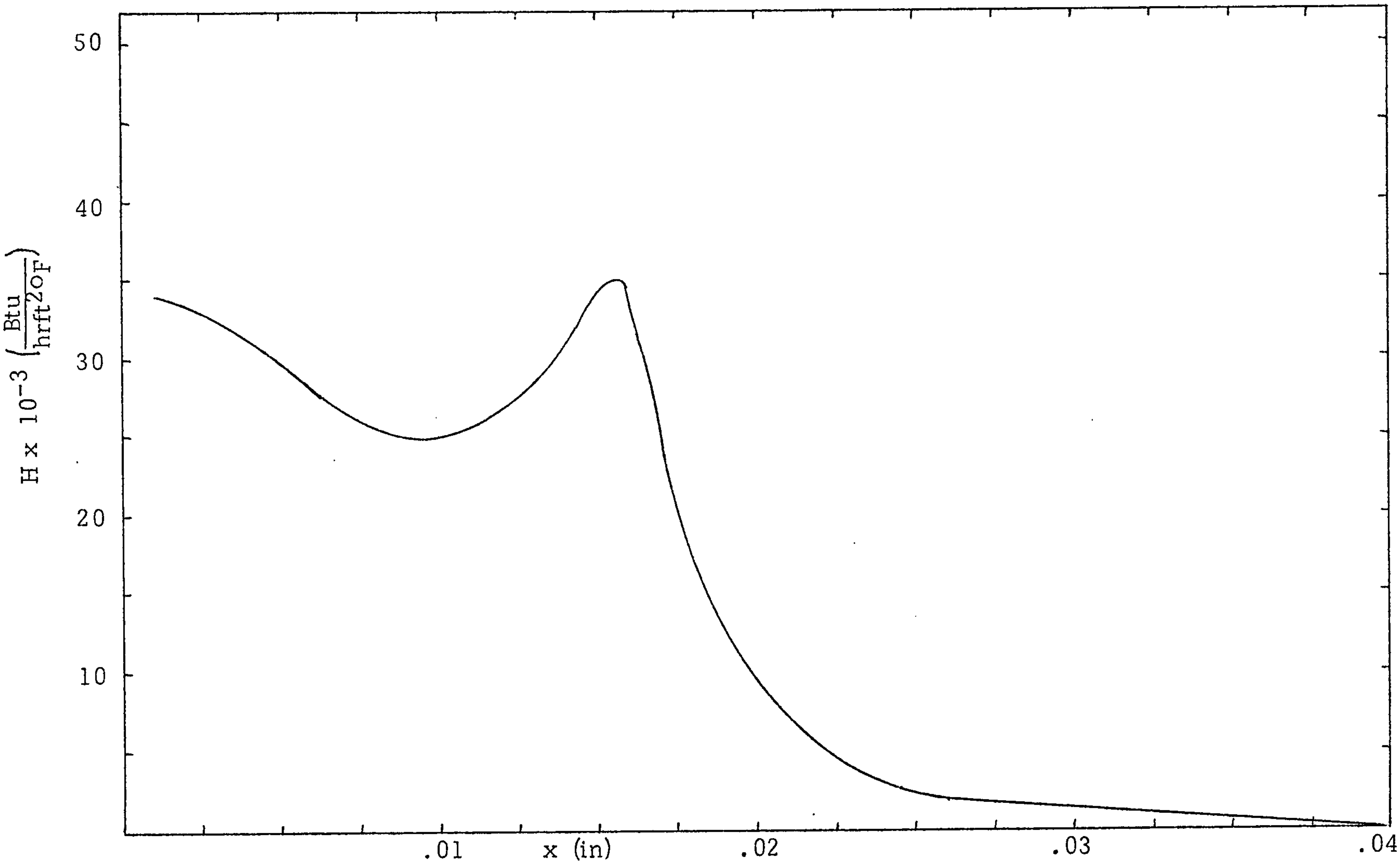

Figure 34

Local Heat Transfer Coefficient as a Function of Position Along the Flute at z = 1.036 Feet

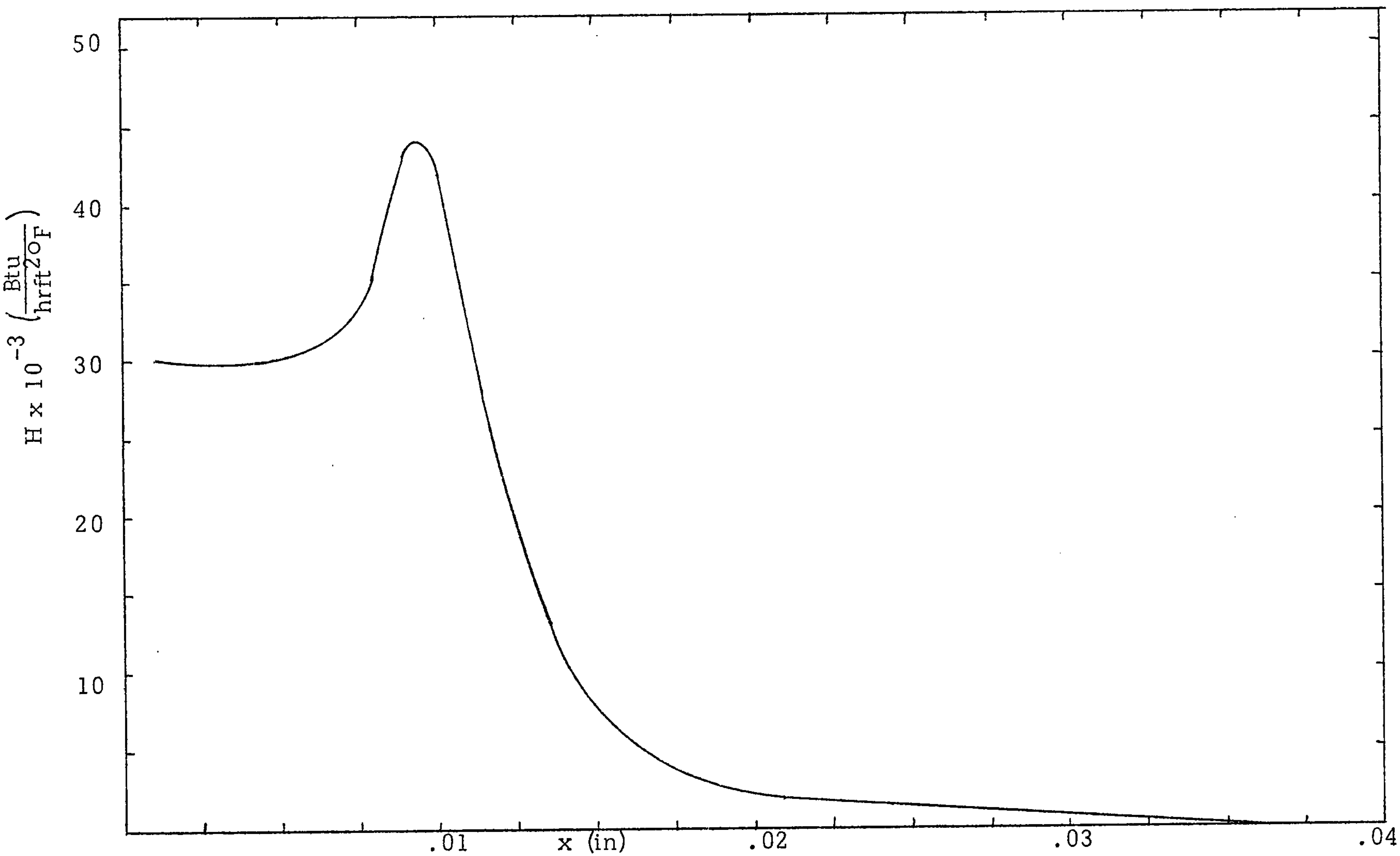

Figure 35

Local Heat Transfer Coefficient as a Function of Position Along the Flute at 2.337 Feet

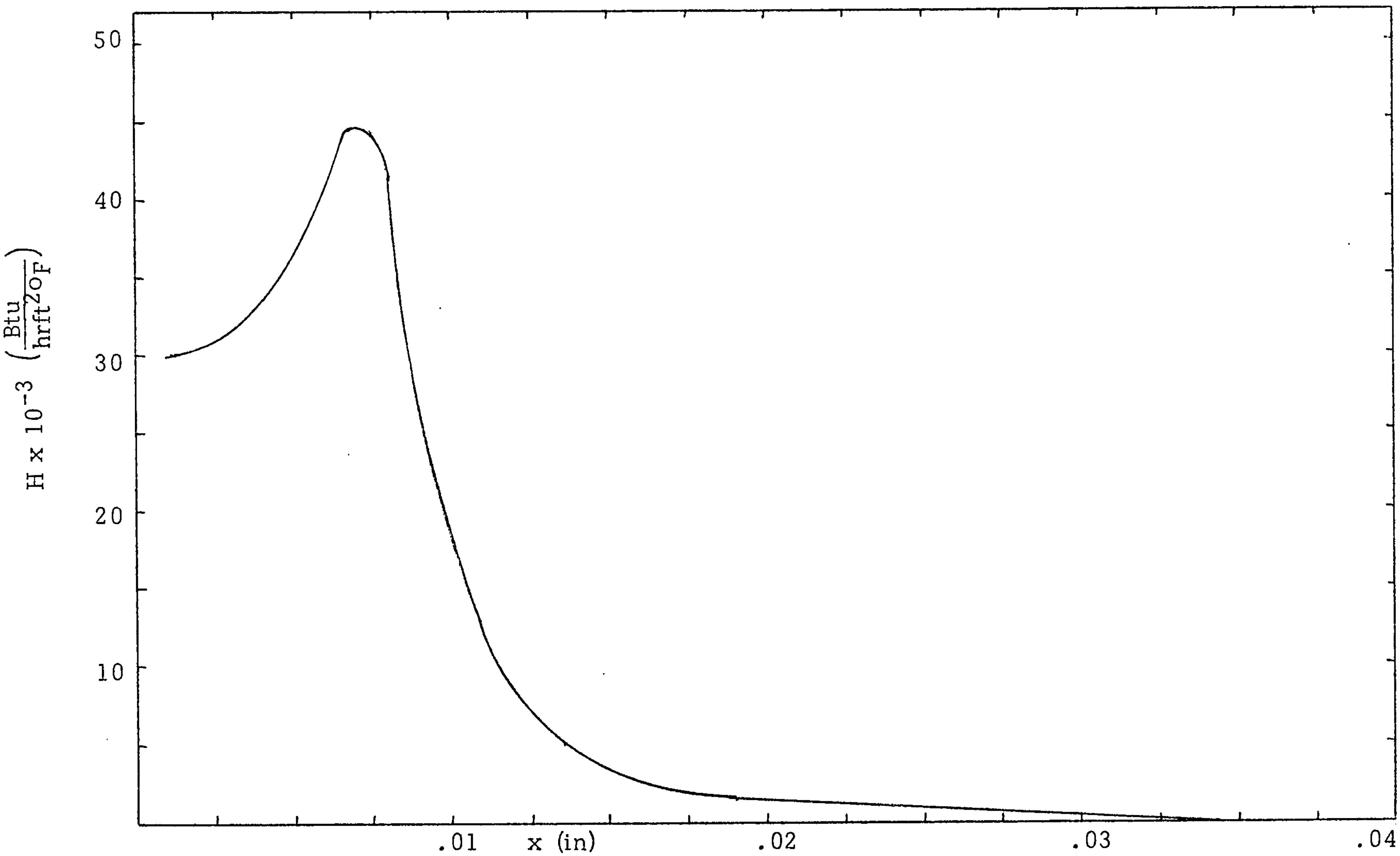

Figure 36

Local Heat Transfer Coefficient as a Function of Position Along the Flute at z = 5.777 Feet

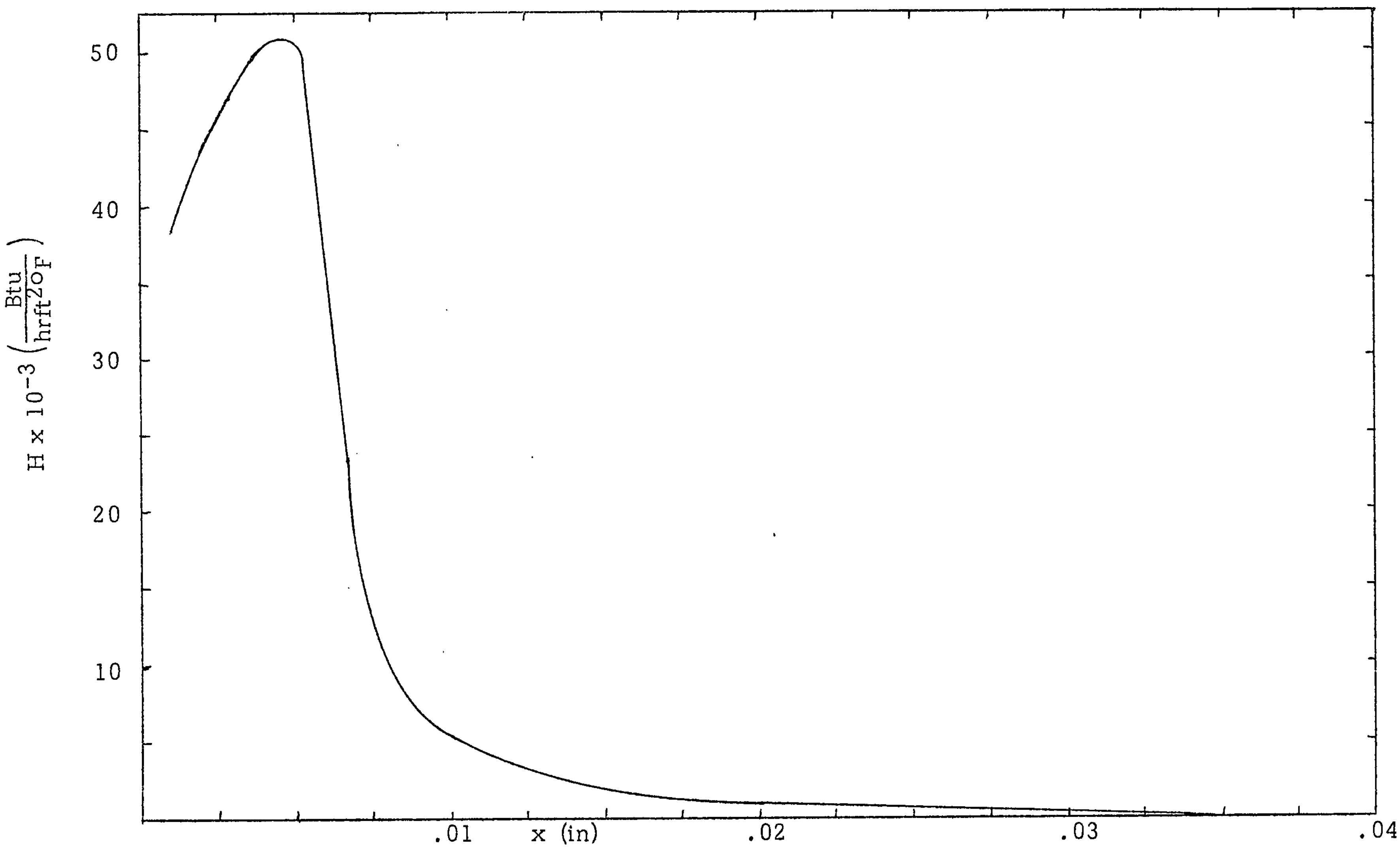

Figure 37

crest. It would definitely be helpful to have an experimental determination of the film thickness to find out whether or not this decrease in film thickness actually does occur or whether it is merely an artificiality of the computational procedure. As one proceeds farther down the condenser, the increase in local heat transfer coefficient becomes larger and larger, and approaches the crest more and more closely.

The average heat transfer coefficient as a function of length for various temperature driving forces is shown in Figure 38. The curves are fairly similar to those for the local heat transfer coefficient, but are somewhat flatter; and the sudden drop resulting from flooding is less pronounced.

Figures 13-16 show the variation of the peak film thickness h_o with vertical position, and indicate that this thickness does not increase steadily, as one would expect, but seems to oscillate. This oscillation is due to the spiral relationship between the peak film thickness and the radius of curvature at the peak, as shown in Figure 12. This oscillation does not seem to be physically reasonable, and is almost certainly a result of the approximations made in developing the computational procedure. Because the horizontal velocity varies considerably from the peak to the valley, as shown in Figures 28-32, it is likely that the viscous term, which was neglected in going from equation (1) to equation (2), is, in fact, not negligible. This may be one reason why the predicted film thickness varies unreasonably.

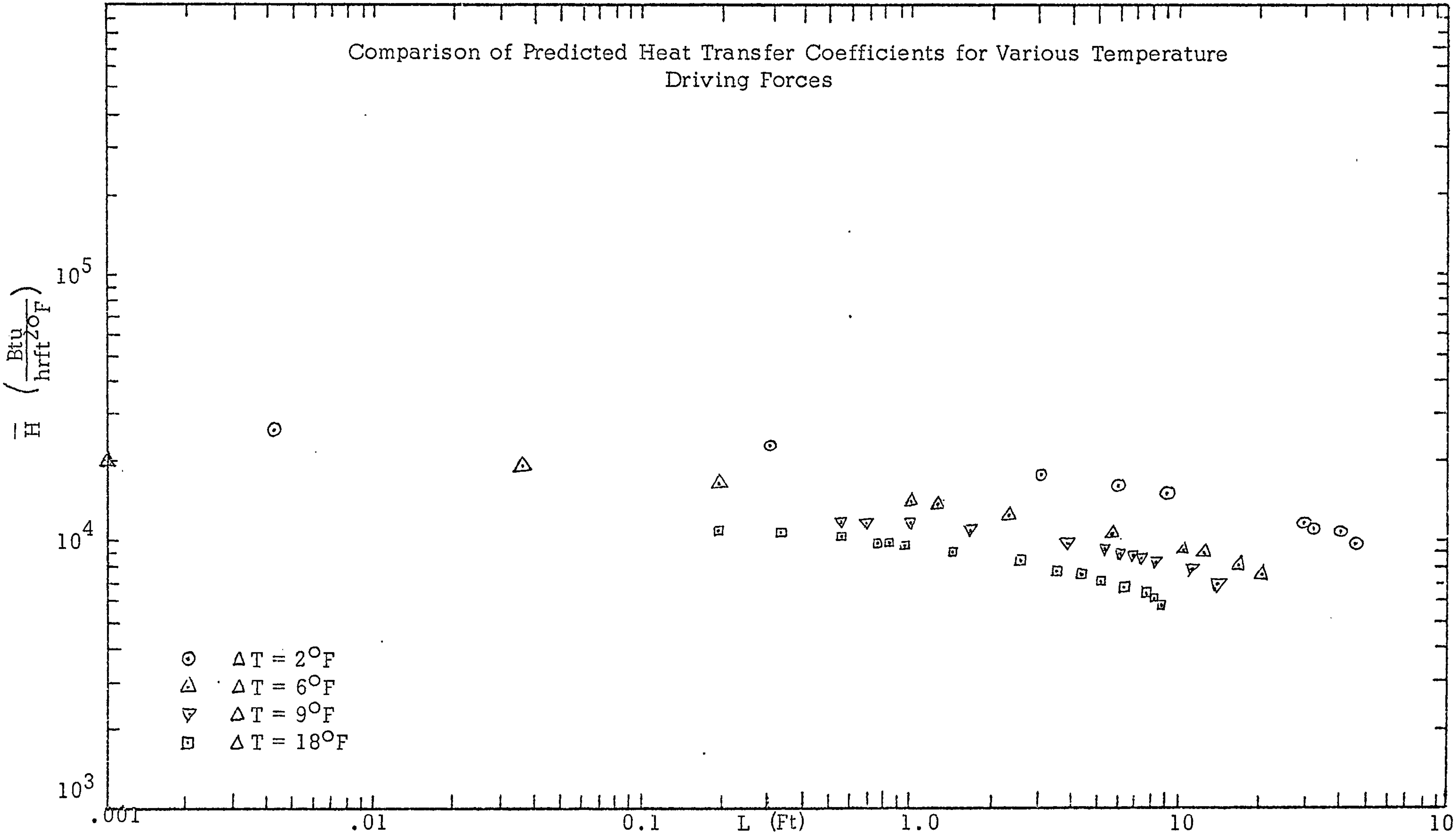
Comparison of Predicted Heat Transfer Coefficients for Various Temperature
Driving Forces
$\bar{H}$ $\left(\frac{Btu}{hrft^2 {}^oF}\right)$
10^5
10^4
10^3
.001
.01
0.1
1.0
10
100
L (Ft)
$\Delta T = 2^oF$
$\Delta T = 6^oF$
$\Delta T = 9^oF$
$\Delta T = 18^oF$
Figure 38

Average heat transfer coefficient versus the temperature driving force as predicted by the modified method is compared to experimental data found by Christ (7) on 6 foot and 13 foot condensing tubes in Figures 39 and 40. Considering the wide scattering of data, the calculated valued agree reasonably well with the experimental values, particularly for Figure 40 (13 foot tube), which includes more experimental data points.

The film profiles at various vertical positions are shown in Figure 41. It may be noted that the film thickness is practically the same for all the vertical positions in the region near the peak, and that the primary difference between any two profiles is the point where the free surface begins to deviate seriously from a parallel to the metal surface.

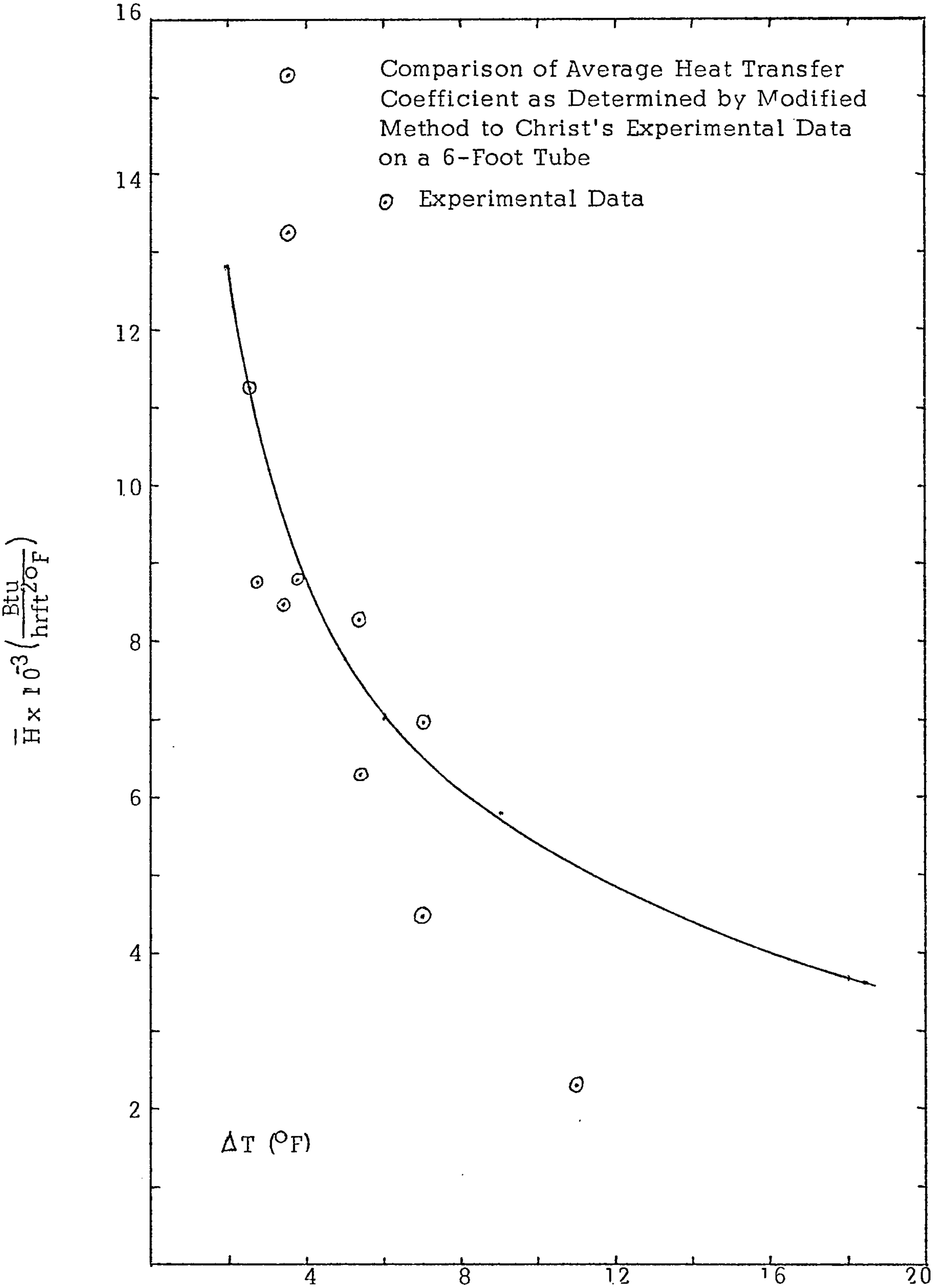
Comparison of Average Heat Transfer Coefficient as Determined by Modified Method to Christ's Experimental Data on a 6-Foot Tube
Experimental Data
$\bar{H} \times 10^{-3} \left(\frac{Btu}{hrft^2 {}^oF}\right)$
ΔT (°F)
16
14
12
10
8
6
4
2
4
8
12
16
20

Figure 39

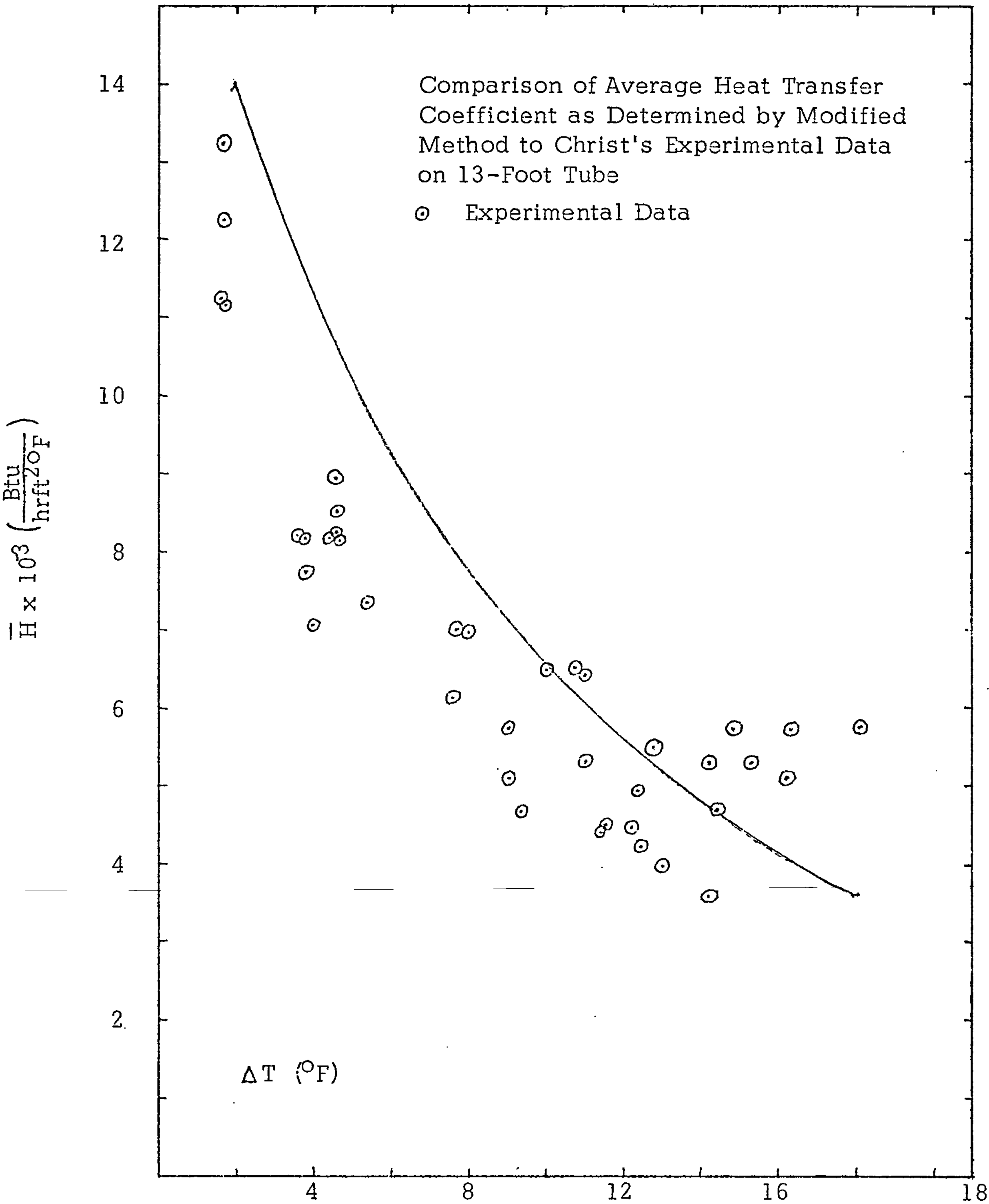
Comparison of Average Heat Transfer Coefficient as Determined by Modified Method to Christ's Experimental Data on 13-Foot Tube
Experimental Data
$\overline{H} \times 10^3 \left(\frac{Btu}{hr ft^2 {}^oF}\right)$
ΔT (^oF)
14
12
10
8
6
4
2
4
8
12
16
18

Figure 40

Condensate Profiles Determined by Modified Method for $\Delta T = 6^{o}F$

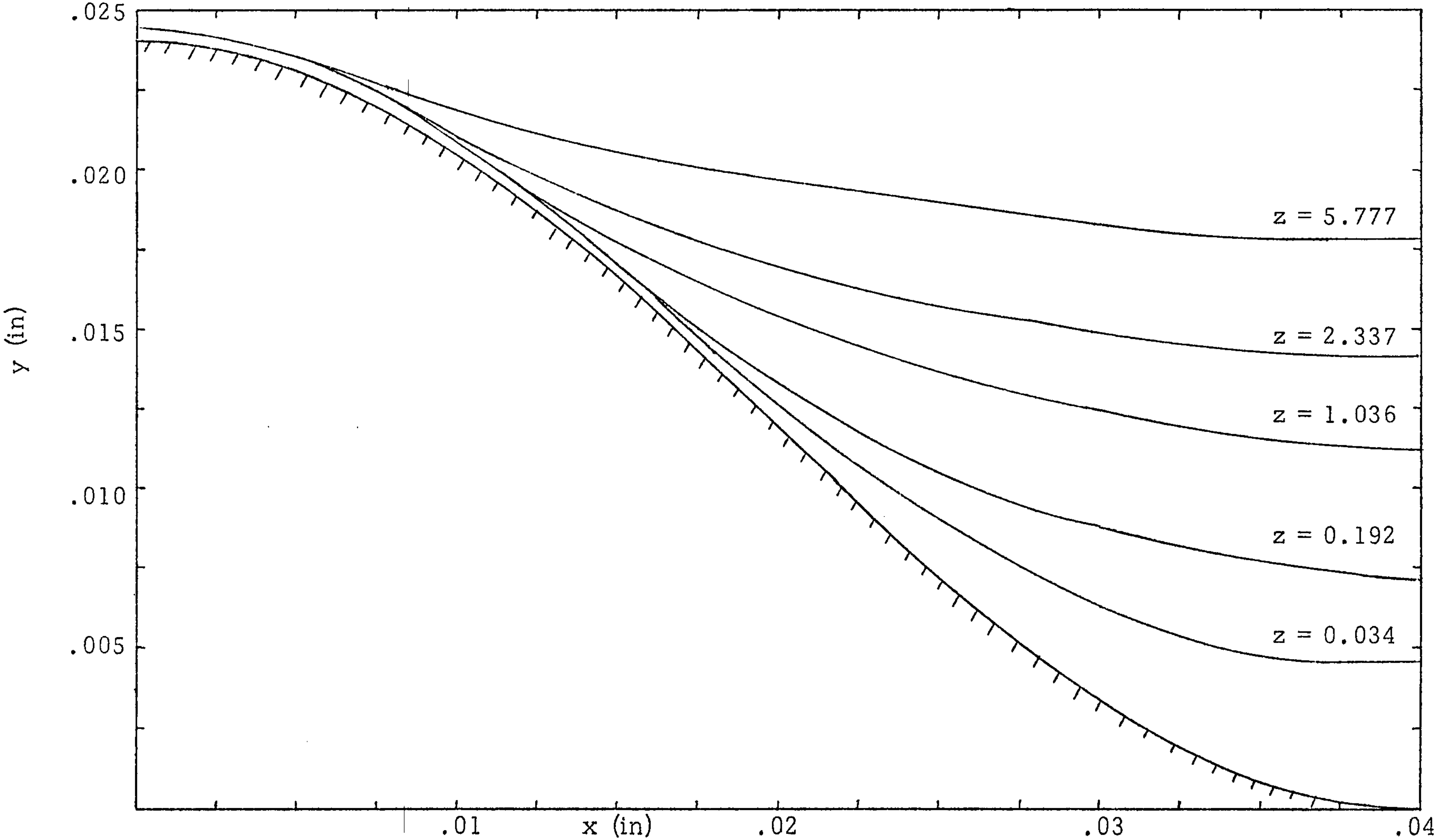

Figure 41

Chapter VIII

EFFECT OF FLUTE GEOMETRY

In order to determine the effect of changing the separation and depth of fluting, simulations were run using sinusoidal profiles with wavelengths of 0.02, 0.04, and 0.08 inches and amplitudes of 0.006, 0.012, and 0.024 inches (see Figure 42). The results of these experiments are shown in Figures 43-48. Clearly, increasing the amplitude results in a higher heat transfer coefficient and a depression of the flooding point. This occurs because, when the amplitude increases, the valley deepens; so it is possible for more condensate to flow down in the trough. This leaves more of the surface covered by a thin film, which is conducive to improved heat transfer. As the amplitude increases, this assumption becomes less tenable. On the other hand, increasing the wavelength makes the surface much flatter; and there is less chance for surface tension to have an effect. Thus the heat transfer coefficient is decreased substantially, but there is little danger of flooding. In contrast, decreasing the wavelength causes a very great increase in heat transfer, but the flooding point occurs at substantially smaller values of z. It would appear that the limit on the shortness of the wavelength would be the same as was the limit on the size of the amplitude --

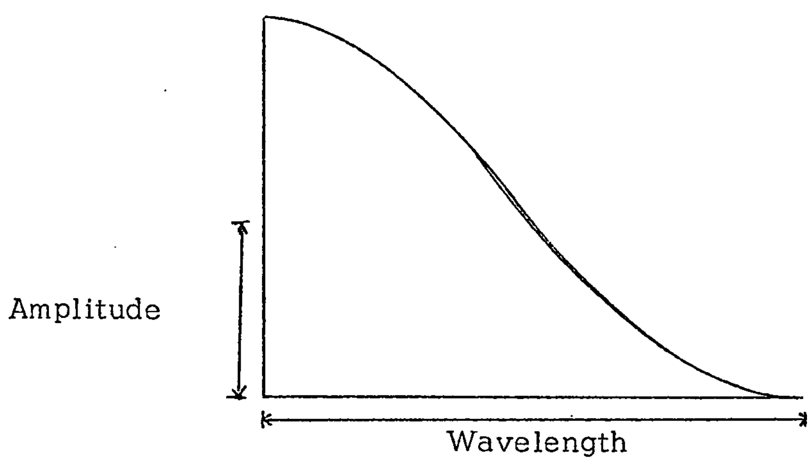

Figure 42
Profile of Fluted Surface Showing
Amplitude and Wavelength

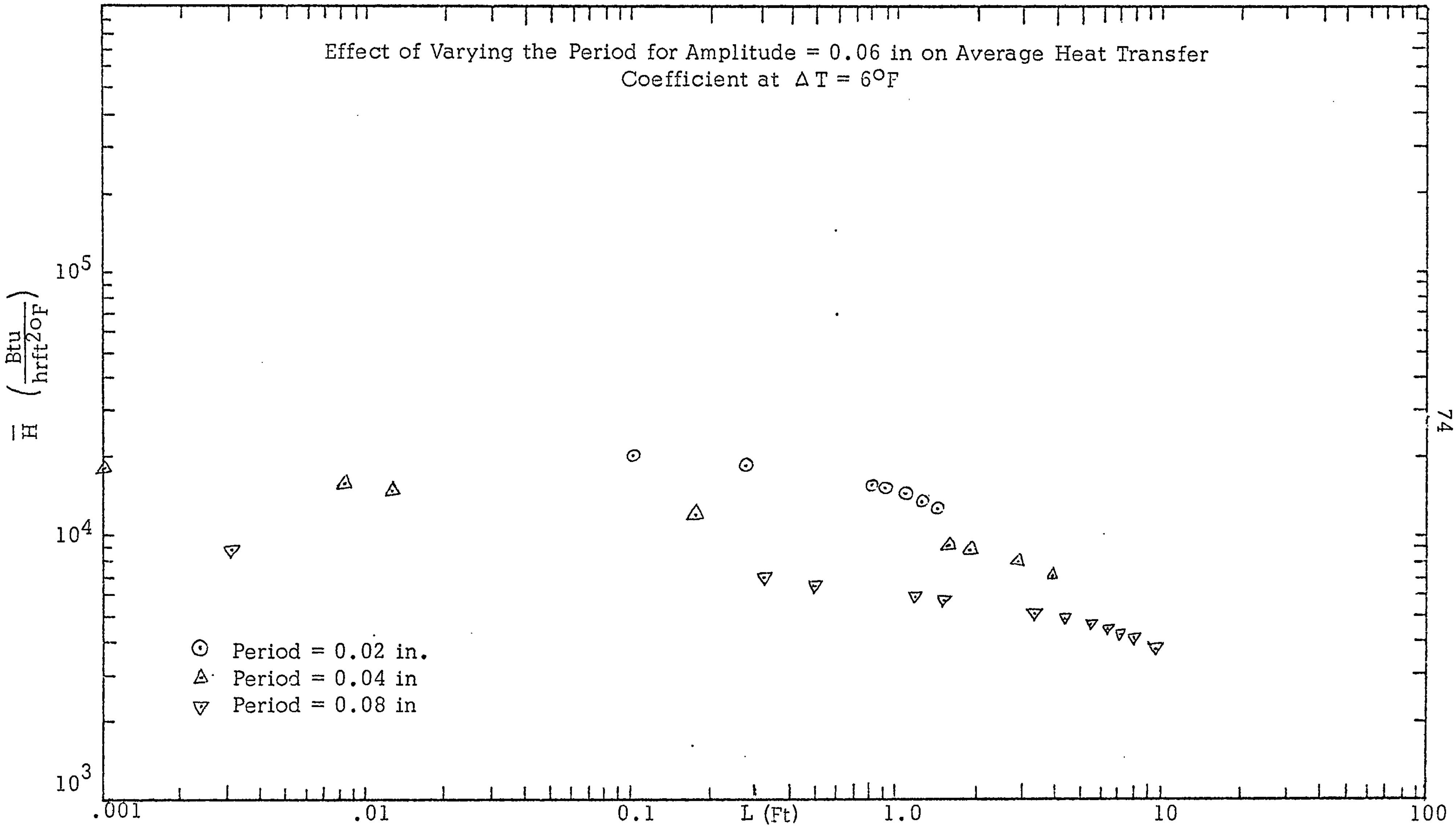
Effect of Varying the Period for Amplitude = 0.06 in on Average Heat Transfer Coefficient at $\Delta T = 6^{o}F$
$\bar{H}\ \left(\frac{Btu}{hrft^{2}\,{}^{o}F}\right)$
10^5
10^4
10^3
Period = 0.02 in.
Period = 0.04 in
Period = 0.08 in
.001
.01
0.1
L (Ft)
1.0
10
100

Figure 43

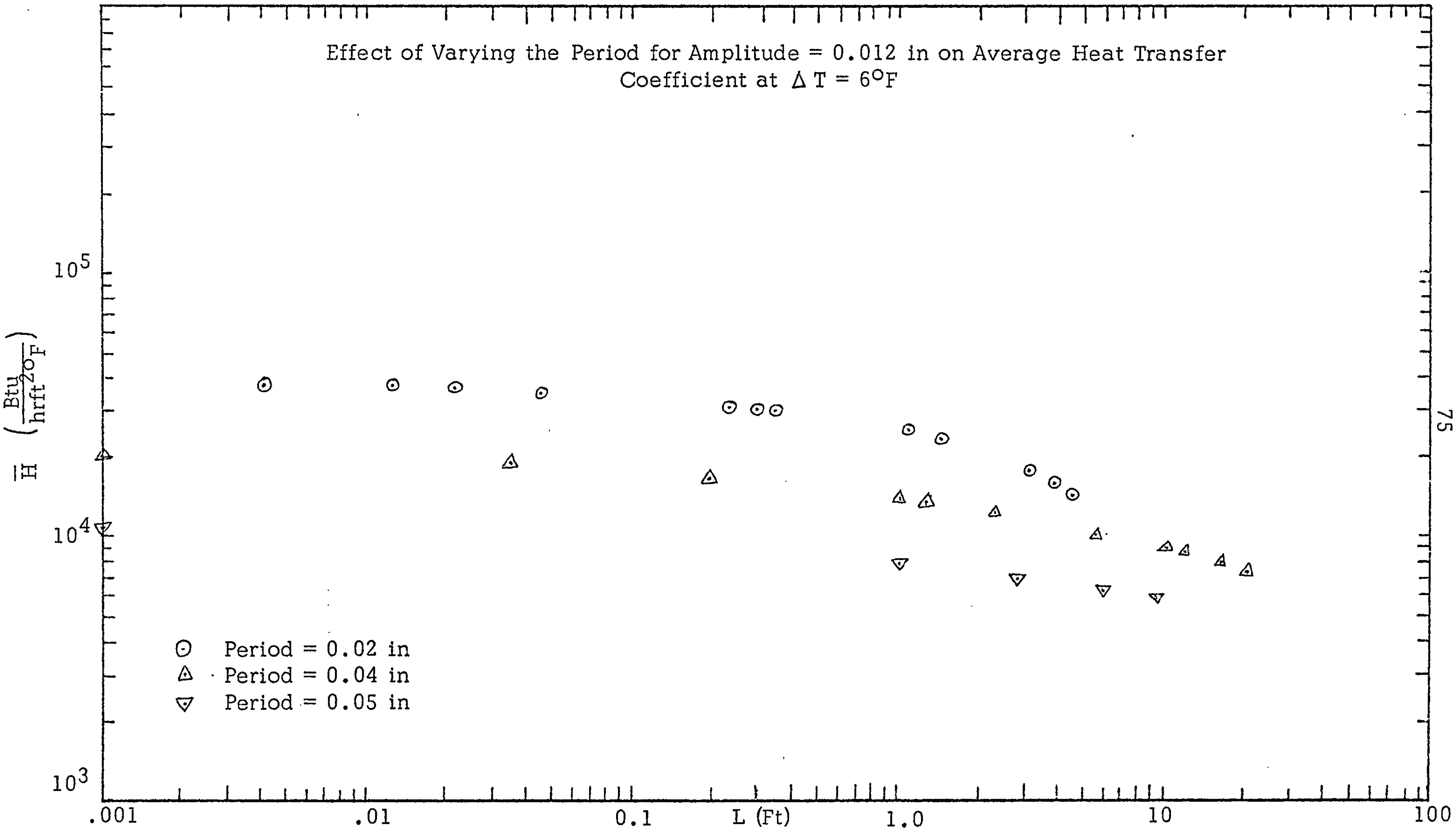
Effect of Varying the Period for Amplitude = 0.012 in on Average Heat Transfer Coefficient at $\Delta T = 6^{\circ}F$
10^5
10^4
10^3
$\overline{H} \left(\frac{Btu}{hrft^2 {}^{\circ}F}\right)$
Period = 0.02 in
Period = 0.04 in
Period = 0.05 in
.001
.01
0.1
1.0
10
100
L (Ft)
Figure 44

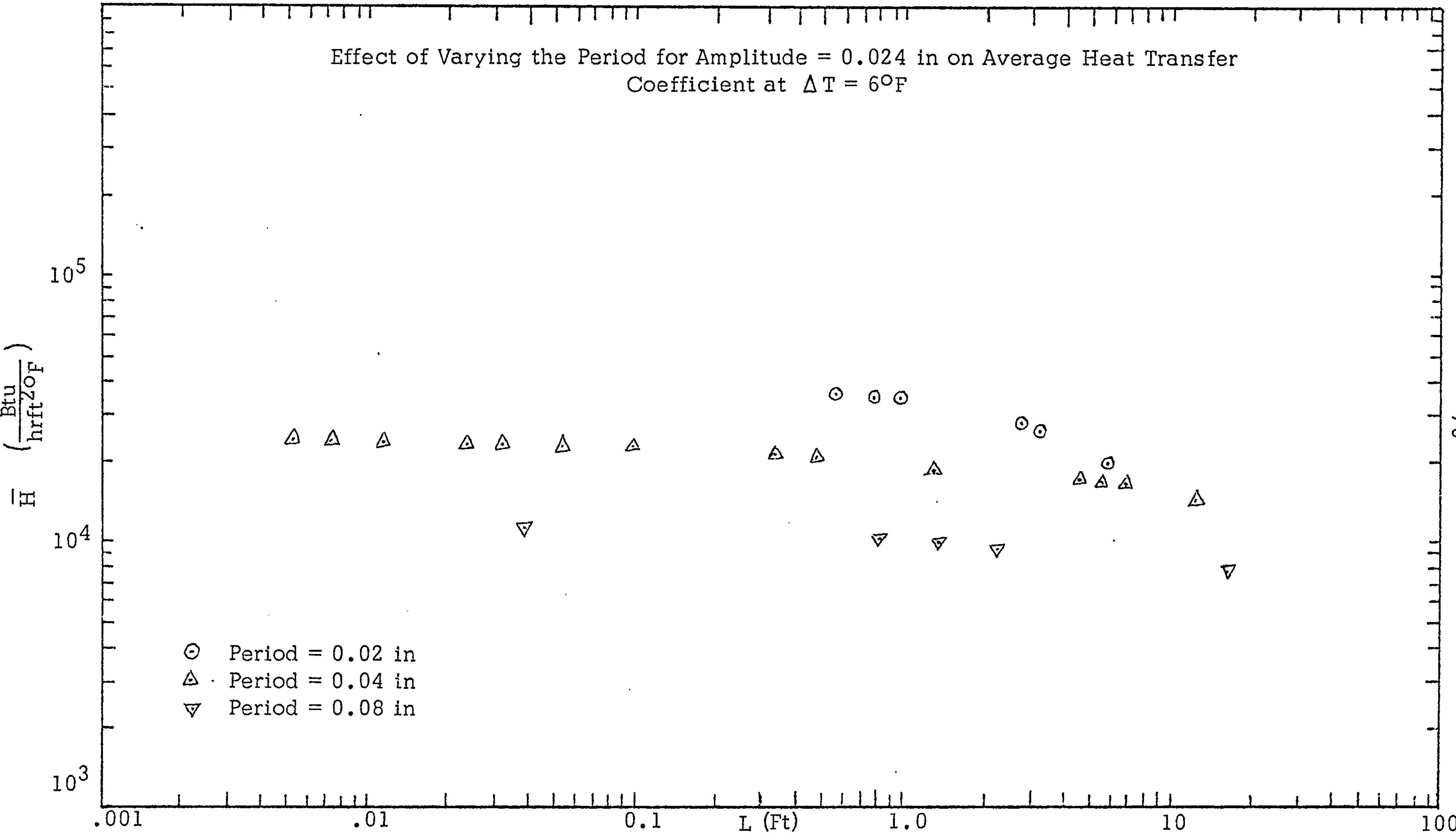
Effect of Varying the Period for Amplitude = 0.024 in on Average Heat Transfer Coefficient at ΔT = 6°F
$\bar{H}$ $\left(\frac{Btu}{hrft^2 {}^oF}\right)$
10^5
10^4
10^3
.001
.01
0.1
1.0
10
100
L (Ft)
Period = 0.02 in
Period = 0.04 in
Period = 0.08 in

Figure 45

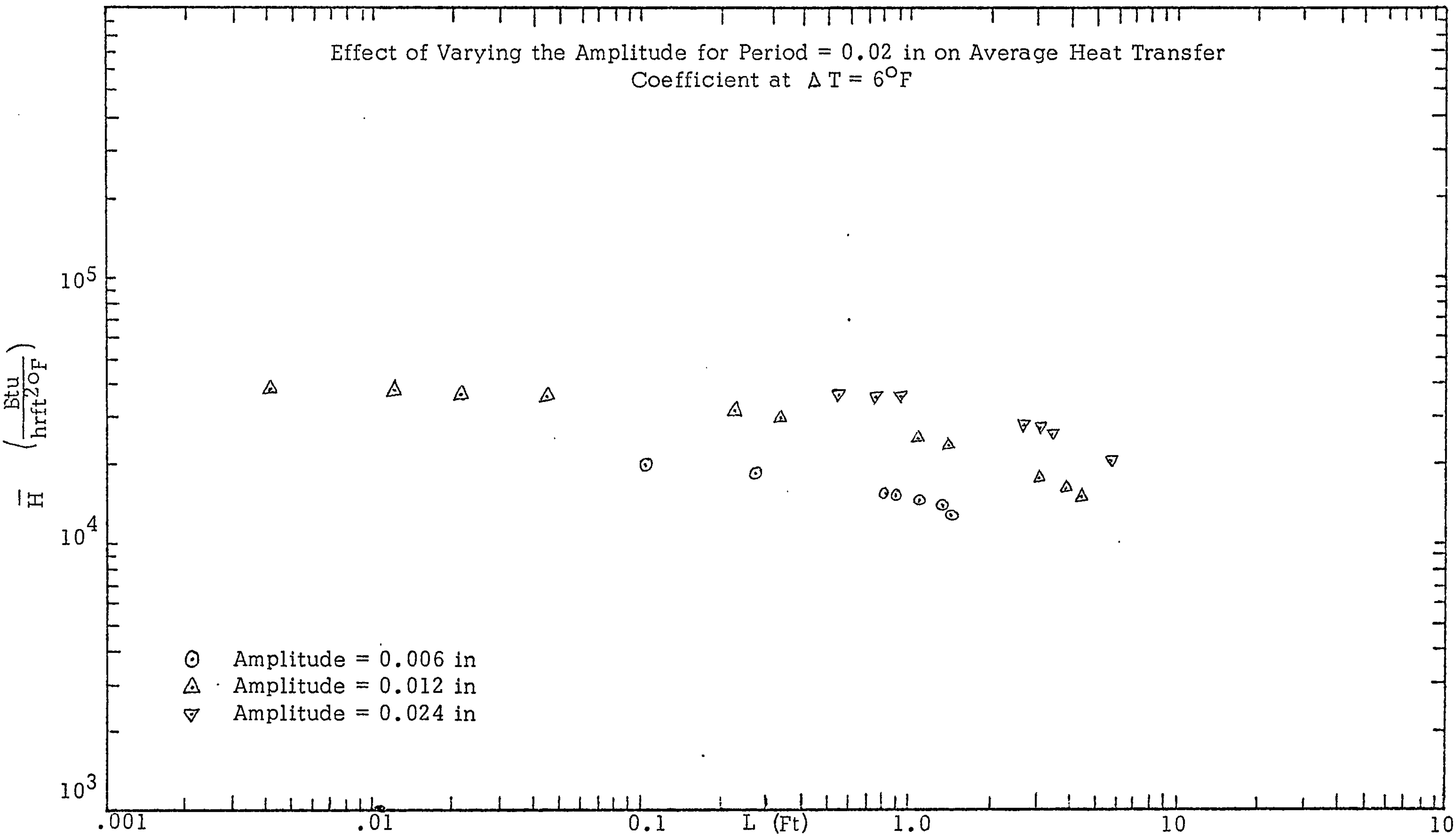

Effect of Varying the Amplitude for Period = 0.02 in on Average Heat Transfer Coefficient at $\Delta T = 6^oF$

Figure 46

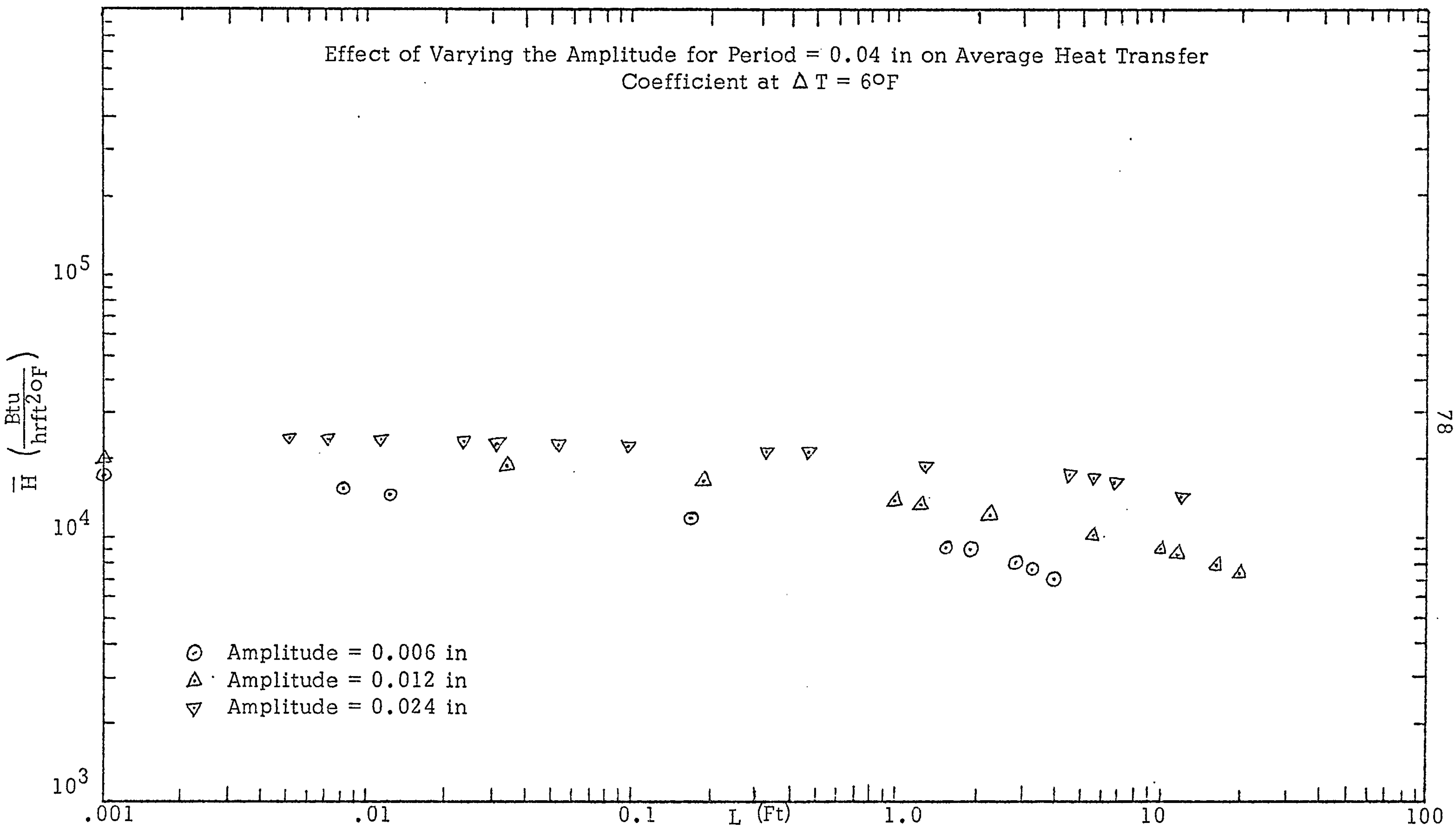
Effect of Varying the Amplitude for Period = 0.04 in on Average Heat Transfer
Coefficient at Δ T = 6°F
$\overline{H}$ $\left(\frac{Btu}{hrft^2 {}^oF}\right)$
10^5
10^4
10^3
.001
.01
0.1
L (Ft)
1.0
10
100
Amplitude = 0.006 in
Amplitude = 0.012 in
Amplitude = 0.024 in

Figure 47

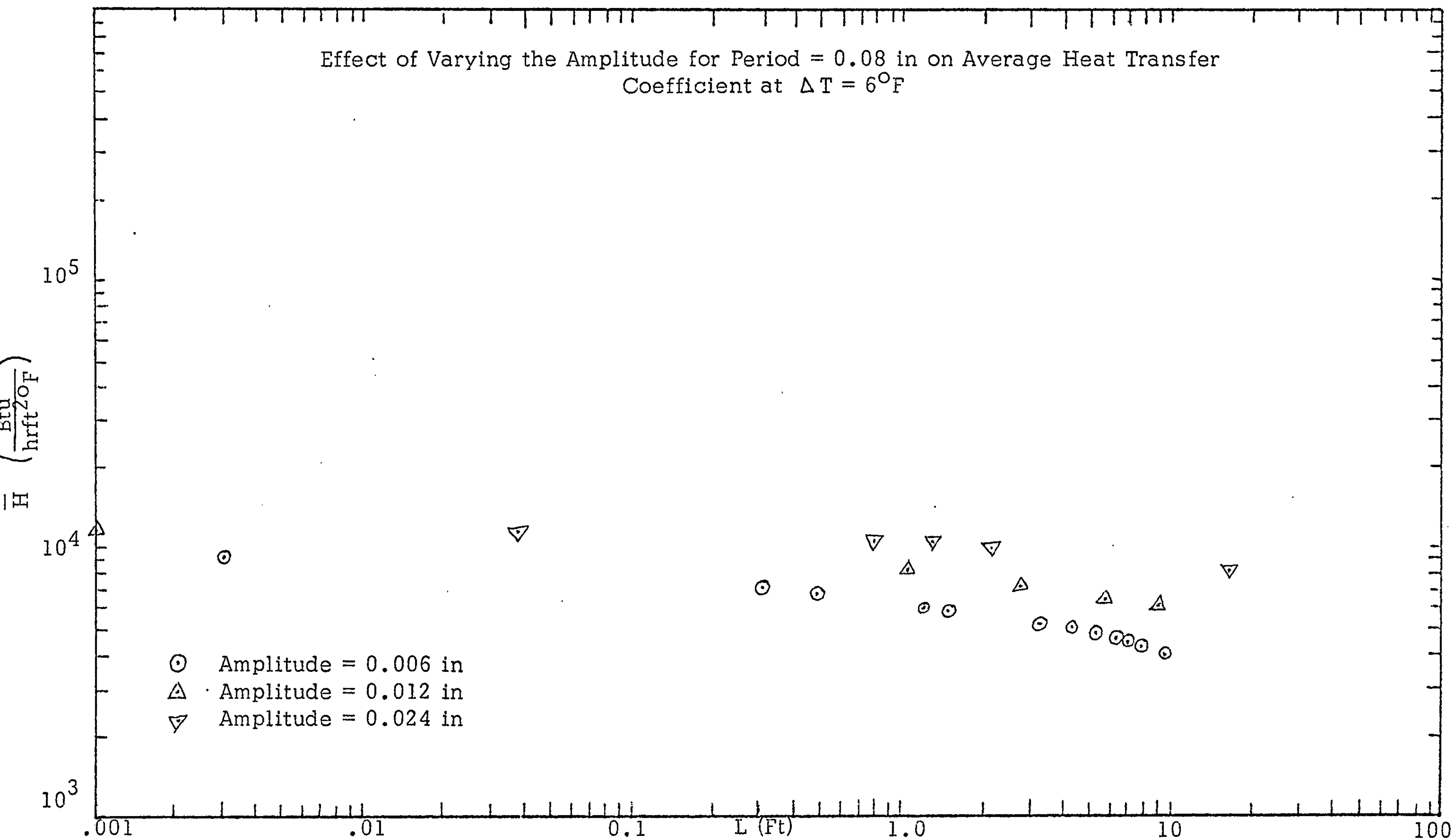

Effect of Varying the Amplitude for Period = 0.08 in on Average Heat Transfer Coefficient at ΔT = 6°F
10^5
10^4
10^3
$\overline{H}$ $\left(\frac{Btu}{hrft^2 {}^oF}\right)$
Amplitude = 0.006 in
Amplitude = 0.012 in
Amplitude = 0.024 in
.001
.01
0.1
L (Ft)
1.0
10
100

Figure 48

can such a tube be manufactured? The most promising combination of these two modifications is increasing the amplitude and decreasing the wavelength, for even though flooding occurs fairly early, the heat transfer coefficient obtained for a surface whose amplitude is 0.024 and wavelength is 0.02 inches is about three times as high as that obtained for a surface whose amplitude is 0.012 and wavelength is 0.04 inches. However, the difficulty of manufacture of fine, deep flutes will, along with the earlier onset of flooding, limit the extent of this modification.

Experiments were made with a metal surface that approximated the General Electric Company's Profile-9 fluted tube, but scaled so as to have a wavelength of 0.04 and an amplitude of 0.012 inches (see Figure 49). The results are somewhat unusual (Figure 50), in that near the top of the tube the film thickness at the peak is large, then decreases to a small value before flooding occurs. Because the radius of curvature of the metal surface (and thus that of the free surface for the film near the top of the condenser) at point A is large and positive, there is a pressure gradient from that point toward both the crest and the trough of the flute. This results in a thickening of the film at the crest, and the thin region of the film is from point A to point B (somewhere along the flute between A and the trough). As one proceeds down the condenser he finds that the film thickness at point A is nearly constant, but that the crest thickness decreases. The result is that when flooding is approached

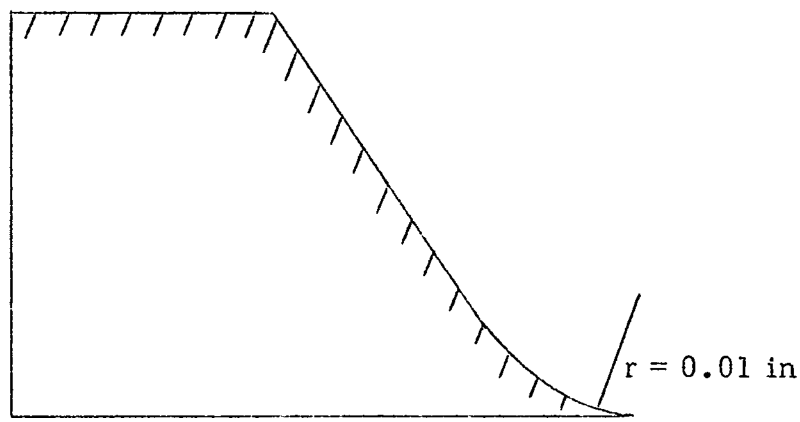

Figure 49
General Electric Profile-9

Condensate Profiles for General Electric Profile-9 Surface

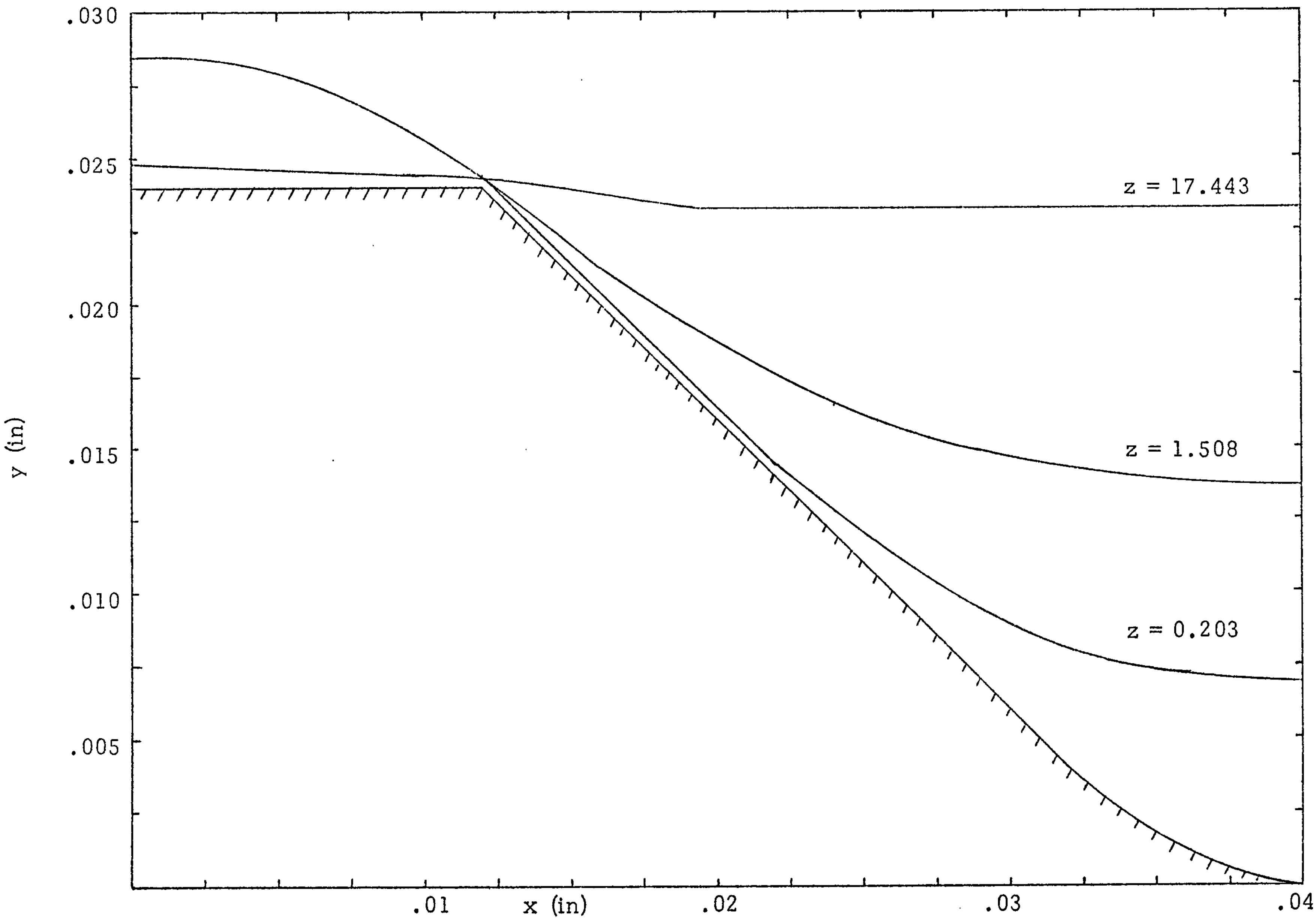

Figure 50

(that is, when the trough is full), the crest has a very thin film. Thus, improved local heat transfer is observed over a somewhat longer condenser length than when the sinusoidal profile is used. However, the heat transfer coefficient associated with Profile-9 is significantly lower than that associated with the sinusoidal surface for most condenser lengths, as shown in Figure 51. From this experiment, it was found that rounding the peak was very advantageous, since that would greatly increase the size of the region of thin film and thus high heat flux.

Because the greatest impedance to good heat transfer is the rate at which the material can flow downward (keeping in mind the relative sizes of the horizontal and vertical velocities, as shown in Figure 28), it was felt that an improved condensing surface would, of necessity, allow for greater run-off. In keeping with the note made in discussion of the Profile-9 results, it was thought necessary to use a curved surface at the peak, one whose radius of curvature was steadily increasing. Thus the profile shown in Figure 52 was designed. The film profiles obtained from this surface are shown in Figure 53. It may be noted that the thickest part of the condensate film at high positions in the condenser is at the point where the slope of the solid is discontinuous, and thus the heat transfer occurs over both the peak and most of the valley for this configuration at these high vertical positions. The heat transfer coefficients found using this profile are compared to those using the sinusodial

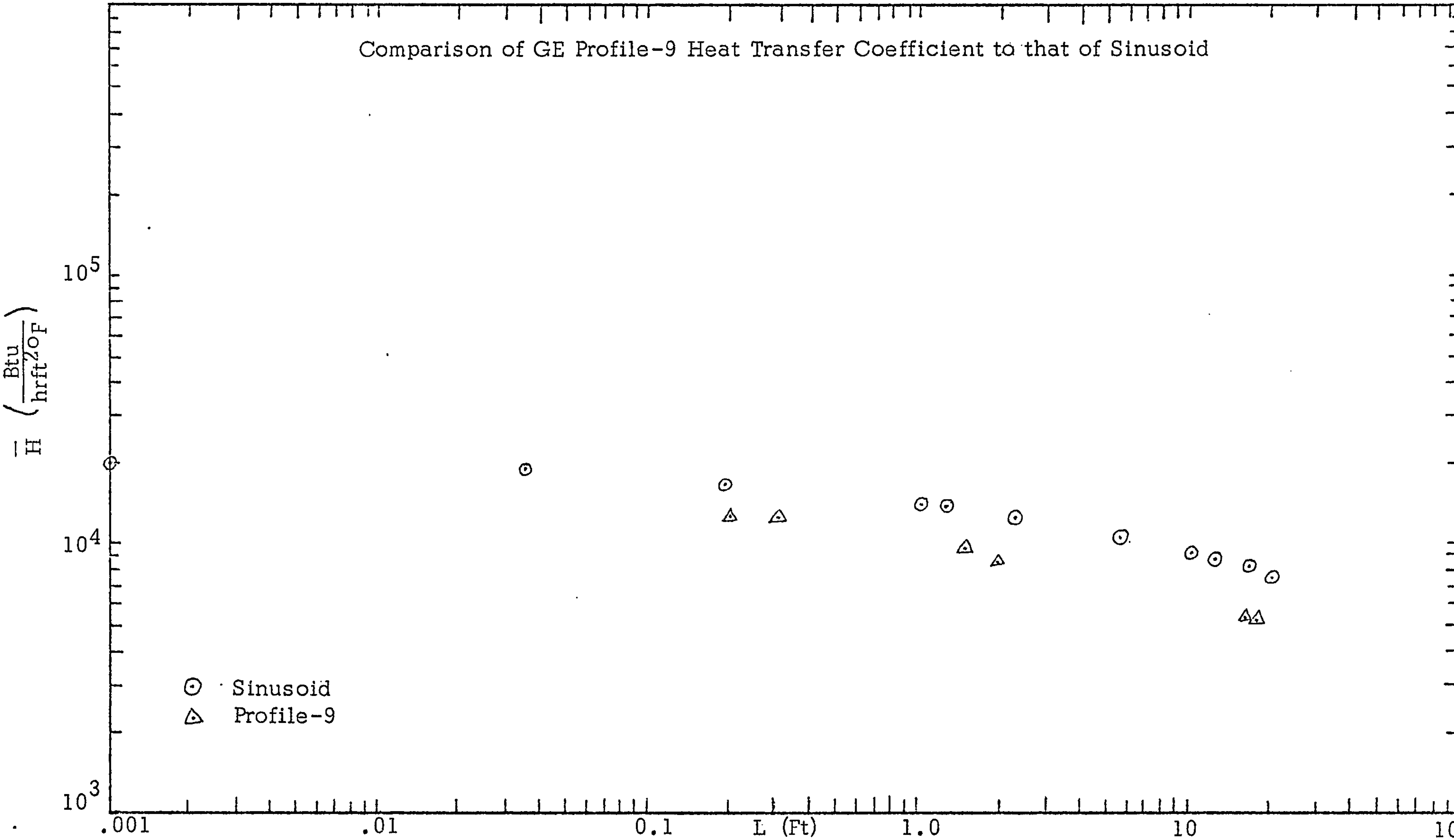
Comparison of GE Profile-9 Heat Transfer Coefficient to that of Sinusoid
$\bar{H}$ $\left(\frac{Btu}{hrft^2 {}^oF}\right)$
10^5
10^4
10^3
.001
.01
0.1
L (Ft)
1.0
10
100
Sinusoid
Profile-9

Figure 51

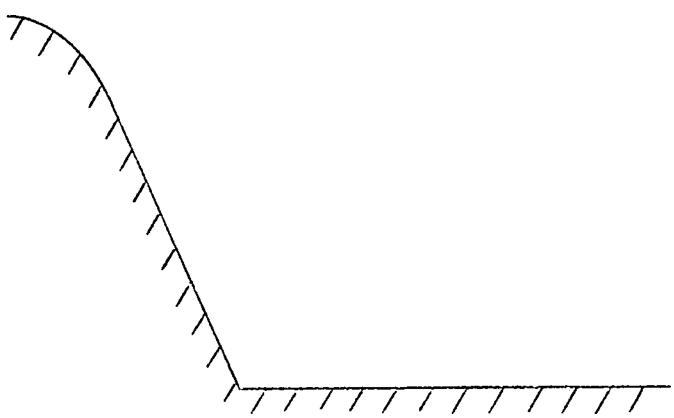

Figure 52
Improved Profile for Enhanced Condensation

Condensate Profiles for Improved Surface

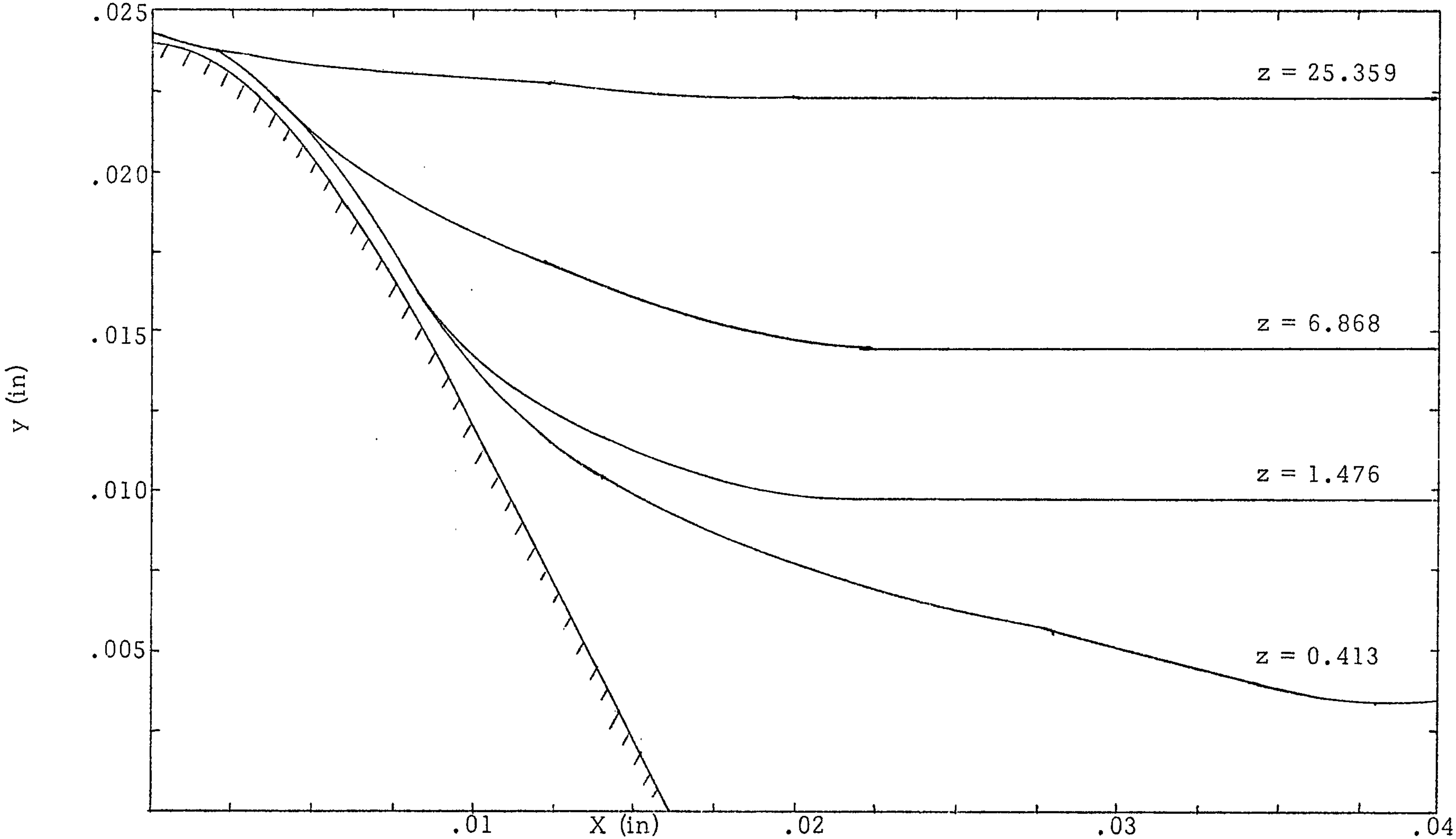

Figure 53

profile in Figure 54, and show that the new profile is slightly more efficient than the sinusoid.

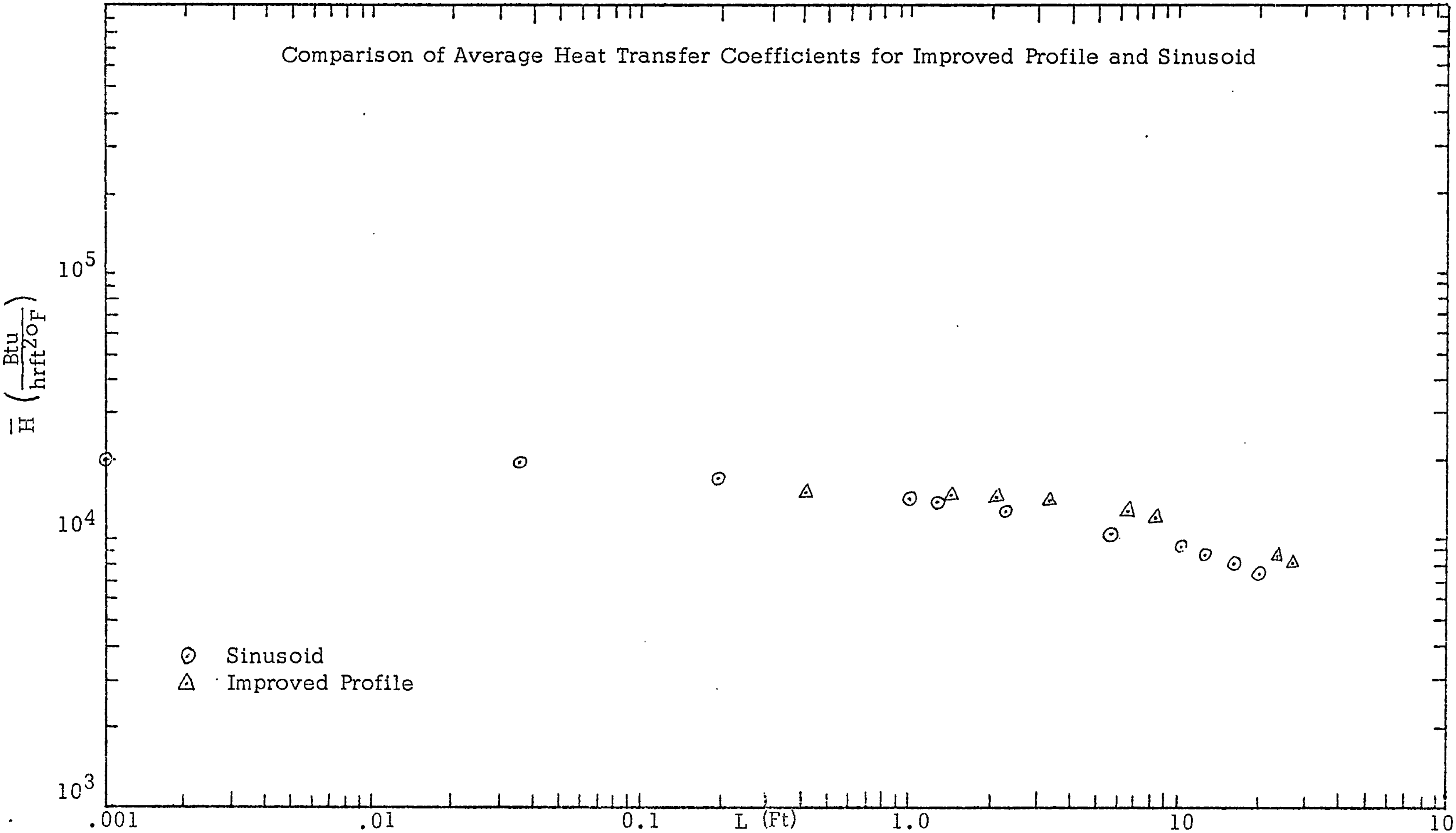
Comparison of Average Heat Transfer Coefficients for Improved Profile and Sinusoid
10^5
10^4
10^3
$\overline{H} \left(\frac{Btu}{hrft^2 °F}\right)$
Sinusoid
Improved Profile
.001
.01
0.1
1.0
10
100
L (Ft)

Figure 54

Chapter IX

CONCLUSIONS

The new model appears to be slightly better than Gregorig's model, in that it agrees somewhat better with experimental results. However, the same problem that is encountered in Gregorig's method is also encountered in the new method - - the fact that h_o, the film thickness at the peak of the flute, is not a unique function of R_o, the radius of curvature of the free surface at the peak.

Optimization work shows that increasing the amplitude and decreasing the spacing between flutes causes the greatest sustained increase in heat transfer. It is found that the widely-used GE Profile-9 surface does not yield heat transfer coefficients as high as does the sinusoidal profile, primarily because the film thickness is large at the peak of the profile. The profile developed as an improvement on the sinusoidal and GE Profile-9 surfaces, which has a curved peak and a large area for downward flow, produces heat transfer coefficients which are somewhat better than the other profiles, with little danger of flooding the grooves.

Chapter X

RECOMMENDATIONS

The next stage in the development of a mathematical model for steam condensing on fluted surfaces should be the solution of the more complete equations of motion, including at least the $\frac{\partial^2 u_x}{\partial x^2}$ viscous term.

It would be helpful, in view of the fact that deep, closely-spaced flutes are predicted to be best, to eliminate the assumption of uniform temperature driving force.

Experimental determination of the film thickness along the flute would be beneficial, since it might point the way toward further improvements in the model.

Appendix 1

Derivation of Equation 22

$$\alpha = \pi - \phi - \Delta\phi \qquad (1)$$

$$\beta = \pi - \alpha - \psi \qquad (2)$$

$$= \phi + \Delta\phi - \psi$$

$$\gamma = \tfrac{1}{2}(\pi - \Delta\psi) \qquad (3)$$

$$\theta_2 = \gamma - \tau \qquad (4)$$

$$\epsilon = \tfrac{1}{2}(\pi - \Delta\phi) \qquad (5)$$

$$\theta_1 = \pi - (\pi - \epsilon) - \xi \qquad (6)$$

$$= \tfrac{1}{2}(\Delta\phi - \pi) - \xi$$

$$\delta = \pi - \theta_1 - \theta_2 \qquad (7)$$

$$\xi = \pi - \alpha - \psi - \omega \qquad (8)$$

$$\omega = \tau + \Delta\psi \qquad (9)$$

$$\xi = \pi - \alpha - \psi - \tau - \Delta\psi \qquad (10)$$

substituting into (7)

$$\delta = \pi - \tfrac{1}{2}(\Delta\phi - \pi) + \pi - \pi + \phi + \Delta\phi - \psi - \tau - \Delta\psi - \gamma + \tau \qquad (11)$$

$$= \phi - \psi + \tfrac{1}{2}(\Delta\phi - \Delta\psi) \qquad (12)$$

Appendix 2

Derivation of Equation 43

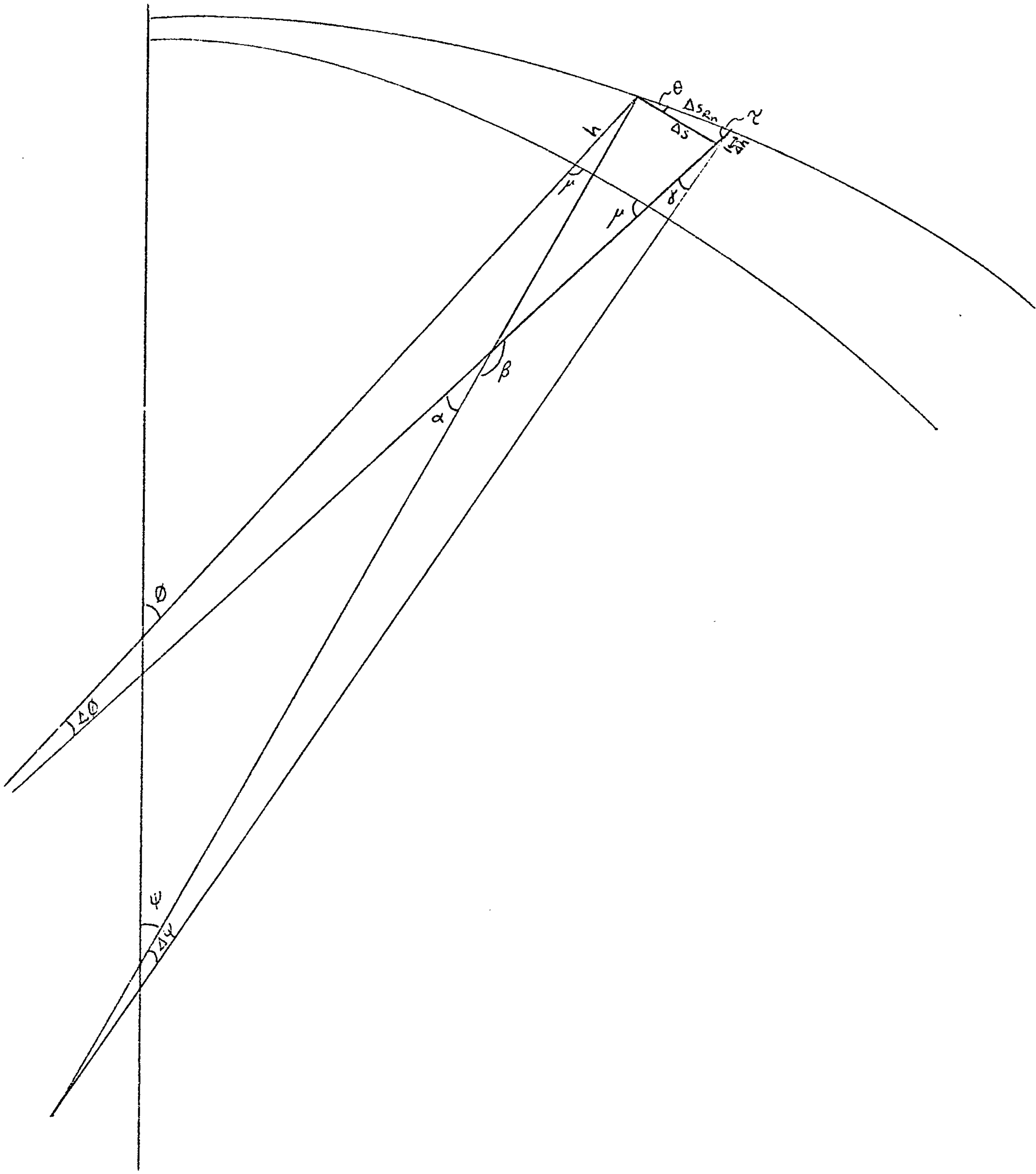

θ
Δs_{Rn}
τ
h
Δs
Δh
μ
μ
γ
β
α
Ø
ΔØ
ψ
Δψ

$$\alpha = \phi + \Delta\phi - \psi$$

$$\beta = \pi - \alpha$$

$$= \pi - \phi - \Delta\phi + \psi$$

$$\mu = \tfrac{1}{2}(\pi - \Delta\phi)$$

$$\theta = \pi - (\pi - \mu) - \tau$$

$$= \tfrac{1}{2}(\pi - \Delta\phi) - \tau$$

$$\gamma = \pi - \Delta\psi - \beta$$

$$= \phi - \psi + \Delta\phi - \Delta\psi$$

$$\tau + \gamma = \tfrac{1}{2}(\pi - \Delta\psi)$$

$$\Rightarrow \quad \tau = \tfrac{1}{2}(\pi - \Delta\psi) - \gamma$$

$$= \tfrac{1}{2}(\pi - \Delta\psi) - \phi + \psi - \Delta\phi + \Delta\psi$$

$$= \tfrac{1}{2}(\pi + \Delta\psi) - \phi + \psi - \Delta\phi$$

$$\theta = \tfrac{1}{2}(\pi - \Delta\phi) - \tau$$

$$= \tfrac{1}{2}(\pi - \Delta\phi) - \tfrac{1}{2}(\pi + \Delta\psi) + \phi - \psi + \Delta\phi$$

$$= \tfrac{1}{2}(\Delta\phi - \Delta\psi) + \phi - \psi$$

by the law of sines

$$\frac{\sin \tau}{\Delta s_R} = \frac{\sin \theta}{\Delta h} = \frac{\sin\left(\frac{\pi}{2} + \frac{\Delta\phi}{2}\right)}{\Delta s_{e_n}}$$

Appendix 3

Computer Program for

Original Gregorig Method

```
      C
      C     PROGRAM FOR DETERMINATION OF PROFILE OF CONDENSATE ON FLUTED TUBE,
      C     AS WELL AS HEAT TRANSFER COEFFICIENT AND DOWNWARD FLOW RATE.
      C     SUBROUTINE GREGOR DETERMINES THE PROFILE AND HEAT TRANSFER COEFF-
      C     ICIENT,BASED ON THE GREGORIG METHOD
      C     FUNCTION FUNC IS THE EQUATION OF THE SOLID SURFACE
      C     FUNCTION DERIV IS THE SLOPE OF THE SOLID SURFACE
      C     SUBROUTINE RELAX DETERMINES THE DOWNWARD FLOW RATE, BASED ON THE
      C     TWO-DIMENSIONAL POISSON EQUATION
      C     DELTA         THE SIZE OF THE (SQUARE) DIFFERENTIAL DISTANCE ELEMENT
      C                   FOR CALCULATION OF THE DOWNWARD FLOW RATE.  (INCHES)
      C     DELT          THE TEMPERATURE DRIVING FORCE BETWEEN THE STEAM AND
      C                   THE METAL SURFACE  (DEGREES F)
      C     RHO           THE DENSITY OF THE CONDENSATE  (G/CC)
      C     MU            THE VISCOSITY OF THE CONDENSATE  (CENTIPOISE)
      C     RO            RADIUS OF CURVATURE AT PEAK  (INCHES)
      C     HMIN          INITIAL ESTIMATE OF THE LIQUID HEIGHT AT THE PEAK (IN)
      C     NEXP          0.1 IS RAISED TO THIS POWER TO DETERMINE THE STEP SIZE
      C                   FOR ESTIMATES OF THE HEIGHT
      C     KEY           DETERMINES THE TYPE OF ROOT SOUGHT--
      C                   0  LOWER ROOT
      C                   1  UPPER ROOT
      C                   2  NO CONVERGENCE SOUGHT
            DIMENSION AH(11)
            COMMON/BLOCKH/AH
            COMMON/BLOCKG/VX(11),        VDS(11),VDPHI(11),VPHI(11),VDM(11),
           1VPN(11),VDPSI(11),VPSI(11)
            REAL NUMBY
            COMMON/BLOCKY/NUMBY(121)
            COMMON/BLOCKU/U(105,68)
            DOUBLE PRECISION DH
            EXTERNAL FUNC,DERIV
            REAL MU,M,K,LAMDA
            WRITE (6,751)
        751 FORMAT (2X,'ORIGINAL GREGORIG METHOD USED')
            MKEY=0
            READ (5,14) AMP,PERIOD
         14 FORMAT (2F10.0)
            READ (5,3) DELTA
          3 FORMAT (F10.0)
            READ (5,9) DELT
          9 FORMAT (F4.0)
            READ (5,15) LAMDA,K,SIGMA
         15 FORMAT (3F10.0)
            SIGMA=SIGMA*0.0001837
            K=K/3600.
            READ (5,1) RHO,MU,RO,HMIN,NEXP,KEY
          1 FORMAT (F10.0,F5.0,F10.0,        F10.0,I2,I2)
            MU=MU*0.000671969
            RHO=RHO*62.42621
         12 DH=10.0**(-NEXP)
            CALL GREGOR (RO,RHO,MU,M,W,HMIN,DH,DELTA,DELT,KEY,MKEY,PERIOD,
           #LAMDA,K,SIGMA)
```

```
      WRITE (6,750) NUMBY
  750 FORMAT (1X,20F6.0)
      IF (MKEY.EQ.1) GO TO 11
      WRITE (6,10) DELT
   10 FORMAT (2X,'TEMPERATURE DRIVING FORCE IS ',F5.0,'  DEGREES F')
      WRITE (6,2) RO,M
    2 FORMAT (2X,'THE TOTAL MASS CONDENSED FOR A PEAK RADIUS OF ',
     1'CURVATURE OF',2X,F8.6,2X,'IS',E11.4,2X,'POUNDS PER SECOND PER ',
     2'FOOT'/)
      RHO1=RHO/144.0
      GX=32.174
      DO 6 I=1,11
    6 WRITE (6,5) VX(I),       VDS(I),VDPHI(I),VPHI(I),AH(I),VDM(I),
     1VRM(I),VDPSI(I),VPSI(I)
    5 FORMAT (2X,9E11.4)
      CALL RELAX(MU,RHO1,GX,FLOW,DELTA,AMP)
      RATE =FLOW*RHO1*144.0
      WRITE (6,7) FLOW,RATE
    7 FORMAT (2X,'VOLUMETRIC FLOW RATE=',F11.7,'FT**3/SEC'/2X,'WEIGHT',
     2' RATE OF FLOW=',F11.7,'LB/SEC')
      HTC= M*970.0*3600.0*12.0/PERIOD/DELT
      WRITE (6,8) HTC
    8 FORMAT (2X,'THE HEAT TRANSFER COEFFICIENT IS',F10.0,
     $'  BTU/HR/FT/F')
      IF (KEY.EQ.0) GO TO 13
      IF (KEY.EQ.2) CALL EXIT
      KEY=0
      GO TO 12
   13 KEY=1
      GO TO 12
   11 KEY=0
      MKEY=0
      GO TO 12
      END
```

```
C
      SUBROUTINE GREGOR(RO,RHC,MU,M,W,HC,DH,DELTA,DELT,KEE,MKEY,
     $PERIOD,LAMDA,K,SIGMA)
C     DELM = CHANGE IN M    LB/(SEC FT)
C     DELS = CHANGE IN S    INCHES
C     DELT=TEMPERATURE GRADIENT   DEGREES F
C     H = HEIGHT OF LIQUID   INCHES
C     K = THERMAL CONDUCTIVITY  BTU/(SEC FT**2 F)/FT
C     RHO = DENSITY  LB/FT**3
C     MU = VISCOSITY  LB/(FT SEC)
C     LAMDA=HEAT OF VAPORIZATION BTU/LB
C     M=RATE OF CONDENSATION    LB/(SEC FT)
C     PSI = ANGLE   RADIANS
C     RA= RADIUS OF CURVATURE OF METAL SURFACE   INCHES
C     RN = RADIUS OF CURVATURE OF CONDENSATE   INCHES
C     S=DISTANCE ALONG SURFACE     INCHES
C     SIGMA = SURFACE TENSION    DYNES/CM
C     THETA= ANGLE   RADIANS
C     X= DISTANCE ALONG PIPE CIRCUMFERENCE   INCHES
C     ITER = ITERATION COUNTER FOR ENTIRE SUBROUTINE LIMITED TO 40
C     DIFF = DISTANCE FROM CENTER-LINE TO THE POINT ON THE FREE SURFACE
C
      REAL LAMDA,MU,K,M
      COMMON/BLOCKG/VX(11),         VDS(11),VDPHI(11),VPHI(11),VDM(11),
     1VRN(11),VDPSI(11),VPSI(11)
      DIMENSION AH(11)
      COMMON/BLOCKH/AH
      REAL NUMBY
      COMMON/BLOCKY/NUMBY(121)
      DOUBLE PRECISION DH,DHO
        ITER=0
      PI=3.14159265
      DHO=HC
      CX=0.0001
   73 DHO=DHO+DH
      HO=DHO
      X1=0.0
      Y1=HO
      IY=2
      NUMBY(1)=HC/DELTA +0.5
      XC=DELTA
      WRITE (6,815) X,THETA,H,M,PSI,DIFF,DPSI,HO
  815 FORMAT (2X,8E14.7)
      ITER=ITER+1
      IF (ITER.GT.40) CALL EXIT
C
C     INITIALIZING THE VECTORS TO BE SAVED
C
      DO 103 I=1,11
      VX(I)=0.0
      VDS(I)=0.0
      VDPHI(I)=0.0
      VPHI(I)=0.0
```

```
      VDM(I)=0.0
      VRN(I)=0.0
      VDPSI(I)=0.0
      VPSI(I)=0.0
  103 AH(I)=0.0
C
C     SETTING THE INITIAL VALUES OF PARAMETERS
C
      RN=RO
      W=0.0
      EX=0.0
      THETA=0.0
      PSI=0.0
      H=HO
      AH(1)=HO
      S=0.0
      M=0.0
      J=0
       X=0.0
      I=2
C     FINDING DELS
    2   BX=X
      J=J+1
      P1=FUNC(X)
      P2=FUNC(X+DX)
      DELS=SQRT((P2-P1)**2+DX*DX)
C
C     FINDING THE ANGLE ON THE METAL SURFACE SWEPT BY DELS (DTHET)
C
      D1=DERIV(X)
      D2=7.5*PI**2*COS(X*PI/0.04)
      IF (D2.EQ.0.0) D2=0.000001
      RA=(1.0+D1**2)**1.5/ABS(D2)
      IF (X.LE.0.02) GO TO 100
      D5=DERIV(X+DX)
      IF (D5.EQ.0.0) D5=0.000001
      D4=7.5*PI**2*COS((X+DX)*PI/0.04)
      RA=-(1.0+D5**2)**1.5/ABS(D4)
  100 DTHET=DELS/RA
      DPSI=DELS/RN
      DELM=K*DELT*DELS/LAMDA/H
      M=M+DELM
      RAN=1.0/RN-3.0*MU*M*DELS/(H**3*RHO*SIGMA)
      IF (RAN.EQ.0.0) RAN=0.000001
      RN=1.0/RAN
      H=H+((THETA-PSI)+0.5*(DTHET-DPSI))*DELS
C
C     IS H NEGATIVE--IMPOSSIBLE
C
      IF (H.LT.0.0) GO TO 73
      X2=X+H*SIN(THETA+DTHET)
  304 IF (X2.LT.X0) GO TO 303
      Y2=FUNC(X)+H*COS(THETA+DTHET)-FUNC(X2)
C
```

```
C     FINDING THE LOCUS OF THE FREE SURFACE IN THE GRID USED FOR
C     INTEGRATION OF DOWNWARD FLOW
C
      Y0=(Y2-Y1)*(X0-X1)/(X2-X1)+Y1
      NUMBY(IY)=Y0/DELTA+0.5
      IY=IY+1
      X0=X0+DELTA
      Y1=Y2
      GO TO 304
  303 DIFF=PERIOD-X-H*SIN(THETA+DTHET)
      IF (J.NE.1) GO TO 300
C
C     LOADING VECTORS
C
      VX(1)=X
      VDS(1)=DELS
      VDPHI(1)=DTHET
      VPHI(1)=THETA
      VDM(1)=DELM
      VRN(1)=RN
      VDPSI(1)=DPSI
      VPSI(1)=PSI
C
C     HAS THE CENTER-LINE BEEN REACHED
C
  300 DIFF=PERIOD-X-H*SIN(THETA)
      IF (DIFF.LE.0.0) GO TO 74
      EYE=I-1
      PX=EYE*PERIOD/10.0
      DSX=ABS(PX-X)
      IF(DSX.GT.DX/2.0) GO TO 99
C
C     LOADING VECTORS
C
      VX(I)=X
      VDS(I)=DELS
      VDPHI(I)=DTHET
      VPHI(I)=THETA
      VDM(I)=DELM
      VRN(I)=RN
      VDPSI(I)=DPSI
      VPSI(I)=PSI
      AH(I)=H
      I=I+1
C
C     RESETTING PARAMETERS
C
   99 THETA=THETA+DTHET
      PSI=PSI+DPSI
      S=S+DELS
      X=X+DX
C
C     WAS MINIMUM ON FREE SURFACE REACHED TOO SOON
C
```

```
      IF (PSI.LT.-0.0001) GO TO 75                                      GREG1620
      DDX=X-PERIOD+DX                                                   GREG1630
      IF (DDX.LT.DX/2.0) GO TO 2                                        GREG1640
      GO TO 223                                                         GREG1650
   72 IF (KEE.EQ.2) GO TO 73                                            GREG1660
C                                                                       GREG1670
C     HALVING THE INTERVAL BETWEEN SUCCESSIVE APPROXIMATIONS OF THE     GREG1680
C     PEAK FILM THICKNESS                                               GREG1690
C                                                                       GREG1700
      DHO=DHO-DH                                                        GREG1710
      DH=DH/2.0                                                         GREG1720
      GO TO 73                                                          GREG1730
C                                                                       GREG1740
C     WAS MINIMUM ON FREE SURFACE REACHED TOO SOON                       GREG1750
C                                                                       GREG1760
   74 IF (PSI.LT.-0.0001) GO TO 75                                      GREG1770
C                                                                       GREG1780
C     WAS MINIMUM ON FREE SURFACE REACHED TOO LATE                       GREG1790
C                                                                       GREG1800
      IF (PSI.GT.0.0001) GO TO 76                                       GREG1810
      GO TO 10                                                          GREG1820
C                                                                       GREG1830
C     WAS MINIMUM ON FREE SURFACE REACHED TOO LATE                       GREG1840
C                                                                       GREG1850
  223 IF (PSI.GE.0.0001) GO TO 76                                       GREG1860
      IF (ABS(PSI).LT.0.0001) GO TO 10                                  GREG1870
      GO TO 73                                                          GREG1880
   75 IF (KEE.EQ.0) GO TO 73                                            GREG1890
      GO TO 72                                                          GREG1900
   76 IF (KEE.EQ.0) GO TO 72                                            GREG1910
      GO TO 73                                                          GREG1920
   10 WRITE (6,36) HO                                                   GREG1930
   36 FORMAT (2X,E15.8//)                                               GREG1940
      RETURN                                                            GREG1950
   80 MKEY=1                                                            GREG1960
      IF (KEE.EQ.2) GO TO 73                                            GREG1970
      RETURN                                                            GREG1980
      END                                                               GREG1990
```

```
      SUBROUTINE RELAX(MU,RHO,GX,FLOW,DELTA,AMP)
C
C     USES SUCCESSIVE-OVER-RELAXATION TO DETERMINE THE DOWNWARD FLOW
C     RATE
C     OMEGA IS THE ACCELERATION PARAMETER
C     JMIN IS THE POINT IN THE FLOW REGION NEAREST THE METAL SURFACE
C     JMAX IS THE FREE SURFACE
C     ERROR IS THE FRACTIONAL CHANGE OF THE VELOCITY FROM ONE ITERATION
C     TO ANOTHER
C     FLOW IS THE INTEGRAL OF THE DOWNWARD FLOW RATE
C
      REAL NUMBY,MU
      COMMON/BLOCKY/NUMBY(121)
      COMMON/BLOCKU/U(105,78)
      PI=3.141592653
      OMEGA=1.9
C
C     INITIALIZING U'S TO ZERO
C
      DO 7 I=1,105
      DO 7 J=1,78
    7 U(I,J)=0.0
      KOUN=1
      ICOUNT=1
C
C     SETTING ERROR AND INTEGRAL OF DOWNWARD FLOW TO ZERO
C
    5 ERROR=0.0
      FLOW=0.0
      ICOUNT=ICOUNT+1
      X=0.0
      DO 6 I=1,78
C
C     SETTING SYMMETRY BOUNDARY CONDITION AT PEAK
C
      U(1,I)=U(3,I)
C
C     SETTING SYMMETRY BOUNDARY CONDITION AT VALLEY
C
    6 U(102,I)=U(100,I)
      DO 1 I=2,101
      KEY=2
      IF (I.EQ.2) GO TO 8
C
C     DETERMINING FREE AND METAL SURFACE BOUNDARIES
C
      Y1=FUNC(FLOAT(I-1)*DELTA)+AMP+NUMBY(I-1)
      Y2=FUNC(FLOAT(I-2)*DELTA)+AMP+NUMBY(I-2)
C
C     IF THE MAGNITUDE OF THE SLOPE OF THE SURFACE IS GREATER THAN OR
C     EQUAL TO 1/2, THE DERIVATIVE BOUNDARY CONDITION MUST INVOLVE
C     POINTS WHICH ARE NOT ON THE SAME VERTICAL COLUMN.  IF THIS IS TRUE
C     THEN KEY=1.
```

```
C
      SLOPE=(Y2-Y1)/DELTA
      IF (SLOPE.GE.0.5) KEY=1
    8 JMIN=(FUNC(X)+AMP)/DELTA+1.5
      JMAX=JMIN+IFIX(NUMBY(I-1))
      IF (I.EQ.2) JMAX1=JMAX
      IF (JMAX.GT.JMAX1) JMAX=JMAX1
      JMM=JMAX+1
      JMN=JMAX-1
      JM=JMIN+1
      IF (JM.GT.JMN) GO TO 10
C
C     THIS IS THE ACTUAL RELAXATION LOOP
C
      DO 4 J=JM,JMN
      UE=U(I,J)+OMEGA*(0.25*(GX*DELTA**2/MU*RHO+U(I-1,J)+U(I+1,J)+
     $U(I,J-1)+U(I,J+1))-U(I,J))
      ERROR=AMAX1(ABS((UE-U(I,J))/UE),ERROR)
      IF (J.EQ.JM) GO TO 11
      FLOW=UE*DELTA**2/144.0+FLOW
      GO TO 4
   11 FLOW=UE*DELTA**2/288.0+FLOW
    4 U(I,J)=UE
   10 U(I,JMM)=U(I,JMN)
      IF (KEY.EQ.1) U(I,JMM)=U(I-1,JMN)
      J=JMAX
C
C     THIS STAGE CALCULATES THE VELOCITY OF THE FREE SURFACE
C
      UE=U(I,J)+OMEGA*(0.25*(GX*DELTA**2/MU*RHO+U(I-1,J)+U(I+1,J)+
     $U(I,J-1)+U(I,J+1))-U(I,J))
      ERROR=AMAX1(ABS((UE-U(I,J))/UE),ERROR)
      FLOW=UE*DELTA**2/288.0+FLOW
      U(I,J)=UE
    1 X=X+DELTA
      IF (KOUN.LT.10) GO TO 3
      WRITE (6,9) ICOUNT,ERROR
    9 FORMAT (2X,I5,E15.8)
      KOUN=0
    3 KOUN=KOUN+1
      IF (ERROR.GT.0.001) GO TO 5
      WRITE (6,2) ICOUNT
    2 FORMAT (2X,'THE NUMBER OF ITERATIONS REQUIRED FOR CONVERGENCE OF T
     #HE DOWNWARD FLOW IS',I5)
      RETURN
      END
```

PAGE 1

```
      FUNCTION FUNC(Z)                                                  FUNC  10
      PI=3.1415926                                                      FUNC  20
      FUNC=0.012*COS(Z*PI/0.04)                                         FUNC  30
      RETURN                                                            FUNC  40
      END                                                               FUNC  50
```

PAGE 1

```
      FUNCTION DERIV(Z)                                 DERI  10
      PI=3.1415926                                      DERI  20
      DERIV=0.3*PI*SIN(Z*PI/0.04)                       DERI  30
      RETURN                                            DERI  40
      END                                               DERI  50
```

Appendix 4

Computer Program for

Modified Method

```
C        PROGRAM FOR DETERMINATION OF PROFILE OF CONDENSATE ON FLUTED TUBE,
C        AS WELL AS HEAT TRANSFER COEFFICIENT AND DOWNWARD FLOW RATE.
C        SUBROUTINE GREGOR DETERMINES THE PROFILE AND HEAT TRANSFER COEFF-
C        ICIENT,BASED ON IMPROVEMENTS OF THE GREGORIG METHOD
C        SUBROUTINE RELAX DETERMINES THE DOWNWARD FLOW RATE, BASED ON THE
C        TWO-DIMENSIONAL POISSON EQUATION
C        FUNCTION FUNC IS THE EQUATION OF THE SOLID SURFACE
C        FUNCTION DERIV IS THE SLOPE OF THE SOLID SURFACE
C        DELTA        THE SIZE OF THE (SQUARE) DIFFERENTIAL DISTANCE ELEMENT
C                     FOR CALCULATION OF THE DOWNWARD FLOW RATE.  (INCHES)
C        DELT         THE TEMPERATURE DRIVING FORCE BETWEEN THE STEAM AND
C                     THE METAL SURFACE  (DEGREES F)
C        RHO          THE DENSITY OF THE CONDENSATE  (G/CC)
C        MU           THE VISCOSITY OF THE CONDENSATE  (CENTIPOISE)
C        K            THERMAL CONDUCTIVITY  (BTU/(HR FT**2 F)/FT)
C        LAMDA        HEAT OF VAPORIZATION  (BTU/LB)
C        SIGMA        SURFACE TENSION  (DYNES/CM)
C        RO           RADIUS OF CURVATURE AT PEAK  (INCHES)
C        HMIN         INITIAL ESTIMATE OF THE LIQUID HEIGHT AT THE PEAK (IN)
C        NEXP        0.1 IS RAISED TH THIS POWER TO DETERMINE THE STEP SIZE
C                    FOR ESTIMATES OF THE HEIGHT
C        KEY         DETERMINES THE TYPE OF ROOT SOUGHT--
C                    0  LOWER ROOT
C                    1  UPPER ROOT
C                    2  NO CONVERGENCE SOUGHT
C
         DIMENSION AH(11)
         COMMON/BLOCKH/AH
         COMMON/BLOCKU/U(105,78)
         REAL NUMBY,LAMDA,K
         COMMON/BLOCKY/NUMBY(121)
         COMMON/BLOCKG/VX(11),        VDS(11),VDPHI(11),VPHI(11),VDM(11),
        1VRN(11),VDPSI(11),VPSI(11)
         DOUBLE PRECISION DH
         EXTERNAL FUNC,DERIV
         REAL MU,M
         READ (5,14) AMP,PERIOD,DELTA
      14 FORMAT (3F10.0)
         READ (5,15) LAMDA,K,SIGMA,RHO,MU
      15 FORMAT (5F10.0)
         SIGMA=SIGMA*0.0001837
         K=K/3600.
         MU=MU*0.000671969
         RHO=RHO*62.42621
         READ (5,1) RO,HMIN,NEXP,KEY,DELT
       1 FORMAT (F10.0,F10.0,I2,I2,F4.0)
      12 DH=10.0**(-NEXP)
         CALL GREGOR (RO,RHO,MU,M,HMIN,DH,DELTA,DELT,KEY,PERIOD,LAMDA,
        #K,SIGMA)
         WRITE (6,750)
     750 FORMAT (1X,'THE VERTICAL FILM THICKNESS IN UNITS OF DELTA ALONG',
        #' THE SURFACE IS')
         WRITE (6,751) NUMBY
```

```
  751 FORMAT (1X,20F6.0)
      WRITE (6,10) DELT
   10 FORMAT (2X,'TEMPERATURE DRIVING FORCE IS ',F5.0,'  DEGREES F')
      WRITE (6,2) RO,M
    2 FORMAT (2X,'THE TOTAL MASS CONDENSED FOR A PEAK RADIUS OF ',
     1'CURVATURE OF',2X,F8.6,2X,'IS',E11.4,2X,'POUNDS PER SECOND PER ',
     2'FOOT'/)
      RHO1=RHO/144.0
      GX=32.174
      WRITE (6,3)
    3 FORMAT (6X,'X',9X,'DS',8X,'DPHI',8X,'PHI',8X,'H',11X,'DM',9X,
     #'RN',8X,'DPSI',7X,'PSI')
      DO 6 I=1,11
    6 WRITE (6,5) VX(I),          VDS(I),VDPHI(I),VPHI(I),AH(I),VDM(I),
     1VRN(I),VDPSI(I),VPSI(I)
    5 FORMAT (2X,9E11.4)
      CALL RELAX(MU,RHO1,GX,FLOW,DELTA,AMP)
      RATE =FLOW*RHO1*144.0
      WRITE (6,7) FLOW,RATE
    7 FORMAT (2X,'VOLUMETRIC FLOW RATE=',F11.7,'FT**3/SEC'/2X,'WEIGHT',
     2' RATE OF FLOW=',F11.7,'LB/SEC')
      HTC= M*970.0*3600.0*12.0/PERIOD/DELT
      WRITE (6,8) HTC
    8 FORMAT (2X,'THE HEAT TRANSFER COEFFICIENT IS',F10.0,
     #'  BTU/HR/FT**2/F')
      CALL EXIT
      END
```

```
      SUBROUTINE GREGOR (RO,RHO,MU,M,HO,DH,DELTA,DELT,KEE,
     $PERIOD,LAMDA,K,SIGMA)
C
C     M         RATE OF CONDENSATION  LB/(SEC FT)
C     S         DISTANCE ALONG SURFACE  INCHES
C     DELM      CHANGE IN M  LB/(SEC FT)
C     DELS      CHANGE IN S  INCHES
C     DELT      TEMPERATURE GRADIENT DEGREES F
C     H         HEIGHT OF LIQUID  INCHES
C     K         THERMAL CONDUCTIVITY  BTU/(SEC FT**2 F)/FT
C     LAMDA     HEAT OF VAPORIZATION BTU/LB
C     RHO       DENSITY  LB/FT**2
C     MU        VISCOSITY  LB/(FT SEC)
C     SIGMA     SURFACE TENSION  POUNDALS/IN
C     PSI       ANGLE  RADIANS
C     RA        RADIUS OF CURVATURE OF METAL SURFACE  INCHES
C     RN        RADIUS OF CURVATURE OF CONDENSATE  INCHES
C     THETA     ANGLE  RADIANS
C     X         DISTANCE ALONG PIPE CIRCUMFERENCE  INCHES
C     ITER      ITERATION COUNTER FOR ENTIRE SUBROUTINE LIMITED TO 40
C     DSRN      DISTANCE ALONG OUTSIDE SURFACE OF CONDENSATE  INCHES
C     X2        X-POSITION OF FREE SURFACE CORRESPONDING TO POSITION
C         X+DELX ON THE METAL SURFACE
C     X1        LAST VALUE OF X2
C     X0        X-POSITION OF NEXT POSITION ON THE GRID USED TO DETERMINE
C          THE DOWNWARD FLOW
C     Y2        Y-POSITION OF X2
C     Y1        LAST VALUE OF Y2
C     Y0        Y-POSITION OF X0
C     DIFF      DISTANCE FROM CENTER-LINE TO THE POINT ON THE FREE SURFACE
C     DDX       DISTANCE BETWEEN NEW POINT ON METAL SURFACE AND CENTER
C     LINE  INCHES
C
      REAL LAMDA,MU,K,M
      COMMON/BLOCKG/VX(11),        VDS(11),VDPHI(11),VPHI(11),VDM(11),
     1VRN(11),VDPSI(11),VPSI(11)
      DIMENSION AH(11)
      COMMON/BLOCKH/AH
      REAL NUMBY
      COMMON/BLOCKY/NUMBY(121)
      DOUBLE PRECISION DH,DHO
      ITER=0
      PI=3.14159265
      DHO=HO
      DX=0.0001
   73 DHO=DHO+DH
      HO=DHO
      X1=0.0
      Y1=HO
      IY=2
      NUMBY(1)=HO/DELTA +0.5
      X0=DELTA
      WRITE (6,815) X,THETA,H,M,PSI,DIFF,DPSI,HO
```

```
  815 FORMAT (2X,8E14.7)
      ITER=ITER+1
      IF (ITER.GT.40) CALL EXIT
C
C     INITIALIZING THE VECTORS TO BE SAVED
C
      DO 103 I=1,11
      VX(I)=0.0
      VDS(I)=0.0
      VDPHI(I)=0.0
      VPHI(I)=0.0
      VDM(I)=0.0
      VRN(I)=0.0
      VDPSI(I)=0.0
      VPSI(I)=0.0
  103 AH(I)=0.0
C
C     SETTING THE INITIAL VALUES OF PARAMETERS
C
      RN=RO
      EX=0.0
      THETA=0.0
      PSI=0.0
      H=HO
      AH(1)=HO
      S=0.0
      M=0.0
      J=0
      X=0.0
      I=2
C
C     FINDING DELS
C
    2 BX=X
      J=J+1
      P1=FUNC(X)
      P2=FUNC(X+DX)
      DELS=SQRT((P2-P1)**2+DX*DX)
C
C     FINDING THE ANGLE ON THE METAL SURFACE SWEPT BY DELS (DTHET)
C
      D1=DERIV(X)
      D5=DERIV(X+DX)
      IF (D1.EQ.0.0) D1=0.000001
      IF (D5.EQ.0.0) D5=0.000001
  100 DTHET=ATAN(1.0/D1)-ATAN (1.0/D5)
      AT=DTHET
C
C     CHECK TO MAKE SURE THAT ARGUMENT OF LOG FUNCTION IS NON-ZERO
C
      IF (AT.EQ.0.0) GO TO 307
      TEST=AT*H/DELS+1.0
C
C     CHECK TO MAKE SURE THAT ARGUMENT OF LOG FUNCTION IS NOT NEGATIVE
```

```
      C
            IF (TEST.LE.0.0) GO TO 73
            DELH=K*DELT*AT/LAMDA/ALOG(AT*H/DELS+1.0)
            GO TO 308
        307 DELH=K*DELT/LAMDA/H*DELS
        308 HHG=H**3
            H=H+DELH
      C
      C     INITIAL ESTIMATE OF CHANGE IN DISTANCE ALONG FREE SURFACE DSRN
      C     THIS IS DONE TO GET AN ESTIMATE OF DELH, WHICH MUST BE USED IN
      C     DETERMINING THE ACTUAL VALUE OF THE DISTANCE ALONG THE FREE
      C     SURFACE
      C
            DSRN=DELS+AT*H
            RAN=1.0/RN-3.0*MU*M*DSRN/(HHG*RHO*SIGMA)
            IF (RAN.EQ.0.0) RAN=0.000001
            RQ =1.0/RAN
            RS=RN
            IF (RQ.LT.0.0.AND.RN.GT.0.0) RS=RQ
            DPSI=DSRN/(RS+RQ)*2.0
            IF (RN.LT.0.0) DPSI=DSRN/(RN+RQ)*2.0
            DELH=DSRN*(SIN(THETA-PSI+0.5*(DTHET-DPSI))/SIN((PI+DPSI)/2.0-DTHET
           $+PSI-THETA))
      C
      C     IMPROVING THE ESTIMATE OF DSRN
      C
            DSRN=SQRT(DELH**2+DSRN**2-2.0*DELH*DSRN*COS((PI+DTHET)/2.0))
            RAN=1.0/RN-3.0*MU*M*DSRN/(HHG*RHO*SIGMA)
            RQ=1.0/RAN
            DPSI=DSRN/(RS+RQ)*2.0
            IF (RN.LT.0.0) DPSI=DSRN/(RN+RQ)*2.0
            DELH=DSRN*SIN(THETA-PSI+0.5*(DTHET-DPSI))/SIN((PI+DTHET)/2.0)
        301 H=H+DELH
      C
      C     IS H NEGATIVE--IMPOSSIBLE
      C
            IF (H.LT.0.0) GO TO 73
            X2=X+H*SIN(THETA+DTHET)
            Y2=FUNC(X)+H*COS(THETA+DTHET)-FUNC(X2)
      C
      C     CHECK TO SEE IF H IS THE SHORTEST DISTANCE TO THE METAL SURFACE
      C
            IF (Y2.LE.H) GO TO 78
        304 IF (X2.LT.X0) GO TO 303
            Y2=FUNC(X)+H*COS(THETA+DTHET)-FUNC(X2)
      C
      C     FINDING THE LOCUS OF THE FREE SURFACE IN THE GRID USED FOR
      C     INTEGRATION OF DOWNWARD FLOW
      C
            IF (ABS(AT).LT.E-8.AND.THETA.EQ.0.0) GO TO 309
            Y0=(Y2-Y1)*(X0-X1)/(X2-X1)+Y1
            NUMBY(IY)=Y0/DELTA+0.5
            GO TO 310
        309 NUMBY(IY)=H/DELTA+0.5
```

```
  310 IY=IY+1                                                           GREG1620
      XO=XO+DELTA                                                       GREG1630
      GO TO 304                                                         GREG1640
C                                                                       GREG1650
C     THIS IS WHERE YOU GO IF THE SHORTEST DISTANCE TO THE METAL SURFACEGREG1660
C     IS ALONG AN X=CONSTANT LINE                                       GREG1670
C                                                                       GREG1680
   78 P2=FUNC(X2)                                                       GREG1690
      DELS=SQRT((P2-P1)**2+(X2-X)**2)                                   GREG1700
      D5= DERIV(X2)                                                     GREG1710
      H=H-DELH                                                          GREG1720
      H=AMIN1(H,Y2)                                                     GREG1730
      M=M-DELM                                                          GREG1740
      IF (D1.EQ.0.0.AND.D5.EQ.0.0) GO TO 171                            GREG1750
      IF (D5.EQ.0.0.AND.D1.NE.0.0) GO TO 172                            GREG1760
      DTHET=ATAN(1.0/D1)-ATAN(1.0/D5)                                   GREG1770
      GO TO 174                                                         GREG1780
  171 DTHET=0.0                                                         GREG1790
      GO TO 174                                                         GREG1800
  172 DTHET=-THETA                                                      GREG1810
  174 AT=DTHET                                                          GREG1820
      IF (AT.EQ.0.0) GO TO 1307                                         GREG1830
      TEST=AT*H/DELS+1.0                                                GREG1840
      IF (TEST.LE.0.0) GO TO 173                                        GREG1850
      DELM=K*DELT*AT/LAMDA/ALOG(TEST)                                   GREG1860
      GO TO 1308                                                        GREG1870
  173 TEST=1.0-AT*H/DSRN                                                GREG1880
      DELM=-K*DELT*AT/LAMDA/ALOG(TEST)                                  GREG1890
      GO TO 1308                                                        GREG1900
 1307 DELM=K*DELT/LAMDA/H*DELS                                          GREG1910
 1308 HHG=H**3                                                          GREG1920
      DSRN=DELS+AT*H                                                    GREG1930
      RAN=1.0/RN-3.0*MU*M*DSRN/(HHG*RHO*SIGMA)                          GREG1940
      IF (RAN.EQ.0.0) RAN=0.000001                                      GREG1950
      RQ=1.0/RAN                                                        GREG1960
      RS=RN                                                             GREG1970
      IF (RQ.LT.0.0.AND.RN.GT.0.0) RS=RQ                                GREG1980
      DPSI=DSRN/(RS+RQ)*2.0                                             GREG1990
      IF (RN.LT.0.0) DPSI=DSRN/(RN+RQ)*2.0                              GREG2000
      DELH=DSRN*(SIN(THETA-PSI+0.5*(DTHET-DPSI))/SIN((PI+DPSI)/2.0-DTHETGREG2010
     $+PSI-THETA))                                                      GREG2020
      DSRN=SQRT(DELH**2+DSRN**2-2.0*DELH*DSRN*COS((PI+DTHET)/2.0))      GREG2030
      RAN=1.0/RN-3.0*MU*M*DSRN/(HHG*RHO*SIGMA)                          GREG2040
      RQ=1.0/RAN                                                        GREG2050
      DPSI=DSRN/(RS+RQ)*2.0                                             GREG2060
      IF (RN.LT.0.0) DPSI=DSRN/(RN+RQ)*2.0                              GREG2070
      DELH=DSRN*SIN(THETA-PSI+0.5*(DTHET-DPSI))/SIN((PI+DTHET)/2.0)     GREG2080
      H=H+DELH                                                          GREG2090
      X=X2                                                              GREG2100
      GO TO 304                                                         GREG2110
  303 DIFF=PERIOD-X-H*SIN(THETA+DTHET)                                  GREG2120
  102 RN=RQ                                                             GREG2130
      Y1=Y2                                                             GREG2140
      X1=X2                                                             GREG2150
```

```
C
C     LOADING VECTORS
C
      IF (J.NE.1) GO TO 300
      VX(1)=X
      VDS(1)=DELS
      VDPHI(1)=DTHET
      VPHI(1)=THETA
      VDM(1)=DELM
      VRN(1)=RN
      VDPSI(1)=DPSI
      VPSI(1)=PSI
C
C     HAS THE CENTER LINE BEEN REACHED
C
  300 IF (DIFF.LE.0.0) GO TO 74
      EYE=I-1
      PX=EYE*PERIOD/10.0
      DSX=ABS(PX-X)
C
C     LOADING VECTORS
C
      IF(DSX.GT.DX/2.0) GO TO 99
      VX(I)=X
      VDS(I)=DELS
      VDPHI(I)=DTHET
      VPHI(I)=THETA
      VDM(I)=DELM
      VRN(I)=RN
      VDPSI(I)=DPSI
      VPSI(I)=PSI
      AH(I)=H
      I=I+1
C
C     RESETTING PARAMETERS
C
   99 THETA=THETA+DTHET
      PSI=PSI+DPSI
      S=S+DELS
      X=X+DX
C
C     WAS MINIMUM ON FREE SURFACE REACHED TOO SOON
C
      IF (PSI.LT.-0.0001) GO TO 75
      DDX=X-PERIOD+DX
      IF (DDX.LT.DX/2.0) GO TO 2
      GO TO 223
   72 IF (KEE.EQ.2) GO TO 73
C
C     HALVING THE INTERVAL BETWEEN SUCCESSIVE APPROXIMATIONS OF THE
C     PEAK FILM THICKNESS
C
      DHO=DHO-DH
      DH=DH/2.0
```

```
      GO TO 73                                                          GREG2700
C                                                                       GREG2710
C     WAS MINIMUM ON FREE SURFACE REACHED TOO SOON                      GREG2720
C                                                                       GREG2730
   74 IF (PSI.LT.-0.0001) GO TO 75                                      GREG2740
C                                                                       GREG2750
C     WAS MINIMUM ON FREE SURFACE REACHED TOO LATE                      GREG2760
C                                                                       GREG2770
      IF (PSI.GT.0.0001) GO TO 76                                       GREG2780
      GO TO 10                                                          GREG2790
C                                                                       GREG2800
C     WAS MINIMUM ON FREE SURFACE REACHED TOO LATE                      GREG2810
C                                                                       GREG2820
  223 IF (PSI.GE.0.0001) GO TO 76                                       GREG2830
      IF (ABS(PSI).LT.0.0001) GO TO 10                                  GREG2840
      GO TO 73                                                          GREG2850
   75 IF (KEE.EQ.0) GO TO 73                                            GREG2860
      GO TO 72                                                          GREG2870
   76 IF (KEE.EQ.0) GO TO 72                                            GREG2880
      GO TO 73                                                          GREG2890
   10 WRITE (6,36) HO                                                   GREG2900
   36 FORMAT (2X,E15.8//)                                               GREG2910
      RETURN                                                            GREG2920
      END                                                               GREG2930
```

```
      SUBROUTINE RELAX(MU,RHO,GX,FLOW,DELTA,AMP)
C
C     USES SUCCESSIVE-OVER-RELAXATION TO DETERMINE THE DOWNWARD FLOW
C     RATE
C     OMEGA IS THE ACCELERATION PARAMETER
C     JMIN IS THE POINT IN THE FLOW REGION NEAREST THE METAL SURFACE
C     JMAX IS THE FREE SURFACE
C     ERROR IS THE FRACTIONAL CHANGE OF THE VELOCITY FROM ONE ITERATION
C     TO ANOTHER
C     FLOW IS THE INTEGRAL OF THE DOWNWARD FLOW RATE
C
      REAL NUMBY,MU
      COMMON/BLOCKY/NUMBY(121)
      COMMON/BLOCKU/U(105,78)
      PI=3.141592653
      OMEGA=1.9
C
C     INITIALIZING U'S TO ZERO
C
      DO 7 I=1,105
      DO 7 J=1,78
    7 U(I,J)=0.0
      KOUN=1
      ICOUNT=1
C
C     SETTING ERROR AND INTEGRAL OF DOWNWARD FLOW TO ZERO
C
    5 ERROR=0.0
      FLOW=0.0
      ICOUNT=ICOUNT+1
      X=0.0
      DO 6 I=1,78
C
C     SETTING SYMMETRY BOUNDARY CONDITION AT PEAK
C
      U(1,I)=U(3,I)
C
C     SETTING SYMMETRY BOUNDARY CONDITION AT VALLEY
C
    6 U(102,I)=U(100,I)
      DO 1 I=2,101
      KEY=2
      IF (I.EQ.2) GO TO 8
C
C     DETERMINING FREE AND METAL SURFACE BOUNDARIES
C
      Y1=FUNC(FLOAT(I-1)*DELTA)+AMP+NUMBY(I-1)
      Y2=FUNC(FLOAT(I-2)*DELTA)+AMP+NUMBY(I-2)
C
C     IF THE MAGNITUDE OF THE SLOPE OF THE SURFACE IS GREATER THAN OR
C     EQUAL TO 1/2, THE DERIVATIVE BOUNDARY CONDITION MUST INVOLVE
C     POINTS WHICH ARE NOT ON THE SAME VERTICAL COLUMN.  IF THIS IS TRUE
C     THEN KEY=1.
```

```
C                                                                         RELA 540
      SLOPE=(Y2-Y1)/DELTA                                                 RELA 550
      IF (SLOPE.GE.0.5) KEY=1                                             RELA 560
    8 JMIN=(FUNC(X)+AMP)/DELTA+1.5                                        RELA 570
      JMAX=JMIN+IFIX(NUMBY(I-1))                                          RELA 580
      IF (I.EQ.2) JMAX1=JMAX                                              RELA 590
      IF (JMAX.GT.JMAX1) JMAX=JMAX1                                       RELA 600
      JMM=JMAX+1                                                          RELA 610
      JMN=JMAX-1                                                          RELA 620
      JM=JMIN+1                                                           RELA 630
      IF (JM.GT.JMN) GO TO 10                                             RELA 640
C                                                                         RELA 650
C     THIS IS THE ACTUAL RELAXATION LOOP                                  RELA 660
C                                                                         RELA 670
      DO 4 J=JM,JMN                                                       RELA 680
      UE=U(I,J)+OMEGA*(0.25*(GX*DELTA**2/MU*RHO+U(I-1,J)+U(I+1,J)+        RELA 690
     $U(I,J-1)+U(I,J+1))-U(I,J))                                          RELA 700
      ERROR=AMAX1(ABS((UE-U(I,J))/UE),ERROR)                              RELA 710
      IF (J.EQ.JM) GO TO 11                                               RELA 720
      FLOW=UE*DELTA**2/144.0+FLOW                                         RELA 730
      GO TO 4                                                             RELA 740
   11 FLOW=UE*DELTA**2/288.0+FLOW                                         RELA 750
    4 U(I,J)=UE                                                           RELA 760
   10 U(I,JMM)=U(I,JMN)                                                   RELA 770
      IF (KEY.EQ.1) U(I,JMM)=U(I-1,JMN)                                   RELA 780
      J=JMAX                                                              RELA 790
C                                                                         RELA 800
C     THIS STAGE CALCULATES THE VELOCITY OF THE FREE SURFACE              RELA 810
C                                                                         RELA 820
      UE=U(I,J)+OMEGA*(0.25*(GX*DELTA**2/MU*RHO+U(I-1,J)+U(I+1,J)+        RELA 830
     $U(I,J-1)+U(I,J+1))-U(I,J))                                          RELA 840
      ERROR=AMAX1(ABS((UE-U(I,J))/UE),ERROR)                              RELA 850
      FLOW=UE*DELTA**2/288.0+FLOW                                         RELA 860
      U(I,J)=UE                                                           RELA 870
    1 X=X+DELTA                                                           RELA 880
      IF (KOUN.LT.10) GO TO 3                                             RELA 890
      WRITE (6,9) ICOUNT,ERROR                                            RELA 900
    9 FORMAT (2X,I5,E15.8)                                                RELA 910
      KOUN=0                                                              RELA 920
    3 KOUN=KOUN+1                                                         RELA 930
      IF (ERROR.GT.0.001) GO TO 5                                         RELA 940
      WRITE (6,2) ICOUNT                                                  RELA 950
    2 FORMAT (2X,'THE NUMBER OF ITERATIONS REQUIRED FOR CONVERGENCE OF TRELA 960
     #HE DOWNWARD FLOW IS',I5)                                            RELA 970
      RETURN                                                              RELA 980
      END                                                                 RELA 990
```

PAGE 1

```
      FUNCTION FUNC(Z)                                    FUNC  10
      PI=3.1415926                                        FUNC  20
      FUNC=0.012*COS(Z*PI/0.04)                           FUNC  30
      RETURN                                              FUNC  40
      END                                                 FUNC  50
```

```
      FUNCTION DERIV(Z)
      PI=3.1415926
      DERIV=0.3*PI*SIN(Z*PI/0.04)
      RETURN
      END
```

BIBLIOGRAPHY

1) Sephton, H. H.: "Heat Transfer Enhancement by Vortex Shear Flow" Symposium on Enhanced Tubes for Desalination Plants Office of Saline Water, U.S. Department of Interior, Washington, DC p. 99 (1970)

2) Lustenader, E. L. and Staub, F. W.: "Development Contributions to Compact Condenser Design" INCO Power Conference Session II May 5-8 (1964)

3) Gregorig, R.: "Film Condensation on Finely-Waved Surfaces with Consideration of Surface Tension," Zeitschrift fur angewandte Mathematik und Physik V p. 36 (1954)

4) Lustenader, E. L., Richter, R., and Neugebauer, F. J.: "The Use of Thin Films for Increasing Evaporation and Condensation Rates in Process Equipment," Journal of Heat Transfer 81 p. 297 (1959)

5) Trefethen, L. M.: Discussion of Lustenader, et al paper Journal of Heat Transfer 81 p. 306 (1959)

6) Carnavos, T. C.: Proceedings of 1st International Symposium on Water Desalination Washington, DC, October 3-9, 1965 2 p. 205 (1967)

7) Christ, A.: "Steam Turbine Preheater Tubes with Grooved Surface," Escher Wyss News, 35 p. 94 (1962)

8) Carnavos, T. C.: "Augmenting Heat Transfer in Desalination Equipment with Fluted Surfaces" Office of Saline Water Symposium: "Enhanced Tubes for Distillation Plants" Washington, D C, March 11 & 12 (1969)

9) Thomas, D. G.: "Enhancement of Film Condensation Heat Transfer Rates on Vertical Tubes by Vertical Wires" I&EC Fund. VI p. 97 Feb. (1967)

10) Thomas, D. G.: "Enhancement of Film Condensation Rate on Vertical Tubes for Longitudinal Fins" AIChE J. XIV #4 p. 644 (1968)

11) Kays, D. D., and Chia, W. S.: "Development and Application of Mechanically Enhanced Heat Transfer Surfaces" ASME preprint 71-HT-40

12) Morkowitz, A., Mikic, B. B., and Bergles, A. E.: "Condensation on a Downward-Facing Horizontal Rippled Surface" Journal of Heat Transfer 94 #3 p. 315 (1972)

13) Nusselt, W.: Zeitschrift vor Deutschen Ingeneuer 60 541, 569 (1916)

14) Ames, W. F.: Numerical Methods for Partial Differential Equations, Barnes & Noble (1969)

NOMENCLATURE

A	Area for heat transfer
D	Angle shown in Figure 8
g	Acceleration due to gravity
g_c	Conversion factor
h	Film thickness
H	Local heat transfer coefficient
$\overline{H}$	Average heat transfer coefficient
k	Thermal conductivity
m	Rate of condensation
P	Pressure
q	Heat flow
Q	Heat flow per unit area
R	Radius of curvature of free surface
R_a	Radius of curvature of solid surface
s	Distance measured along solid surface
t	Time
T	Temperature
U	Velocity
W	Mass flow rate
x	Coordinate
y	Coordinate
z	Coordinate

greek letters

δ	Angle in Figure 5
ΔS_R	Distance in Figure 11
ΔS_{Rn}	Distance in Figure 10
ΔT	Temperature driving force
ΔX	Change in distance along surface
λ	Latent heat of vaporization
μ	Viscosity
ρ	Density
σ	Surface Tension
ϕ	Angle see Figure 5
ψ	Angle see Figure 5
ω	Acceleration parameter for relaxation

subscripts

n	Represents horizontal position
p	Represents vertical position
x	Coordinate direction
y	Coordinate direction
z	Coordinate direction

superscripts

n	Result of n^{th} iteration in relaxation